Microtubule nucleation controlled by testis-specific γ-TuRC in Drosophila spermatogenesis

PhD Thesis

Elham Alzyoud

SUPERVISOR:
Dr. habil. Rita Sinka
Associate Professor

University of Szeged, Faculty of Science and Informatics,
Department of Genetics
Doctoral School of Biology

Szeged
2022

Table of Contents

List of abbreviations

3'UTR: 3' untranslated region
3-AT: 3-amino-1, 2, 4-aminotrizole
5'UTR: 5' untranslated region
Ana: anastral spindle 1
Asl: Aasterless
Bb8: big bubble 8
CA: centriole adjuncts
Cas9: CRISPR-associated protein 9
CB: cystic bulge
CDS: Coding sequence
Cep: Centrosomal protein
CLR: cilium like region
Cnn: centrosomin
CnnT: testis-specific Centrosomin isoform
CRISPR: clustered regularly interspaced short palindromic repeats
CySC: somatic cyst stem cells
DAPI: 4′,6-Diamidino-2-Phenylindole, Dihydrochloride
DNA: deoxyribonucleic acid
ER: Endoplasmic reticulum
GCP: gamma-tubulin complex proteins
GFP: green fluorescent protein
Grip: gamma-ring complex proteins
GSC: germline stem cells
HA: hemagglutinin
IC: individualization complex
IVTT: *In vitro* coupled transcription–translation
LiAc: Lithium Acetate
mCh: mCherry
Msps: MT polymerase mini spindles
MT: Microtubule
MTOC: microtubule organizing center
Mzt1: Mitotic spindle organizing protein 1
Ncd: Non-claret disjunction
ncMTOC: non-centrosomal microtubule-organizing center
PACT: Pericentrin/AKAP450 centrosomal targeting
PBSTB: PBS, Triton-X100, BSA
PBSTX: PBS, Tween-20 and Triton-X100
PBSTXB: PBSTX+BSA
PCM: pericentriolar material
PCNT: Pericentrin
PCR: polymerase chain reaction
Plp: pericentrin like protein
RNA: ribonucleic acid
Sas4: spindle assembly abnormal
sgRNA: small guided RNA
shot: spectraplakin short stop
S-Lap: sperm leucyl aminopeptidase
Spd2: spindle defective 2
ssDNA: salmon sperm DNA
t-γ-TuRC: testis-specific γ Tubulin Ring Complex
TACC: Transforming acidic coiled-coil protein
TEM: transmission electron microscopy
t-Grip: testis-specific gamma-ring complex protein
Tom20: Translocase of outer membrane 20
unc: uncoordinated
WT: wild type
Y2H: yeast two-hybrid
γ-TuRC: γ Tubulin Ring Complex
γ-TuSC: γ Tubulin Small Complex

1 Introduction

1.1 Drosophila melanogaster spermatogenesis

1.1.1 Drosophila as a model organism

Drosophila melanogaster has become one of the most frequently used model organism in genetics, developmental-, cell-, and molecular biology during the last century (Fabian and Brill, 2012). Thomas Hunt Morgan was the first scientist who used Drosophila in genetic research. He established and proved the chromosomal theory of inheritance by utilizing Drosophila as a model. The rapid generation time, the low cost, and the simple maintenance make *D. melanogaster* highly reliable and widely used in laboratories. Thanks to the well-established genetic toolkit of Drosophila, we can conduct various types of genetic manipulation, including classical forward genetic and reverse genetic methods. The wide range of molecular and genetic tools encompass classical mutants' induction with different mutagen agents (EMS, X-ray, etc.), furthermore, a variety of mobile genetic elements are also available to manipulate the genome of Drosophila. The most widely used is the P element which is a powerful tool to induce mutations and its modified versions also serve as a vector to incorporate transgenes into the genome. After the discovery and characterization of the clustered regularly interspaced short palindromic repeats (CRISPR) and CRISPR-associated protein 9 (Cas9) in bacteria, CRISPR-Cas9 technology soon emerged and was optimized in Drosophila as well in many other organisms. CRISPR-Cas9 makes it possible to induce smaller or larger deletions in the gene of interest, alternatively, it can be used to mediate *in vivo* tagging of a target gene. Due to the relatively high sequence homology between Drosophila and human protein-coding genes, *D. melanogaster* was proven to be a suitable model for studying the molecular mechanisms of human diseases, including cancer, physiological, neurological disorders and also a frequently used model for drug screening (Fabian and Brill, 2012; Hales et al., 2015; Ugur et al., 2016).

1.1.2 Drosophila spermatogenesis

Drosophila testis is a coiled pair of blunt-ended tubes, the place of male germ cell development. Drosophila spermato- and spermiogenesis are like mammals, sharing high genetic homology, with multiple conserved proteins. This explains why Drosophila spermatogenesis represents a good

model to study a broad range of biological processes such as stem cell behavior, mitotic and meiotic cell division, and communication between somatic and germ cells. In the developing spermatids, we can investigate the rearrangement and formation of cytoskeletal elements, changes in cellular organelles, the nuclear remodeling with protamine containing chromatin, formation of specialized mitochondria after meiosis and the process responsible for the centrosome and basal body formation (Jana et al., 2016; Siddall and Hime, 2017).

Sperm morphology and structure is highly conserved in animals; however, the size of the sperm is variable among Drosophila species. *D. persimilis* have a sperm with 0.32 mm length, while *D. bifurca* sperm length reaches 58.29 mm (Pitnick et al., 1995). *Drosophila melanogaster* has a giant sperm with a length of 1.85 mm and a diameter of 0.6 µm, which is 30 times bigger than human sperm (Laurinyecz et al., 2019). The insect *Zorotypus impolitus* has the widest sperm described so far with 3 µm width and 1:10-1:13 axoneme:mitochondria size ratio (Dallai et al., 2014).

Drosophila spermatogenesis starts at the apical tip of the testis where the testis stem cell niche resides (Spradling et al., 2008). Three types of cells are found in the stem cell niche; the germline stem cells (GSC), the somatic cyst stem cells (CySCs) and the non-dividing somatic hub cells (Gönczy and DiNardo, 1996). Each GSC is enclosed by two CySCs, and both populations undergo asymmetric divisions to maintain the stem cell pool and differentiate into gonialblast and somatic cyst cells, respectively (White-Cooper and Bausek, 2010; Dominado et al., 2016). Hub cells are a signaling center for the stem cell niche as they support the asymmetrical division of the GSC. The germline cells are supported by the two somatic cyst cells throughout spermatogenesis. The gonialblast undergoes four mitotic divisions producing 16 spermatogonial cells, the primary spermatocytes. The cytokinesis during cell divisions is incomplete, which results in interconnected primary spermatocytes that share cytoplasm through stable intercellular bridges, called the ring canals (White-Cooper and Bausek, 2010; de Cuevas and Matunis, 2011). Once entering premeiotic S phase spermatogonial cells switch to the spermatocyte program, which includes cell growth and intensive gene expression (Demarco et al., 2014). The majority of gene products needed for the spermatocytes and post-meiotic spermatid development are transcribed at this stage (Fabian and Brill, 2012; Demarco et al., 2014).

The meiosis of the 16 mature spermatocytes produces a cyst with 64 interconnected round spermatids. Spermatids in the same cyst develop simultaneously with the same distribution of cellular organelles throughout spermatogenesis. At this stage new organelles are being established,

like the acroblast (Golgi and lysosome derived organelle), which will form the acrosome later (Fabian and Brill, 2012). The acrosome is an evolutionarily conserved organelle of the sperm, which is necessary for proper fertilization (Wilson et al., 2006; Fári et al., 2016). The dense body on one side of the nucleus is a microtubule and actin-rich structure and plays a role in the elongation and shaping of the nucleus (Tokuyasu, 1974b).

After meiosis the transcriptional activity of round spermatids is minimal, despite this, they go through dramatic morphological changes as they continue their development. In round spermatids the haploid nuclei are spherical with a ~5 μm diameter, during cyst elongation the nuclei go through intensive morphological changes, as they gradually elongate too. The intensive compaction of the chromatin also occurs as histones are replaced by protamines, which provides a more compact form for the chromatin. By the end of the spermiogenesis, the apical part of the cysts contains 10 μm long needle-shaped nuclear bundles (Tokuyasu, 1974b). During earlier steps of elongation, nuclei are organized into a group at one side of the cyst, heading toward the basal end of the testis, while the spermatid tails are pointing to the opposite end at the apical part (**Figure 1**) (Fabian and Brill, 2012). Elongation of spermatids is driven by elongation of the mitochondrial derivatives (Noguchi et al., 2011).

Spermatid elongation is followed by individualization, the process of separating spermatids and engulfing each one with an individual membrane. It starts with the formation of the individualization complex (IC), around the needle-shaped nuclei. IC is composed of 64 cone shaped actin-rich cytoskeletal structures (investment cones). The IC starts to migrate towards the basal end of the cyst as it moves, all unnecessary cell components, like membranes, cytoplasm, and organelles are being stripped away and collected in the cystic bulge at the end of the cyst (Tokuyasu et al., 1972; Fabrizio et al., 1998). In the cystic bulge, high caspase activity is present, which is responsible for the facilitation of the degradation of the excess cellular components. This non-apoptotic caspase cascade is also required for the proteolysis of cytoplasmic proteins. At the end of the individualization, the degradation products are separated into the so-called waste bag (Fabian and Brill, 2012). The individualization process is very sensitive, the failure of nucleus basal body attachment, disruption of mitochondrial function or organization, or the impaired degradation of the cytoplasmic proteins all result in abnormal individualization. Asynchronous movement of the ICs could be a good marker of the failure of the above-mentioned defects (Tokuyasu et al., 1972).

The mature sperms are coiled, so their massive length is gathered at the basal end of the testis, later mature sperms are transferred to the seminal vesicle where they are stored until copulation (Fabian and Brill, 2012). The cyst cells also elongate with the 64 spermatids after the meiotic stages and keep a tight contact with the developing germ cells (Demarco et al., 2014). The head cyst cell is required for the coiling process and the transfer of mature sperm to the seminal vesicle.

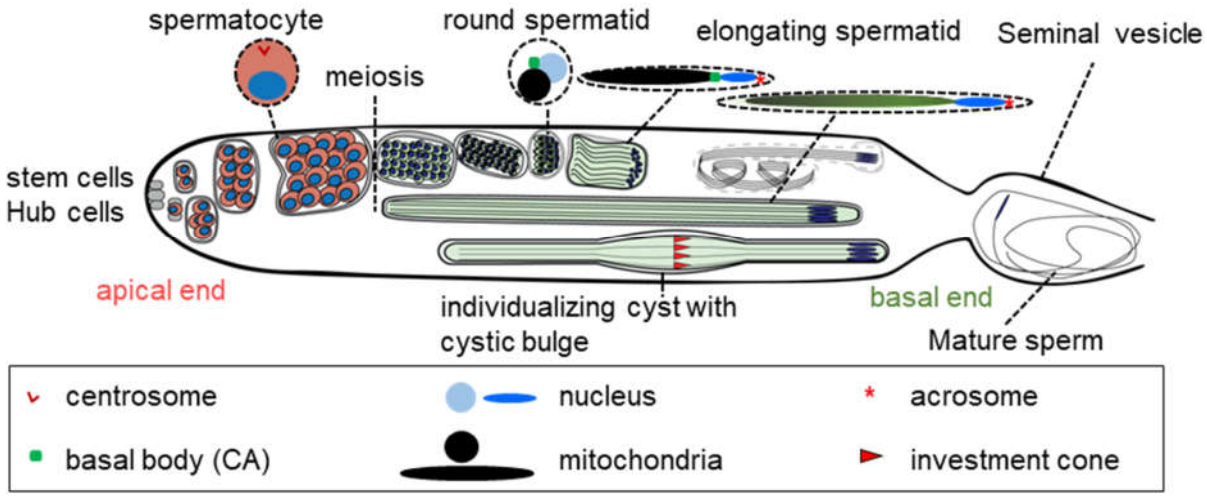

Figure 1. Graphical representation of *Drosophila melanogaster* testis with different stages of spermatogenesis. Hub cells are located at the most apical end of the testis (grey). The pre-meiotic stages contain the spermatocytes (2, 4, 8, 16 cells/cyst; red), meiotic and post-meiotic developmental stages (64 cells/cyst) are towards the basal end of the testis (green). Single cells from different stages are highlighted with dashed lines, with the indication of characteristic cellular organelles for the certain stage (centrosome, basal body, nucleus, mitochondria, acrosome, investment cone). The seminal vesicle with mature sperm is on the basal end of the testis.

1.1.3 Mitochondrial organization during spermatogenesis

Mitochondria are an essential energy supplier of the sperm. Mitochondrial morphogenesis is complex during spermato- and spermiogenesis. Mitochondria in spermatocytes are very similar to the somatic ones. Typical mitochondria are considered to be 3–4 μm in length and 1 μm in diameter. Mitochondrial dynamics, like fission and fusion play an important role in their morphology. Mitochondria can be transported alongside microtubules, and this dynamic is key to the undergoing fusion and fission processes. After meiosis in round spermatids, the individual mitochondria start to aggregate at one side of the nucleus and fuse, forming a structure called the

nebenkern (**Figure 1, 2**). The nebenkern is the size of the haploid nucleus and consists of two mitochondrial derivatives, wrapped around each other forming a structure which resembles an onion (Tokuyasu, 1975). When the 64 round spermatids start to elongate, the nebenkern unfurls and establishes two mitochondrial derivatives. The derivatives start to elongate and drive the elongation of the cyst as it enters first the leaf-blade and later the comet stage. Spermatid elongation is driven by the interdependent extension of giant mitochondria and the microtubule array that is formed around the mitochondrial surface. (Noguchi et al., 2011). During elongation, the two mitochondrial derivatives and the axoneme elongate simultaneously forming the tail of the spermatid (Tokuyasu, 1974a). Both mitochondrial derivatives run parallel with the axoneme, and their lengths are comparable. The initially similar mitochondrial derivatives start to differentiate by the end of elongation, when one of them accumulates paracrystalline material, while the other one loses its volume. Based on the cross-section analysis of the sperm tail, the size ratio between the axoneme and the mitochondria is generally 1:2 or 1:3. Both derivatives have close contact with ER-derived axial membrane along the entire length of the spermatid tail (Tokuyasu, 1974a; Laurinyecz et al., 2019).

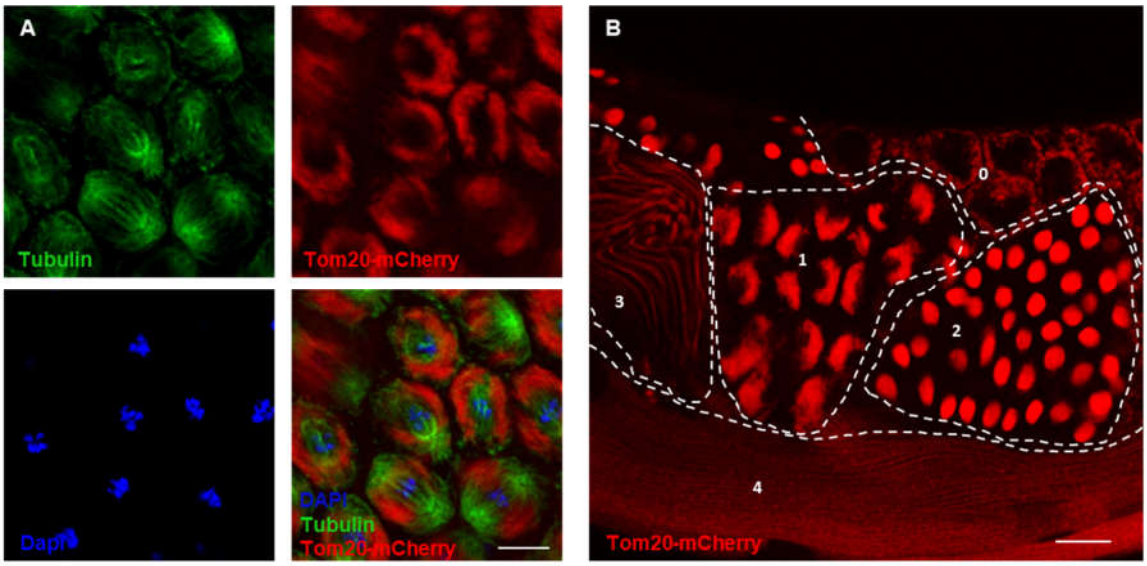

Figure 2. Mitochondrial distribution during spermatogenesis. A. Distribution of the mitochondria (Tom20-mCherry, red) and tubulin (anti-tubulin, green) in meiotic spermatocytes: the mitochondria are forming a barrel-shaped structure around the nuclear region, while tubulin shows the spindle and microtubules attached to the chromosomes. **B.** Mitochondria distribution (Tom20-mCherry) in mature spermatocytes (0), meiotic spermatocytes (1), in round spermatids (Nebenkern) (2), in elongating spermatids (3) and elongated spermatids (4). Scale bars: 20 µm.

The necessity of mitochondrial derivatives and the surrounding microtubule array for elongation was presented with mutants in mitochondria and microtubule-associated factors. Mutations which are causing abnormal nebenkern formation like a mutation in *fuzzy onions* or *no mitochondrial derivative* (*nmd)* results in reduced length of mitochondrial derivatives, as the tails fail to elongate to their full length (Noguchi et al., 2011). Mutations affecting the structural organization of the mitochondria in many cases lead to sterile males with aberrations in the sperm elongation and structure. Examples of such mutants are the testis-specific glutamate dehydrogenase big bubble 8 (*Bb8*) and *nmd,* which lead to elongation defects (Noguchi et al., 2011; Vedelek et al., 2016). It was already shown that the surface of spermatid mitochondrial derivative serves as a microtubule-organizing center (MTOC) (Noguchi et al., 2012). These MTOCs can promote the assembly of the microtubule array, which in turn makes the elongation of the derivatives possible. Despite we know some of the molecular components of these MTOCs they are not fully characterized (Noguchi et al., 2011; Chen et al., 2017).

1.1.4 Cytoskeletal elements during spermatogenesis

As discussed above the mitochondrial derivatives can serve as an MTOC; however, the canonical MTOCs, and the centrosomes also have an important role in cytoskeletal organization during spermatogenesis. The cellular structures and cytoskeletal elements are massively reorganized in most of the spermatogenic stages. Centrosomes are composed of two centrioles surrounded by an amorphous protein matrix called the pericentriolar material (PCM) (Kobayashi and Dynlacht, 2011). Spermatid differentiation is associated with extensive modifications of the centrioles as they transform into basal bodies. Before the spermatocyte growth phase, centrioles are 0.9 μm in length with a 9+1/0 microtubule structure, but upon the spermatocyte growth phase the centrioles grow in length reaching ~2.3 μm (Tates, 1971; Lattao et al., 2017). Development of the basal body starts in primary spermatocytes when centrioles nucleate cilium like region (CLR) on their distal end, protruding from the cell surface. During meiosis, the basal bodies with CLR are internalized with additional plasma membrane caps, and they move to the cell poles where they act as MTOC, nucleating the astral microtubules (MTs). After, centriole–CLR complexes are distributed for the spermatids, and the basal body emerge from the centriole–CLR complex, contributing to the axoneme organization (Lattao et al., 2017). By the end of the meiosis, each

spermatid basal body with CLR moves toward the nucleus, docks at the nuclear membrane, and starts to function as MTOC by nucleating the axoneme of the flagellum. While moving toward the nucleus, the basal body is attached to cytoplasmic MTs, forming the centriole adjuncts (CA) which contain mainly PCM proteins (eg. γ-tubulin, and Cp190) of the centrosomes and testis-specific proteins (eg. Mozart1) (Tates, 1971; Riparbelli et al., 1997; Fabian and Brill, 2012; Lattao et al., 2017; Tovey et al., 2018). Sperm axoneme is motile, with a pair of MTs at the center surrounded by nine outer MT doublets with dynein arms (Fabian and Brill, 2012; Lattao et al., 2017). During elongation, the axial membrane forms out of ER membranes and surrounds the axoneme. The distal end of the axoneme opposite to the basal body is surrounded by a ciliary membrane (Fabian and Brill, 2012). The ring centriole is a structure localizing at the axoneme end opposite to the basal body. The ring centriole anchors the ciliary membrane to the elongating axoneme (Fabian and Brill, 2012). Further known elements of the ring centriole are centrosomal proteins like Unc and Chibby (Cby). (Baker et al., 2004; Enjolras et al., 2012).

1.2 Microtubule organizing centres

The microtubule cytoskeleton plays a crucial role in eukaryotic cells by maintaining cell shape, movement, polarity, organelle positioning, intracellular transport, and facilitating chromosome movement and cytokinesis (Kollman et al., 2011). MTs are polar hollow cylinders composed of α- and β-tubulin heterodimers assemble in a GTP dependent manner, with a slow-growing minus-end with α-tubulin, anchored to the MTOC, and a fast-growing elongating plus end with an exposed β-tubulin (Liu et al., 2020). MT nucleation is the process of new MT filament formation, it can happen *de novo in vitro*; however, it is not stable and kinetically unfavorable (Wiese and Zheng, 2006). MT nucleation in cells is dependent on the conserved protein complex gamma-tubulin ring complex (γ-TuRC), which is one of the requirements to form stable MTOC. These molecular complexes are cellular structures that control MT nucleation, stabilization, and anchoring when there is a temporal or spatial need for them during cellular changes. MTOCs can be organized around the centrosome or independently from it, as non-centrosomal MT organizing centers (ncMTOCs) (Tillery et al., 2018).

Centrosomal MTOCs are the most studied and well-known form of MTOCs. Centrosomes are present in the majority of eukaryotic cells; however, metazoan female meiotic systems, centriole less spindle pole body containing fungi and vascular plants lack centrosomes (Megraw and

Kaufman, 2000; Wasteneys, 2002; Lengefeld and Barral, 2018). Centrosomes are membraneless organelles consisting of a pair of centrioles surrounded by the pericentriolar material (PCM). The centriole is a conserved structure and has typical nine-fold symmetry of MT blades, with ~ 0.2 µm diameter and 0.5 µm length. It can serve as the core of the centrosome or the basal body of ciliated cells (Kobayashi and Dynlacht, 2011; Lattao et al., 2017). Most interphase cells have one centrosome with one centriole, but before cell division, there is a centriole duplication. This duplication results in two centrioles, a mother, and a daughter centriole. The PCM is a protein-rich structural scaffold that surrounds the centrosome, where γ-tubulin and soluble proteins from the cytoplasm are being loaded (Fry et al., 2017). PCM functions in the nucleation and anchoring of MTs, facilitating the formation and the orientation of the spindles during cytokinesis. It plays a role in centriole duplication, and centrosome separation (Glover et al., 1995; Basto et al., 2006; Loncarek et al., 2008; Nigg and Stearns, 2011). Moreover, PCM also regulates and redistributes proteins through the association with MT plus-ends or transport by motor proteins (Zimmerman and Doxsey, 2000; Kumar and Wittmann, 2012). PCM proteins are involved in hedgehog signaling, cell cycle progression, DNA damage signaling, and protein degradation (Takada et al., 2003; Doxsey et al., 2005; Basto et al., 2007; Griffith et al., 2008; D'Angiolella et al., 2010; Atwood et al., 2013). The above-mentioned wide variety of functions is reflected in the structure of the PCM proteins as most of them have a long coiled-coil region which is known to play a role in protein-protein interactions. Protein components strictly define the structure and diameter of PCM and separate PCM into multiple layers by acting as molecular rulers (Woodruff et al., 2014). PCNT /Plp is an important protein for spindle organization, and it is one of the core PCM component proteins. Cep152/ Asl, CDK5RAP2/ Cnn/ Spd5, Cep192/ Spd2, and CPAP/ Sas4 are additional core PCM components, which are involved in PCM formation (Woodruff et al., 2014). During cell divisions, the PCM expands in size and increases its MT nucleation capacity to meet the elevated need for MT nucleation during spindle formation. PCM dynamics is controlled by the balance of phosphorylation and dephosphorylation reactions within the PCM proteins. Plk4 and Aurora A kinase are necessary for proper centrosome maturation and regulation of cell divisions. Protein phosphatase 4 and 2A are known for their role in regulating PCM dynamics (Helps et al., 1998; Giet et al., 2002; Santamaria et al., 2011).

Centriole structure and composition vary based on cell cycle stage and tissue type. After M phase the mother centriole assembles a new centriole (daughter) in G1-S phase, which elongates

in S-G2 stage. The centriole pair disengage after meiosis/mitosis and the daughter centriole becomes capable to duplicate or organize PCM (Nigg and Stearns, 2011; Woodruff et al., 2014). Drosophila embryos and cultured cells centriole have a cartwheel structure with double MTs, in contrast to male germ stem cells. The mother centriole cartwheel structure has triplets of MTs, while the daughter has a mix of doublets and triplets in male germ stem cells. The MT composition of the centriole varies between the mother and the daughter centrioles (Gottardo et al., 2015).

The core basal body components of the spermatids include Ana2, Sas6 and Cep135. Cep135 connects the core with the next layer of proteins, where Sas4 is present. Ana1, Asl, Spd2 and Unc all reside at the same layer as Sas4. The outer layer of centriole consists of Spd2, Plp, Cnn, and the pericentriolar material (**Figure 3**) (Fu et al., 2016; Lattao et al., 2017).

Many cells and tissues in Drosophila are centrosomeless or contain inactive centrosomes. In these cells, cellular structures serve as MTOCs as they become the ncMTOCs (Tillery et al., 2018). Interestingly zygotic development in Drosophila can efficiently proceed without centrosome as in the case of *sas4* mutant (Basto et al., 2006) or with dysfunctional centrosome as in the case of *cnn* mutant (Megraw et al., 2001). ncMTOC is believed to compensate for the loss of the centrosome in these cases. We know little about ncMTOC but based on our already expanding knowledge we can determine that they have diverse cellular localizations and compositions (**Figure 4**). ncMTOCs have a proven role in female meiosis, which occurs in the absence of the centrosome in *Caenorhabditis elegans*, Xenopus, Chicken, rodents, humans and Drosophila (Dumont and Desai, 2012). ncMTOCs function in a similar way to the centrosomal MTOCs, but they might have additional specialized functions as well (Tillery et al., 2018). To form ncMTOCs, the centrosome MTOC function should be attenuated, while simultaneously a location in the cell needs to be defined (Sanchez and Feldman, 2017).

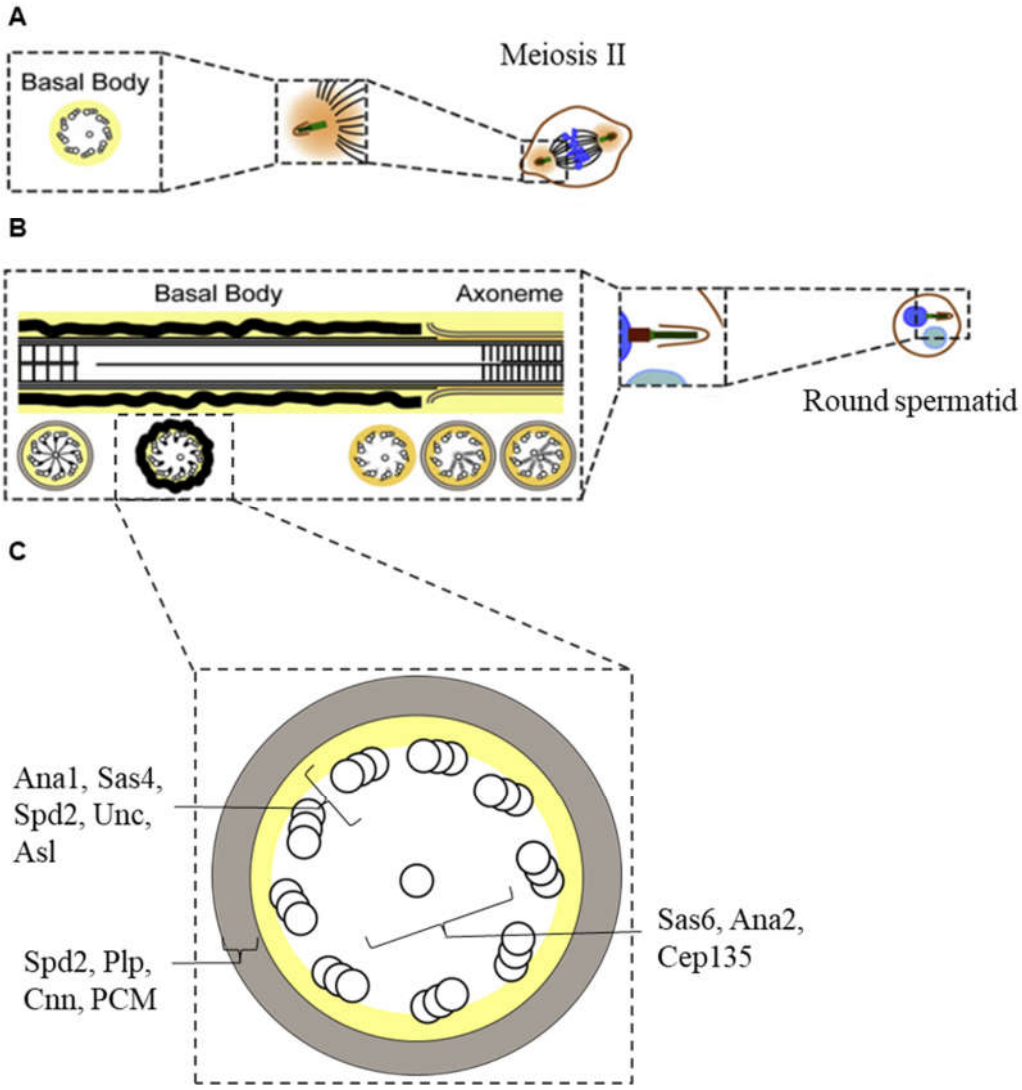

Figure 3. A schematic representation of the cross and the longitudinal section of the basal body in meiosis II (A) and round spermatid (B). C. Cross section of round spermatids basal body with the most important protein components. Based on Carvalho-Santos et al., 2012

During meiosis chromosomes serve as ncMTOC in Drosophila females. The kinesin-14 motor protein family Ncd transports Msps to the spindle poles, where the core centrosomal protein TACC anchors it to the spindle pole. Additionally the maternal isoform of γ-tubulin, γ-Tub37C might contribute to TACC recruitment to the spindle pole (Hughes et al., 2011; Dumont and Desai, 2012). In stage 10 of Drosophila oocyte development, Shot and Patronin organize an anterior cortical ncMTOC. These ncMTOCs are necessary for the development of the anterior-posterior and

dorsoventral axes for the future embryo (van Eeden and St Johnston, 1999; Nashchekin et al., 2016; Takács et al., 2017; Tillery et al., 2018).

Drosophila neuronal cells contain ncMTOCs at their dendrites. Cnn, Plp and γ-tubulin are all localized at these MTOCs; however, the exact mechanism behind these proteins connection and activity still to be investigated (Yalgin et al., 2015).

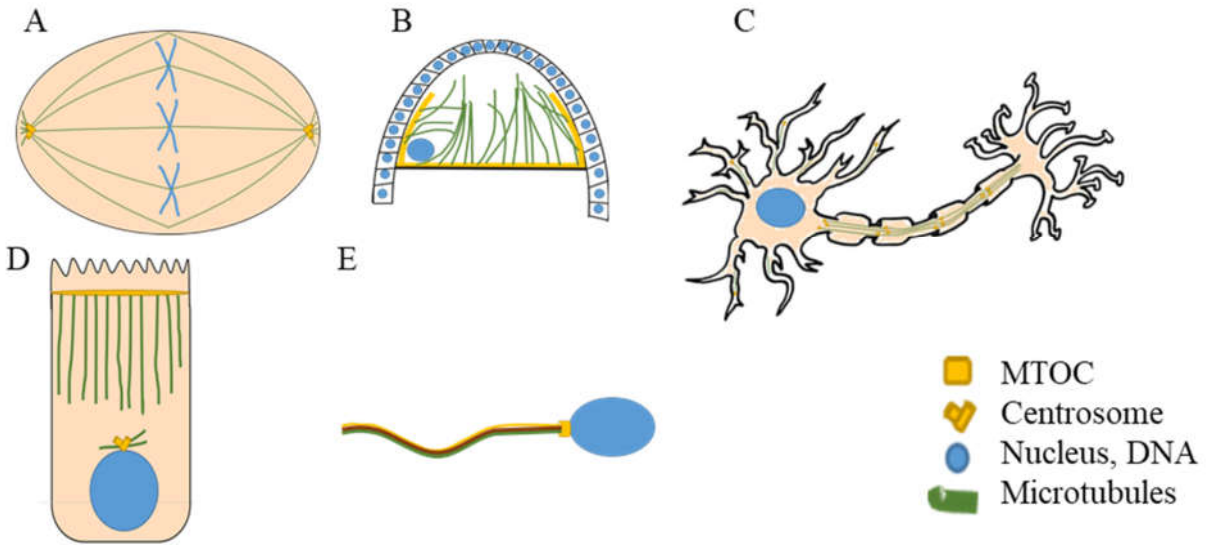

Figure 4. Organization of MTOCs in different Drosophila cell types. **A.** a dividing cell where the centrosome nucleate spindle MTs. **B.** stage 10 Drosophila oocyte with ncMTOCs at the anterior cortex. **C.** Neuron with dendritic ncMTOCs. **D.** Ovarian follicle cell with the centrosome and ncMTOCs **E.** Drosophila sperm the basal body and ncMTOC on the mitochondrial surface

1.3 Gamma tubulin ring complex

Gamma tubulin is a member of the tubulin superfamily sharing homology with α and β tubulins. γ-tubulin is highly conserved among eukaryotes. Human γ-tubulin can rescue the absence of the endogenous γ-tubulin, and restore the viability of *γ-tubulin* mutant in *Schizosaccharomyces pombe* (Wiese, 2008). γ-tubulin is known for its important role in stabilizing MT nucleation, it incorporates into multi-protein complexes within the cell. Proteins that form those complexes with γ-tubulin are gamma-ring complex proteins (Grips) or in human gamma-tubulin complex proteins (GCP). γ-tubulin small complex (γ-TuSC) is a heterotetrameric protein complex with a molecular weight of ~300 kDa, composed of γ-tubulin, GCP2 and GCP3 (γ-Tub23C, Grip84 and Grip91 in

Drosophila) (**Figure 5**). GCP2 and GCP3 are highly conserved. This conservation is proved by replacing the *S. pombe* GCP2 and GCP3 orthologues with their human and budding yeast orthologs (Riehlman et al., 2013).

The γ-TuSC incorporates into a larger complex, the γ-TuRC. In addition to multiple γ-TuSC, γ-TuRC contains additional three GCP proteins, GCP4, GCP5 and GCP6 (Grip75, Grip128 and Grip163 in Drosophila, respectively). γ-TuRC structure resembles a conical open left-handed spiral, with 14 spokes, each is a single GCP protein associated with γ-tubulin (**Figure 5**). Until recently, GCP4, GCP5 and GCP6 were considered to form a cap for γ-TuRC. It was proved in *X. laevis* that they are incorporated into the ring and replace some of GCP2 and GCP3 in γ-TuSC (Liu et al., 2021; Zupa et al., 2021). GCP 2, 3, 4, 5 and 6 have a similar structure, they all harbor N- and C- terminal GCP (Grip) motifs. It was shown that the GCP-N motif is responsible for the interactions between the neighboring GCP proteins, while the GCP-C motif binds to one γ-tubulin (Gunawardane et al., 2000, 2003; Moritz et al., 2000). GCP2 and GCP3 mutants are lethal in Drosophila, Aspergillus, and *S. pombe*. However, GCP 4, 5 and 6 mutants are viable in the same organisms. Some data suggests that GCP4, 5 and 6 may play a role in γ-TuRC incorporation into different types of MTOCs (Teixido-Travesa et al., 2012). GCP4 and GCP6 (Grip75 and Grip163 in Drosophila respectively) are required in the female and male germline cells of Drosophila, additionally, GCP6 (Grip163) plays a role in γ-TuRC localization to the keratin fibers in epithelial cells (Schnorrer et al., 2002; Vogt, 2006; Filigheddu et al., 2007).

The γ-TuRC might contain other proteins in addition to the related GCP2, 3, 4, 5 and 6, such as NEDD1/Grip71, NME7/nmdyn-D7, Mozart1 and 2 (Gunawardane et al., 2003; Bilitou et al., 2009; Hutchins et al., 2010). NEDD1/Grip71 is a γ-TuRC protein lacking the GCP domains but having an N-terminal WD40 domain which is involved in protein-protein interactions and its C-terminal domain is responsible for the interaction with γ-TuRC (Gunawardane et al., 2003; Lüders et al., 2006) (**Figure 5**).

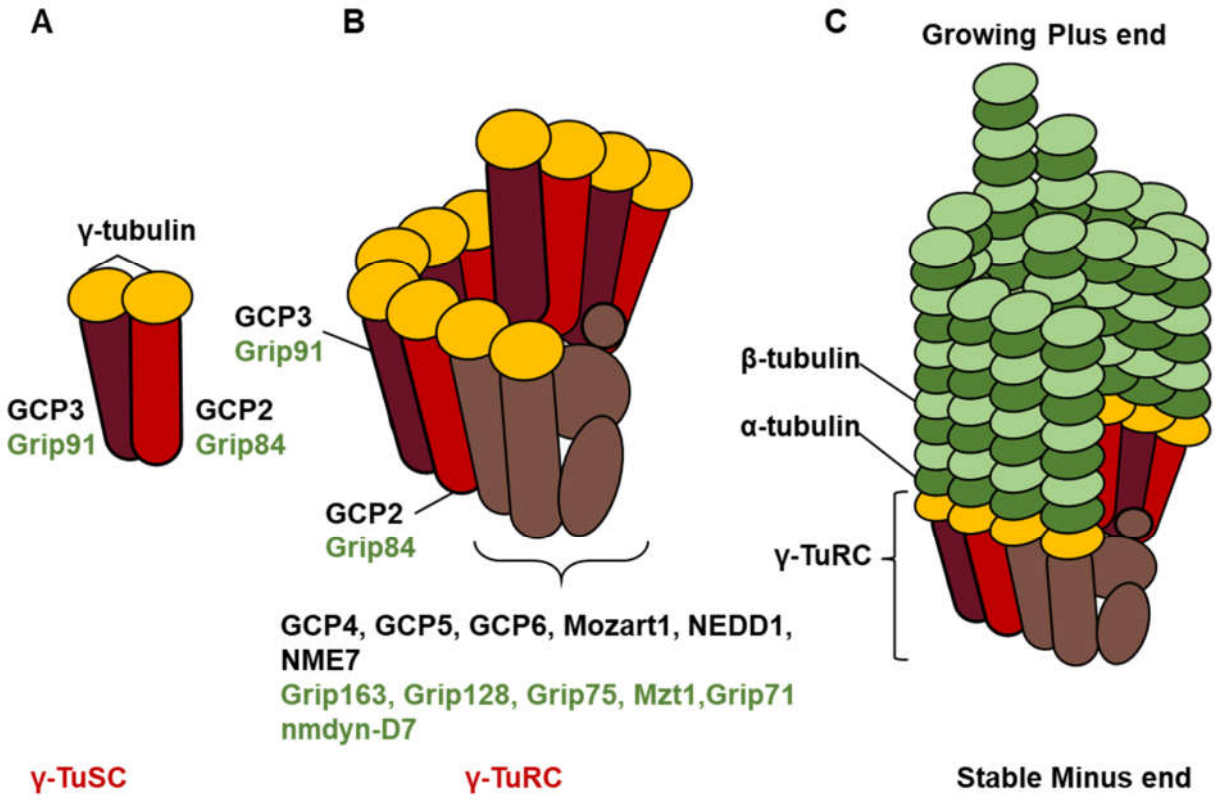

Figure 5. Graphical illustration of γ-TuSC, γ-TuRC and an active γ-TuRC. A. γ-TuSC is composed of two γ-Tubulins in addition to two gamma-tubulin complex proteins, GCP2, and GCP3 in human Grip84, and Grip91 in Drosophila. **B.** γ-TuRC structure, composed of multiple γ-TuSC in addition to other gamma-tubulin complex proteins, and gamma-tubulin complex interacting proteins. **C.** γ-TuRC while nucleating and stabilizing growing MTs, where it is attached to the γ-TuRC through its stable minus end.

In Drosophila γ-TuRC is composed of γ-tubulin, Grip84, Grip91, Grip128, Grip75, Grip163 and Grip71 (Gunawardane et al., 2000). Grip84 and Grip91 with γ-tubulin form the γ-TuSC, the core of the ring complex (Oegema et al., 1999) (**Figure 5**). Mutants of the γ-TuSC proteins, Grip84 and Grip91 are lethal, with defects in the spindle assembly (Barbosa et al., 2000; Colombié et al.,

2006; Vogt, 2006). Grip75 and Grip128 mutants are viable with defects in both male and female germ cell development (Vogt, 2006).

In order to nucleate MTs, multiple γ-TuSCs assemble with additional γ-TuRC or γ-TuRC-interacting proteins to form active γ-TuRC. There are two ways how the complex can assemble: it could happen either in the cytosol or at the MTOCs. The type of assembly is variable among organisms. γ-TuRC assembles in the cytosol in human, Drosophila and Xenopus, on the other hand in *S. pombe* it assembles at the MTOC (Zhang et al., 2000; Anders et al., 2006; Farache et al., 2016; Cota et al., 2017). The orthologs of this complex are the basic units where α-β tubulin polymerization starts, forming MTs in vertebrates. Minus end of the growing MTs is mainly anchored to and capped by the γ-TuRC, the growth of the MT happens at the plus end (**Figure 5**) (Oakley et al., 1990). During nucleation of MTs, α and β-tubulin molecules join to form a heterodimer. Multiple heterodimers together are resulting in protofilaments. 3 laterally connected protofilaments are required to establish a stable association with γ-TuRC. Protofilaments bind strongly to the γ-TuRC through the interactions of α-tubulin to the γ-tubulin of the γ-TuRC (**Figure 5**). 13 protofilaments form the wall of the MT hollow cylinder (Roostalu and Surrey, 2017; Tovey and Conduit, 2018).

A recent study shows ncMTOC-specific recruiter protein for the γ-TuRC during Drosophila spermatogenesis. The testis-specific splice variant of centrosomin protein, contains an N-terminal CM1 domain, a γ-TuRC recruitment domain and a C-terminal mitochondrial targeting domain. The N-terminal CM1 domain of CnnT recruits γ-TuRC to the mitochondria and the C-terminal domain is suggested to stabilize the mitochondrial binding and converts the mitochondria to ncMTOC (Chen et al., 2017). It was also found recently that the conserved γ-TuRC interacting protein, Mzt1 also accumulates in the male germline, and localizes to the centrosome and basal body of the developing spermatids during spermatogenesis (Tovey et al., 2018). Mzt1 is considered to bind the N-terminal of GCP proteins (Zupa et al., 2021). Mzt1 was found to interact with the N-terminal regions of Grip91 and Grip128 in Drosophila; however, the precise molecular function and localization pattern was not tested rigorously (Tovey et al., 2018).

1.4 Gene duplication and retrogenes

Gene duplication is a fundamental process which leads to the evolvement of new genes and functions resulting in biological diversity. Retrogenes are intronless copies of genes originated by

reverse transcription of the mRNA of the original genes, which then integrate into the genome (Bai et al., 2007). Retrogenes can acquire additional exons from the insertion site, increasing the level of complexity of the original gene product. It was shown that many retrogenes gain testis-specific function in primates and Drosophila, contributing to the complex regulation and cellular reorganization during spermatogenesis (Díaz-Castillo and Ranz, 2012).

The retrogenes often result in sex and tissue-specific genes. Many of the testis-specific retrogenes have evolved from genes located on the X chromosome, which is beneficial because they escape the X chromosome inactivation during spermatogenesis (Díaz-Castillo and Ranz, 2012). Testis-specific gene duplication is highly prevalent in cytoskeletal elements, mitochondrial metabolic enzymes and proteasome subunits (Díaz-Castillo and Ranz, 2012; Vedelek et al., 2018). In our group, we previously studied mitochondrial enzymes which have a retrogene origin, the sperm leucyl aminopeptidase (S-Lap) gene family. It was shown that S-Lap proteins lost their enzymatic activity and turn out to be the major component of the paracrystalline material of the major mitochondrial derivative of the sperm (Laurinyecz et al., 2019). The mitochondrial glutamate dehydrogenase enzyme Bb8 is necessary for the proper development of mitochondrial derivatives of the sperm and it was shown to be part of the paracrystalline material. (Vedelek et al., 2016, 2018; Laurinyecz et al., 2019).

Based on FlyBase data of paralogous genes, Grip genes could have served as a template for retrogenes multiple times. We identified 3 genes (*CG7716*, *CG18109* and *CG32232*) with no introns in their coding sequence, and with testis enriched expression (Vedelek 2018). These genes testis enriched expression raises the possibility of their function during spermatogenesis and the existence of a testis-specific γ-TuRC.

2 Aims

Drosophila melanogaster is a good model to study various biological processes, due to the wide variety of available classical and molecular genetic tools. Drosophila spermatogenesis is a suitable model to study basic cellular processes, such as MT organization. It was shown recently that besides the known classical MTOC, such as centrosome and basal body there are alternative ones on the surface of the mitochondria of the developing spermatids.

Our general aim was to explore the molecular components, and function of the different MTOCs during spermatogenesis by studying the predicted testis-specific γ-TuRC members and interacting partners.

Specific aims:

- We aimed to characterize genetically the predicted testis-specific paralogous of the γ-TuRC proteins, t-Grip84, t-Grip91 and t-Grip128, by describing the phenotype of their classical mutants.
- We wanted to describe the subcellular localization of t-Grip84, t-Grip91 and t-Grip128 and also the precise localization of Mzt1, the testis-specific γ-TuRC associated protein.
- Our goal was to identify the molecular composition and interacting partners of the predicted testis-specific γ-TuRC (t-γ-TuRC).

3 Materials and methods

3.1 Fly stocks, mutants, and fertility test

Flies were maintained under standard laboratory conditions on cornmeal agar medium at 25˚C or 18˚C. GFP-PACT line was obtained from Jordan Raff's and Tom20-mCherry from Hong Xu's laboratory (Martinez-Campos et al., 2004) (Zhang et al., 2016). w^{1118} used as wild type (WT) (3605). *Mi{MIC}CG7716*^{MI12921} (58006), *Mi{ET1}CG7716*^{MB07394} (26394), *Df(3L)BSC375*, (24399), *Mi{MIC}CG18109*^{MI05374} (42318) and *Df(2L)osp29* (3078) mutant stocks were obtained from Bloomington Drosophila Stock Center.

To generate *t-Grip128*$^{\Delta 65}$ null mutant alleles, two small guided RNA (sgRNAs) **(Supplementary Table 1)** were cloned into the pCFD4 vector (Addgene #49411) at the BbsI site and stable transgenic lines were established as described in Port et al. (**Figure 6**) (Port et al., 2014) (Galletta et al., 2020).

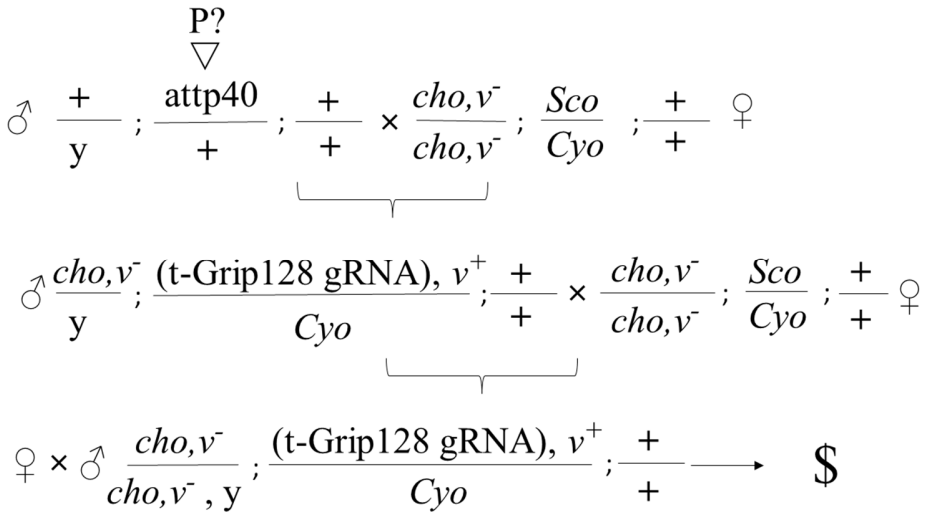

Figure 6. Crossing scheme to establish *t-Grip128 gRNA* stable fly line

The *t-Grip128* gRNA lines were crossed with the Cas9 source line, y1 M{nos-Cas9.P}ZH-2A w- (BDSC 54591) to generate deletions in the *t-Grip128* gene (**Figure 7**). The deletions were screened by amplifying the chromosomal region around *t-Grip128.* From 73 potential candidates, *t-Grip128*$^{\Delta 65}$ stable line was sequenced and chosen for further analysis.

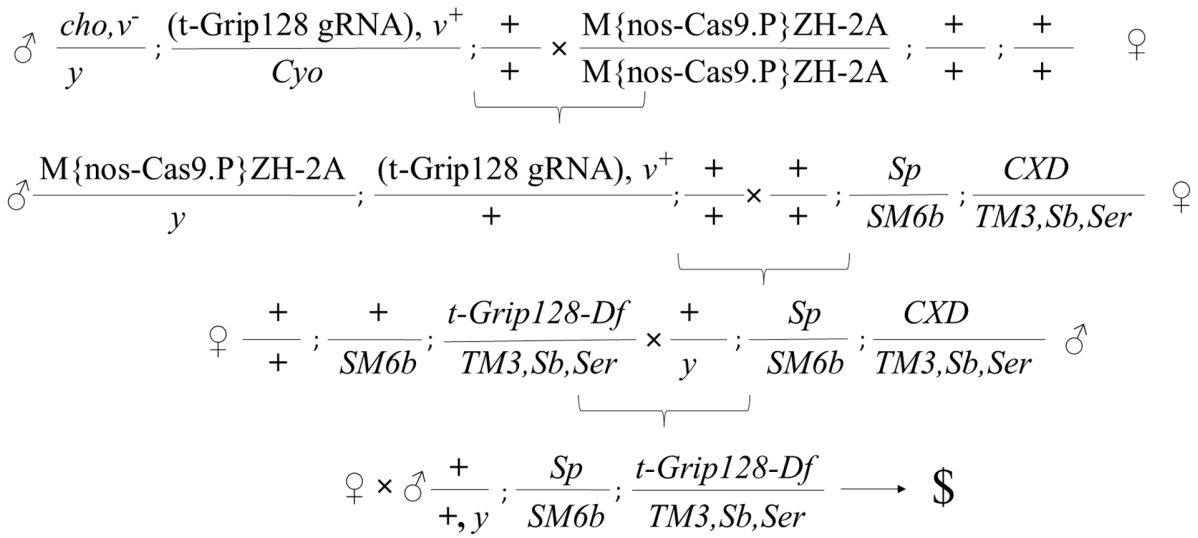

Figure 7. Crossing scheme used for establishing t-Grip128 deletion.

To establish transgenic lines, plasmids containing HA-t-Grip91, HA-t-Grip128, t-Grip84-GFP, t-Grip84-mCh and GFP-Mzt1 were injected into *P{CaryP}attP40* (BDSC 25709) and *P{CaryP}attP2* (BDSC 8622) fly lines (**Supplementary Figure 1**). All transgenic constructs were injected into embryos by the injection facility of ELKH-BRC, Szeged.

For fertility tests, individual males were crossed with three w^{1118} virgin females. 14 days after crossing, the hatched progeny was counted in every tube. The effect of ageing on $t\text{-}Grip128^{\Delta 65}$ fertility was tested by crossing individual males with three w^{1118} virgin females and 7 days later the same males have been crossed again with three w^{1118} virgin females. We repeated this procedure 7 days later. Hatched progeny was counted 14 days after each cross. Fertility tests were repeated independently 4 times, with >10 individual males in each experiment.

3.2 DNA constructs

cDNA of Mzt1, γ-Tub23C were obtained from the Drosophila Golden collection (DGRC) (https://dgrc.bio.indiana.edu/Home). Primer design for the Gibson assembly was done by NEBuilder Assembly Tools (NEB) (https://nebuilder.neb.com). The quantity and quality of DNA were evaluated using Nanodrop 2000c (ThermoFisher Scientific). Primers used for cloning are

listed in **Supplementary Table 1**. HA-t-Grip91, HA-t-Grip128, t-Grip84-mCh, t-Grip84-GFP, γ-Tub23C-GFP and GFP-Mzt1 constructs were made by amplifying the 5' upstream regions (970bp of *t-Grip91*, 2213bp of *t-Grip128*, 2134bp of *t-Grip84*, 1084 of *γ-Tub23C* and 1581bp of *Mzt1*) and the full-length coding sequences of t-γ-TuRC proteins from genomic DNA. Mzt1 and γ-Tub23C CDSs were amplified from the DGRC cDNAs. Phusion DNA polymerase (NEB) was used in all amplification. PCR products were purified using GeneJET PCR Purification Kit (ThermoFisher Scientific) according to the manufacturer's instructions. The amplicons were assembled into pUASTattB-mCherry, pUASTattB-GFP or pUASTattB-3xHA vectors with the Gibson assembly method using HiFi DNA Assembly Master Mix (NEB) according to the manufacturer's protocols. The assembled constructs were transformed into chemically competent 2T1 *Escherichia coli* cells. We tested the transformants by CloneChecker System (ThermoFisher Scientific) or by colony PCR (Bergkessel and Guthrie, 2013), and the plasmid DNA was purified from the positive clones using GeneJET plasmid miniprep kit (ThermoFisher Scientific). Positive clones were sequenced and construct of t-Grip84-mCh, t-Grip84-GFP, HA-t-Grip91, HA-t-Grip128 and GFP-Mzt1 were purified for injection using HiSpeed Plasmid Midi Kit (QIAGEN) according to the manufacturer's instructions. The purified plasmid DNAs were diluted in injection buffer (Sullivan et al., 2000) and injected into the appropriate genotype of embryos.

t-Grip84-GFP for tissue culture experiment, N- and C-terminal t-Grip91, N- and C-terminal t-Grip84, N- and C-terminal t-Grip128 for the GST tagged bait used in the IVTT (*in vitro* transcription and translation) experiment, were made by amplifying the CDSs from genomic DNA with Phusion DNA polymerase (NEB). After purification, the amplified fragments were cloned into pENTR1A (Addgene #17398) in the case of full length, N- and C-terminal t-Grip84 constructs using the enzymes EcoRI and NotI, and pENTR3C (Addgene #97408) in the case of N- and C-terminal t-Grip91 and t-Grip128 using the enzymes KpnI and NotI. The positive clones were sequenced and the clones with the correct sequences were recombined into pAWG (DGRC #1072) Gateway destination vector to establish t-Grip84-GFP and GST-Dest15 for establishing GST-N- and C- terminal t-Grip84, t-Grip91 and t-Grip128. For the LR reaction, we mixed 150 ng from the sequenced construct of pENTR1A full length t-Grip84 with 150 ng destination vector (pAWG), and 150 ng from the sequenced constructs of pENTR3C (N- and C- terminal t-Grip84, t-Grip91 and t-Grip128) with 150 ng destination vector (GST-Dest15), with 2 µl LR Clonase in 10 µl TE

buffer. 1 µl of each reaction was transformed into chemically competent 2T1 *E. coli* cells. Positive colonies were purified using plasmid miniprep kit (ThermoFisher Scientific Scientific).
For yeast two-hybrid analysis we used fragments of each t-γ-TuRC protein, t-Grip84-N: 1-1197 bp, t-Grip84-C 1198-2187 bp; t-Grip128-N: 1-1647 bp, t-Grip128-C 1648-2928 bp and full-length Mzt1. We cloned them into pGAD424 by Gibson Assembly using HiFi DNA Assembly Master Mix (NEB) according to the manufacturer's protocol. t-Grip91-N 1-2898 bp; t-Grip91-C 2899-5796 bp were cloned into pGBT9 and the full-length γ-Tubulin23C were cloned into pGAD424 and pGBT9 using Gibson Assembly using HiFi DNA Assembly Master Mix (NEB) according to the manufacture's protocol. We used SmaI restriction digested and purified pGAD424 and pGBT9 plasmids in the Gibson Assembly reactions according to the manufacturer's instructions. Colonies were checked using clone checker system, and positive colonies were confirmed by sequencing.

IVTT preys, the N-terminal and C-terminal parts of t-Grip84, t-Grip91 and t-Grip128 in addition to the full length Mzt1 and γ-Tubulin23C were made by amplifying the cDNA sequences using Phusion DNA polymerase (NEB). After purification, the PCR products were cloned into pJET1.2 vector using blunt-end cloning (ThermoFisher Scientific) downstream of the T7 promoter. Plasmids were transformed into chemically competent *E. coli*, after checking positive colonies were confirmed by sequencing.

3.3 Tissue Culture

Dmel2 Drosophila tissue culture cells (Life Technologies) were grown at 25°C in Insectagro DS2 serum-free medium (Corning) supplemented with 2 mM L-glutamine (Biosera) and penicillin-streptomycin (100 I.U./mL penicillin and 25 (µg/mL) streptomycin) (Gibco). Cells were transiently transfected using Lipofectamine 2000 transfection reagent (ThermoFisher Scientific). First, the cells were plated in 24 well plates on the surface of the coverslip in a 500 µl medium and grow until cells reach 70% confluency. 500 ng DNA was diluted in 50 µl opti-MEM media and mixed with 4 µl Lipofectamine 2000 transfection reagent diluted in 50 µl opti-MEM media. The transfection mix was incubated for 10 minutes at room temperature and then added to the cells. Cells were tested after ~19 hours by immunostaining.

3.4 Immunostaining and microscopy

Preparation and staining of testes were performed as described by White-Cooper et. al (White-Cooper, 2004). Briefly, testes were dissected in testis buffer (15 mM Potassium Phosphate Buffer (pH 6,7), 80 mM KCl, 16 mM NaCl, 5 mM MgCl2, 1% PEG 6000) on ice. Samples were fixed for 20 minutes at room temperature in freshly prepared 4% formaldehyde in fixative buffer (PBS, 137mM NaCl, 2.7mM KCl, 10Mm $NaHPO_4$, 2mM KH_2PO_4 pH 7.4). After fixation testes were washed and permeabilized 3 times with PBSTX buffer (1x PBS, 0.1% Tween-20, and 0.3% Triton-X100) for 20 minutes each. 1% BSA in PBSTX (PBSTXB) was used to block the samples for 60 minutes. Primary antibodies were diluted in PBSTXB, added to the samples and incubated overnight at 4°C. Primary antibodies were removed and samples were washed 3 times with PBSTX buffer for 20 minutes each (**Table 1**). Secondary antibodies were diluted in PBSTXB solution and samples were incubated in it for 2 hours at room temperature (**Table 1**). Testes were washed 3 times in PBSTX, stained with DAPI (1 µg/ml) (if needed) and mounted with SlowFade Gold antifade reagent (Life Technologies). Images were taken using Olympus BX51 fluorescent microscope or Olympus Fluoview Fv10i Confocal microscope.

Tissue culture cells were fixed at room temperature for 10 minutes in 4% formaldehyde in PBS. They were washed twice for 10 minutes with PBS. Cells were blocked by PBSTB (PBS, 0.1% triton, 1%BSA) for 1-hour, and the diluted primary antibodies (in PBSTB) were added to them and incubated overnight at 4˚C. Cells were washed 3 times with PBSTB (5 minutes each). Secondary antibodies were diluted in PBSTB, and cells were incubated for 2 hours at room temperature. Samples were washed twice with PBSTB and stained with DAPI (1µg/ml) and mounted (**Table 1**).

Antibody /Dye	Dilution	Source	Identifier
Anti-HA (Rat monoclonal)	1:100	Sigma-Aldrich/Roche	Cat# 11867423001
anti-cleaved-Caspase3 (rabbit monoclonal)	1:200	Cell Signalling	Cat# 9664
anti-pan polyglycylated Tubulin (mouse monoclonal)	1:5000	Sigma-Aldrich/Merck	Cat# MABS276
anti-γ-Tubulin (mouse monoclonal)	1:5000	Sigma-Aldrich/Merck	Cat# T6557
anti-Ana1 (rabbit)	1:5000	(Fu et al., 2016)	-
anti-Asl (rabbit)	1:1000	(Fu et al., 2016)	-
anti-Grip163 (rabbit)	1:1000	(Vérollet et al., 2006)	-
Mouse Alexa Fluor 488 secondary	1:400	ThermoFisher	Cat# A-11029
Mouse Alexa Fluor 546 secondary	1:400	ThermoFisher	Cat# A-11030
Mouse Alexa Fluor 633 secondary	1:400	ThermoFisher	Cat# A-21052
Rat Alexa Fluor 488 secondary	1:400	ThermoFisher	Cat# A-21208
Rat Alexa Fluor 568 secondary	1:400	ThermoFisher	Cat# A-11081
Rabbit Alexa Fluor 488 secondary	1:400	ThermoFisher	Cat# A-11008
Rabbit Alexa Fluor 546 secondary	1:400	ThermoFisher	Cat# A-11010
MitoTracker Red CMXRos	0,5 μM	ThermoFisher	Cat#M7512
Hoechst 33342	1:500 (16.2mM)	ThermoFisher	Cat#H3570
4',6-Diamidino-2-Phenylindole, Dihydrochloride (DAPI)	1 μg/ml	ThermoFisher	Cat#D1306

Table1. Summary of the antibodies and fluorescent dyes with the used dilution.

3.5 Transmission Electron microscopy

Transmission Electron microscopy was done like described in Laurinyecz et al. 2016 (Laurinyecz et al., 2016)

3.6 Yeast two Hybrid system

Yeast two Hybrid (Y2H) assays were carried out using the Matchmaker two-hybrid system (Clontech, USA). The baits pGBT9 with the appropriate fragment of DNAs were cotransformed with the preys containing investigated DNAs-pGAD424 vector into PJ69-4A yeast cells (**Figure 33**). One colony of PJ69-4A yeast grow in 3 ml YPDA media at 30˚C with 250 RPM shaking overnight. From the starter culture 1 ml was transferred into 50ml YPDA media and grow at 30˚C by 250 RPM shaking, until OD 0,5-0,6. Yeast cells were centrifuged for 3 minutes at 450 g at 4˚C. Cells were washed in 10 ml sterile H_2O and centrifuged again for 3 minutes. Cells were resuspended in 900 µl H_2O+100 µl 1M Lithium Acetate (LiAc). After yeast cells were incubated at 30˚C for 1 hour with 150 rpm shaking. 80 µl salmon sperm DNA (ssDNA) was heat-inactivated by incubating for 10 minutes at 99˚C, then cooled on ice for another 10 minutes. 80 µl ssDNA was added to the yeast cells, (100 µl yeast-ssDNA mix used per transformation) followed by adding 200 ng DNA constructs (mixture of bait and prey) to each transformation. Yeast cells and DNA mixture was vortexed and then incubated for 30 minutes with gently shacking (150 rpm) at 30˚C. Fresh LiAc-PEG solution prepared by mixing 1:10 1M LiAc:40%PEG. 700 µl LiAc-PEG was added to each transformation reaction and vortexed for 2 seconds and incubated for 1 hour at 30˚C with 150 rpm shaking. After the incubation yeast cells were heat-shocked at 42˚C for 15 minutes and centrifuged at 14500 g for 1 minute at room temperature. The supernatant was removed, and the cells were resuspended in 300 µl H_2O, and spread on selective plates. Cells were grown at 30˚C for 2-3 days on selective plates (-Leu, -Trp). Individual colonies were streaked out on yeast synthetic double drop-out plates lacking tryptophan and leucine.

To test the prey and bait interaction, an overnight culture was diluted in TE buffer (10x, 100x, 1000x). Cells were plated on the double (-Leu, -Trp), triple (-Leu, -Trp, -His) and quadruple (-Leu, -Trp, -His, -Ade) dropout plates (Sigma) and containing 10mM 3-amino-1, 2, 4-aminotrizole (3-AT, Sigma). We documented the growth of the yeast after 4 days at 30°C.

3.7 *In vitro* coupled transcription–translation (IVTT)

In vitro coupled transcription–translation (IVTT) was done as described in Karman at al. 2020 (Karman et al., 2020).

3.8 RNA extraction cDNA synthesis and Quantitative RT-PCR

Total RNA was purified from 25 pairs of testis, for *t-Grip84*^{ms}, *t-Grip91*^{ms} and WT using the Quick-RNA MiniPrep kit (Zymo Research). Briefly, testes were dissected in testis buffer on ice, testis buffer was removed, and samples were frozen in liquid nitrogen. 100 µl RNA Lysis Buffer was added to the samples then homogenized with a plastic pestle and lysed tissues were centrifuged for 30 seconds at 13500 rpm at room temperature. The supernatant was transferred to a spin-away filter and centrifuged for a further 30 seconds at 13500 rpm at room temperature. 100 µl 96% ethanol was added to the flow-through and mixed well by pipetting. The mixture was transferred to Zymo-spin IIICG column centrifuged and the flow-through was discarded. 400 µl RNA wash buffer was added and centrifuged again and the flow-through was discarded. A freshly prepared mixture of 5 µl DNase1 and 75 µl DNA digestion buffer was added to the column and incubated at room temperature for 30 minutes, then centrifuged and the flow-through was discarded. 400 µl RNA Prep buffer was added to the samples and after a spin, the flow-through was discarded. The column was washed with 700 µl RNA wash buffer and the washing was repeated by using 400 µl RNA wash buffer. The column was transferred to an RNase free tube and 30µl RNase-DNase free water was added to the column and centrifuged. RNA concentration was measured by Nanodrop 2000c (Thermo Scientific). For the first-strand cDNA synthesis, RevertAid First Strand cDNA Synthesis Kit (ThermoFisher Scientific) was used. 500 ng total RNA was diluted in 11 µl RNase-DNase free H_2O and mixed with: 1 µl Random Hexamer primer, 4 µl 5X reaction buffer, 1 µl Ribolock RNase inhibitor, 2 µl 10Mm dNTP, 1 µl RevertAid M-MulV RT. The mixture was vortexed and centrifuged briefly, then incubated at 25˚C for 5 minutes, 42˚C for 60 minutes and 70˚C for 5 minutes to terminate the reaction.

Maxima SYBR Green/ROX qPCR Master Mix (ThermoFisher Scientific) was used for the real-time quantitative PCR reaction, according to the manufacturer's instructions. Reactions were run 3 times in triplicates in the Rotor-Gene Q Real-Time PCR Detection System (QIAGEN) with the following reaction conditions: 95°C for 10 minutes, 50 cycles of 95°C for 15 seconds, 54°C

for 30 seconds, 72°C for 30 seconds. Gene-specific and rp49 specific primers were used are listed in **Supplementary Table 1.**

3.9 Quantification and statistical analysis

Testis specificity index was calculated as described by Vedelek et. al 2018 (Vedelek et al., 2018). Data analysis and graph production was done using Origin 9.0 (OriginLab Corporation, Northampton, MA, USA). One-way ANOVA followed by Tukey's HSD test was used to comparisons between WT and the indicated mutants.

4 Results

4.1 Identification of testis-specific γ-TuRC proteins

Analysis of transcript enrichment in different regions of the Drosophila testis (apical, middle, basal) revealed region-specific enrichment of gene families (Vedelek et al., 2018). This analysis identified basal transcript accumulation of several cytoskeletal components, including several dynein, kinesin, and tubulin genes. Detailed analysis of the transcript accumulation of the γ-TuRC revealed that the six complex members (Grip84, Grip91, Grip128, Grip163, Grip75 and Grip71) are all expressed in testis; however, their transcript accumulation is mainly restricted to the apical end of the testis. Based on the gene family search, we identified 3 uncharacterized paralogue genes of three γ-TuRC members. We named them *t-Grip84 (CG7716), t-Grip91 (CG18109),* and *t-Grip128 (CG32232)* relying on sequence similarities.

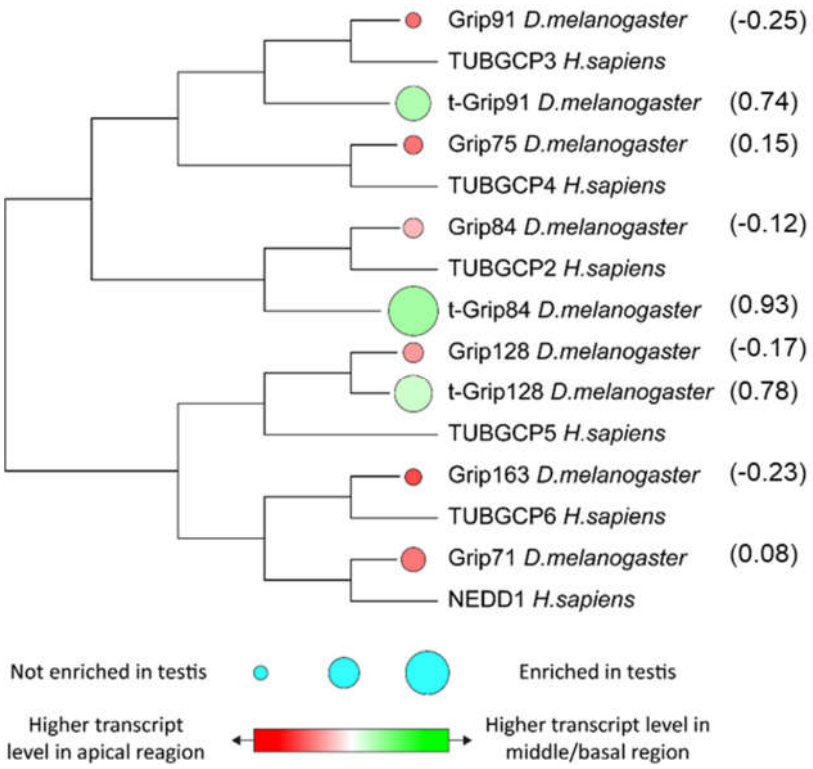

Figure 8. The phylogenetic relationships between human and Drosophila γ-TuRC genes. The Drosophila γ-TuRC transcript accumulation pattern is labelled by colors from red to green according to the transcript accumulation changes from the apical to the middle and the basal parts

of the testis. Testis enrichment is symbolized by the size of the circle in front of the gene name. Testis-specificity indexes of Drosophila γ-TuRC and t-γ-TuRC members are in the brackets.

Tissue specificity of the t-γ-TuRC transcripts was calculated, and we found that the ubiquitously expressed γ-TuRC members have a relatively low testis-specificity index; however, the newly described t-γ-TuRC members show a high testis specificity index (Vedelek et al., 2018). Their transcript accumulation is abundant in the middle and basal regions of the testis (**Figure 8**) (Vedelek et al., 2018). Based on transcript localization and tissue specificity of the t-γ-TuRC members, we expect that these proteins contribute to the post-meiotic development of spermatids. We compared the ubiquitous and the testis-specific γ-TuRC proteins by multiple protein sequence alignment and predicted the conserved GCP-N and GCP-C domains (**Supplementary Figure 2**). All ubiquitous γ-TuRC proteins contain GCP-N and GCP-C domains; however, only t-Grip84 contains both potential GCP domains and t-Grip91 and t-Grip128 only have a predicted GCP-N one (**Figure 9**). These domains were shown to be responsible for γ-tubulin and Grip to Grip binding *in vitro* in the case of γ-TuRC (Farache et al., 2016). t-Grip91 N-terminal part contains a long coiled-coil region, which could be responsible for the protein-protein interaction, nevertheless, further experiments are necessary to determine the precise function of these domains in the case of the individual t-γ-TuRC proteins.

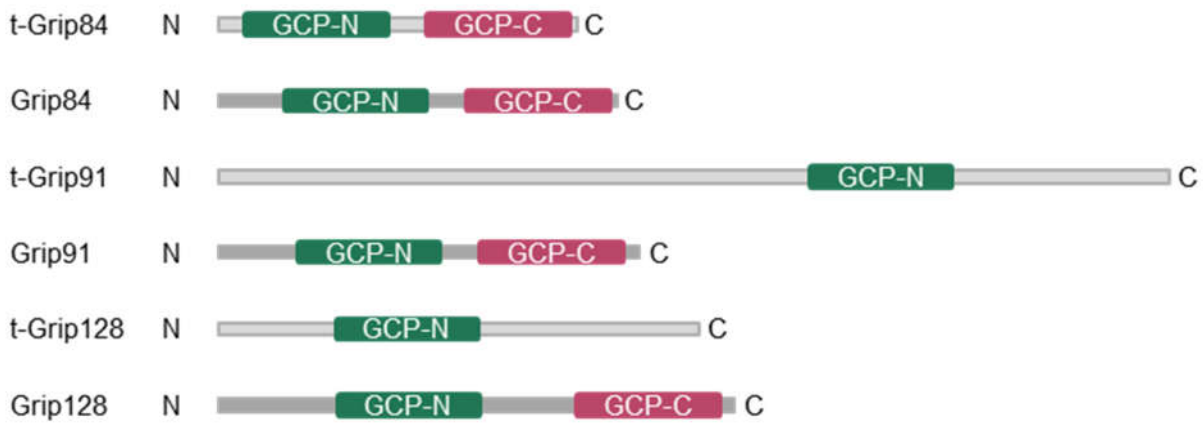

Figure 9. Gene structure and predicted domains of Drosophila ubiquitous and testis-specific γ-TuRC proteins. Drosophila ubiquitous Grip proteins have the typical structure of γ-TuRC proteins with GCP-N and GCP-C domains. Testis-specific Grip proteins all have a GCP-N domain and only t-Grip84 has the GCP-C domain.

4.2 Genetic characterization of the t-γ-TuRC members

We decided to genetically characterize the t-γ-TuRC genes. *t-Grip84* and *t-Grip128* are located on the 3rd (3L:7,588,608..7,590,998 and 3L:4,993,950..4,996,877) and *t-Grip91* on the 2nd chromosome (2L:15,784,085..15,790,146). ubiquitous paralogues of t-γ-TuRC genes, *Grip84*, *Grip91* and *Grip128* contain multiple exons with one transcript for Grip91 and Grip128 and 5 different transcripts for Grip84 (**Figure 10A**). In contrast, the t-γ-TuRC genes all have a similar gene structure that is typical for retrogenes (Bai et al., 2007). All three t-γ-TuRC genes are intronless, whereas *t-Grip84* and *t-Grip91* contain only a very short 5' and 3' untranslated regions and a long coding region. According to the Flybase data, there are no predicted 5' and 3' UTR regions of *t-Grip128*, only consisting of one long exon (**Figure 10B**).

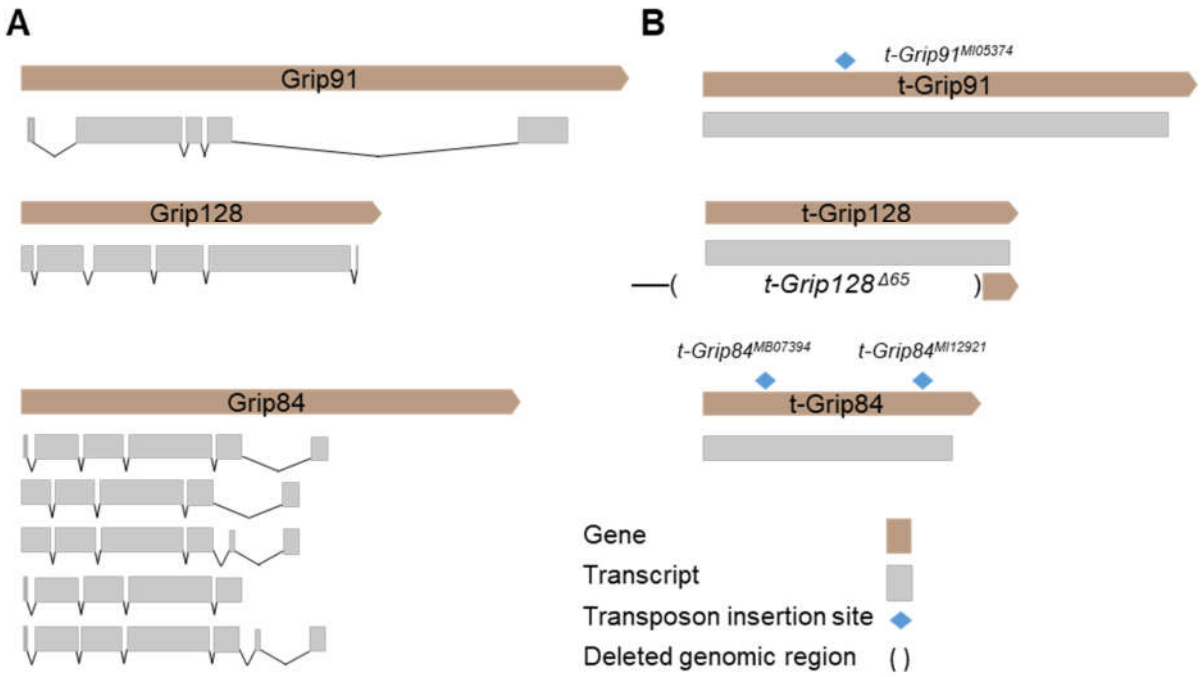

Figure 10. Structure and transcripts of ubiquitous γ-TuRC and t-γ-TuRC genes. A. The structure of the ubiquitously expressed γ-TuRC (Grip91, Grip128 and Grip84). **B.** t-γ-TuRC genes (*t-Grip91, t-Grip128* and *t-Grip84*) are intronless with only one transcript from each gene. The location of the transposon insertion sites in the case of *t-Grip91*, *t-Grip84* and the deleted genomic region of *t-Grip128* are labelled on the schematic gene structure.

To test the mutant phenotypes caused by the lack of *t-Grip84* and *t-Grip91* proteins, we collected the publicly available mutants for *t-Grip84* (*t-Grip84*^{MB07394}, *t-Grip84*^{MI12921}) and *t-Grip91* (*t-Grip91*^{MI05374}) (**Figure 10B**). The fertility of the homozygous mutant females of *t-Grip84*^{MB07394}, *t-Grip84*^{MI1292} and *t-Grip91*^{MI05374} was comparable to the wild type. Homozygotes of *t-Grip84*^{MB07394} (hereafter *t-Grip84*^{ms}), *t-Grip84*^{MI12921} and *t-Grip84*^{MB07394}/*t-Grip84*^{MI12921} transheterozygotes are male-sterile. We further confirmed the male-sterile phenotypes of *t-Grip84*^{ms} by testing the fertility of hemizygous *t-Grip84*^{ms}/*Df(3L)BSC375* males, which also showed male-sterility.

Mutants of the *t-Grip91* either in homozygotes of *t-Grip91*^{MI05374} (hereafter *t-Grip91*^{ms}), or hemizygotes of *t-Grip91*^{MI05374} and *Df(2L)osp29* resulted in male semi-sterility (70%) (**Figure 11**).

A

Gene	Mutant allele	Homozygous Phenotype	Hemizygous Phenotype	Aging Phenotype	Rescue
t-Grip84	*t-Grip84*^{MB07394} (*t-Grip84*^{ms})	male-sterile	male-sterile	-	Fertile
	t-Grip84^{MI12921}	male-sterile	male-sterile		
t-Grip91	*t-Grip91*^{MI05374} (*t-Grip91*^{ms})	male-semisterile	male-semisterile	-	Fertile
t-Grip128	*t-Grip128*$^{\Delta 65}$	fertile	fertile	fertile	-

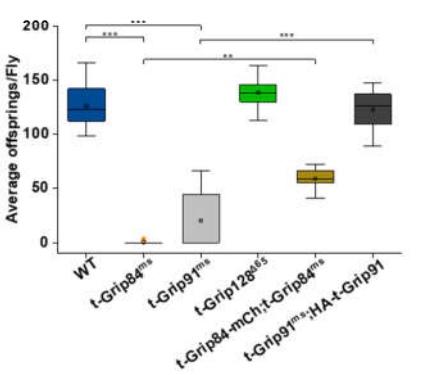

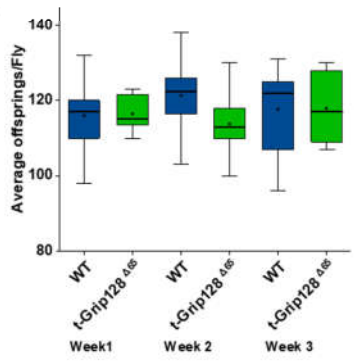

Figure 11. Fertility of the t-γ-TuRC mutants. A. Fertility of *t-Grip84*, *t-Grip91* and *t-Grip128* mutant males in homozygous, transheterozygous and hemizygous combination using overlapping deletion in the chromosomal region of the genes. **B.** Fertility of the wild type and t-γ-TuRC mutants by counting the average offspring after 14 days of crossing them. WT (n=27) *t-Grip84*^{ms} (n=27), *t-Grip91*^{ms} (n=19) and *t-Grip128*$^{\Delta 65}$ (n=20). Male sterility of *t-Grip84*^{ms} and *t-Grip91*^{ms} was partially or fully rescued with the t-Grip84-mCh (n=21) or HA-t-Grip91 (n=12) transgenes. Error bars indicate mean ± SEM Statistical significance was determined by one-way anova ($p<0.001$). **C.** Fertility of WT (n=20) and *t-Grip128*$^{\Delta 65}$ males (n=20) by ageing them for 3 weeks. Error bars indicate mean ± SEM.

Due to the lack of the classical mutant allele of *t-Grip128,* we decided to use the CRISPR-Cas9 gene-editing technology to create a null mutant of *t-Grip128*. We designed two gRNAs and expressed them in pCFD4 vector-based transgenic line in the presence of Cas9 endonuclease, which was driven by a germ-line specific *nanos* promoter. We tested 73 potential deletion lines and identified *t-Grip128*$^{\Delta 65}$ with a 3359bp deletion (genomic coordinates 3L:4994209-4997568), between the gRNA target location, in the coding region of the *t-Grip128* gene (**Figure 10B**). We tested the fertility of *t-Grip128*$^{\Delta 65}$ males and found that despite the deletion removing most of the coding region of *t-Grip128*, the fertility of the homozygous mutant males was comparable to the wild type (**Figure 11 A, B**). According to the literature, mutants of the γ-TuRC interacting proteins only exhibit fertility loss by ageing (Tovey et al., 2018). Therefore, we checked the age-dependent fertility of *t-Grip128*$^{\Delta 65}$ males and found that the homozygous *t-Grip128*$^{\Delta 65}$ fertility was similar to the wild type (**Figure 11C**). Altogether, these results suggest that *t-Grip128* is not essential for normal male fertility in Drosophila.

To further characterize the mutant t-γ-TuRC genes, we measured *t-Grip84*, *t-Grip91* and *t-Grip128* relative gene expression in the testis extracts of *t-Grip84*^{ms}, *t-Grip91*^{ms} and *t-Grip128*$^{\Delta 65}$ mutants respectively. We found a dramatic reduction of the t-γ-TuRC transcripts in the mutant testis samples, suggesting that t-γ-TuRC mutants are null alleles (**Figure 12**).

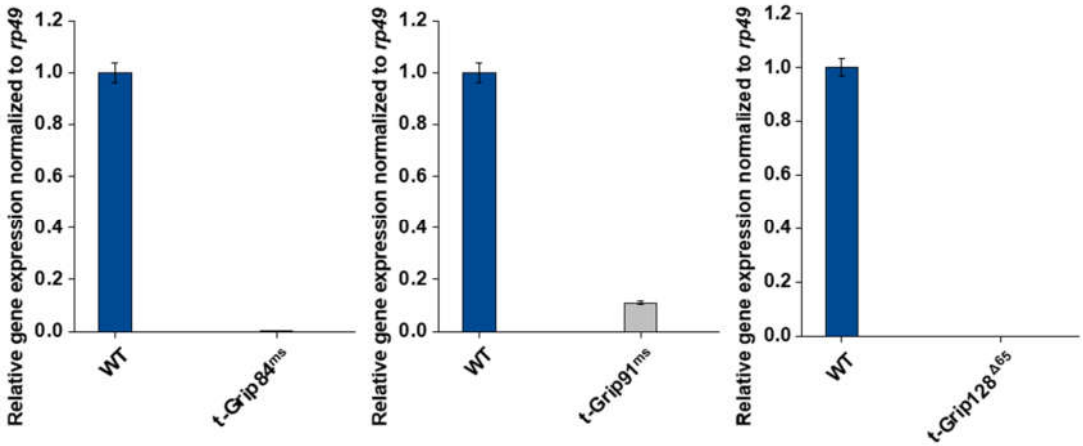

Figure 12. Relative gene expression of t-γ-TuRC mutants. Relative gene expression of *t-Grip84*, *t-Grip91* and *t-Grip128* in the mutant testes extracts of *t-Grip84*^{ms}, *t-Grip91*^{ms} and *t-Grip128*$^{\Delta 65}$ respectively (25 pairs\genotype). *rp49* was used as a reference gene for the normalization.

4.3 Phenotypic characterization of the t-γ-TuRC mutants

We tested the general morphology of the testis in t-γ-TuRC mutants by microscopic observation of different developmental stages of spermatogenesis. Detailed examination of the mutants revealed that the seminal vesicles of the *t-Grip91*^{ms} males both in homozygous and hemizygous combinations contain a reduced number of sperms, while homozygous and trans-heterozygous of *t-Grip84*^{ms} and *t-Grip84*^{MI12921} males which were sterile had empty seminal vesicles (**Figure 11 A, B, Figure 14 B, C arrowhead**). This observation suggested that the process of spermatogenesis is affected in the t-γ-TuRC mutants, therefore we tested the stages of spermato- and spermiogenesis in both *t-Grip91*^{ms} and *t-Grip84*^{ms} mutants. We found that mitotic and meiotic divisions were normal both in *t-Grip84*^{ms} and *t-Grip91*^{ms} testes. Mutants of genes involved in mitotic or meiotic division result in fused cells with abnormal nucleus: nebenkern ratio (different from the 1:1 ratio). Based on the fact, that γ-TuRC is involved in the centrosomal organization, we tested the nebenkern-nucleus ratio in the round spermatids. We found wild type nucleus-nebenkern ratio in the mutants, supporting the previous observation about the normal mitotic and meiotic cell division in the t-γ-TuRC mutants (**Figure 13**).

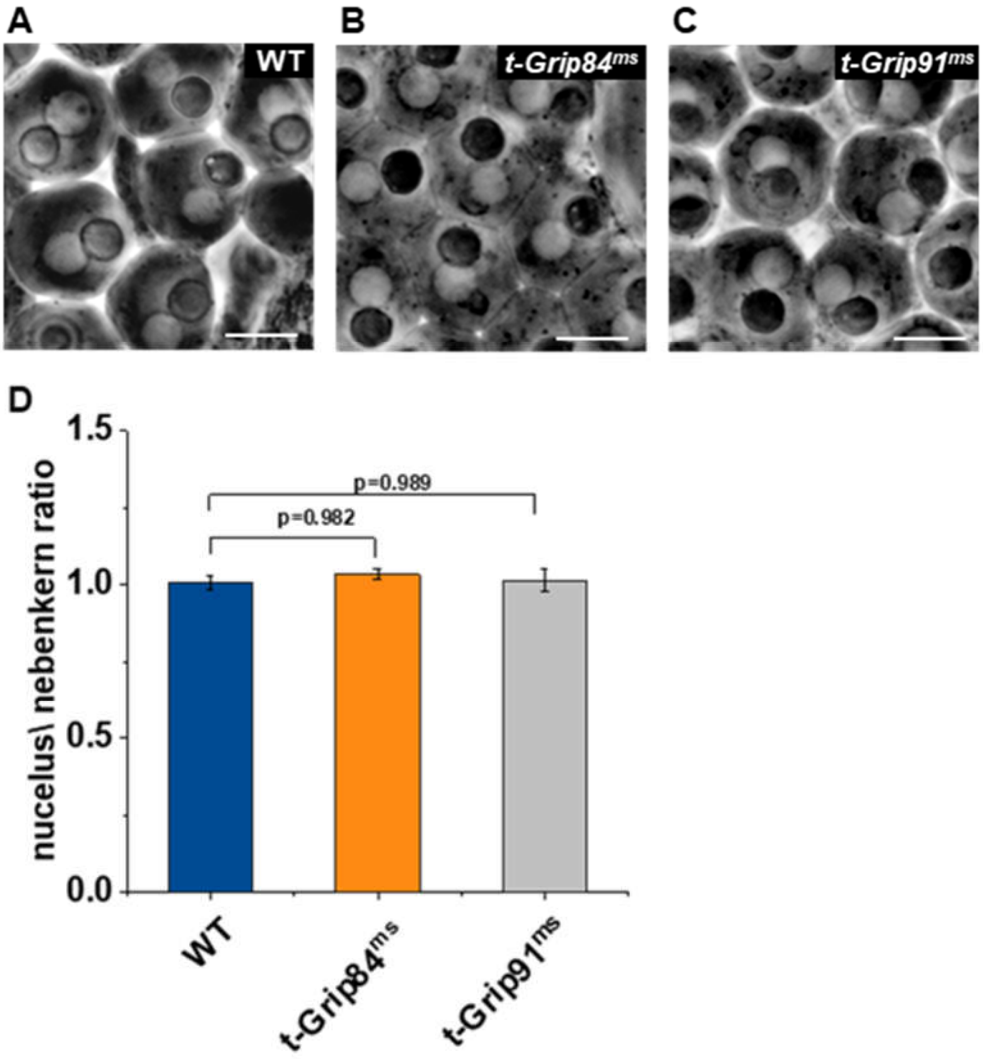

Figure 13. The phenotype of spermatids at the onion stage in t-γ-TuRC mutants. **A-C**. Phase-contrast micrograph of round spermatids from WT, *t-Grip84*^{ms} and *t-Grip91*^{ms}. **D.** Nucleus: Nebenkern ratio was counted in WT, *t-Grip84*^{ms} and *t-Grip91*^{ms}. Scale bars: 20 µm.

Next, we checked axoneme formation and maturation in the t-γ-TuRC mutants. Axonemal MTs are post-translationally modified, and they are important for axoneme assembly and the formation of mature, fertile sperm. Polyglycylation and polyglutamylation occur at the exposed and highly charged C-terminal tails of α- and β-tubulin of the axoneme (Rogowski et al., 2009). Polyglycylation occurs in the late stages of spermiogenesis at the time of individualization, therefore, visualizing polyglycylated tubulin is a good way to investigate the mature and motile axoneme. We used an anti-pan polyglycylated tubulin antibody (Axo49) to test axoneme assembly and maturation. We found that cysts in *t-Grip84*^{ms} and *t-Grip91*^{ms} mutants developed normally and

axonemes are indistinguishable from the WT (**Figure 14**). We did not observe a cyst elongation problem, which could manifest in the abnormal length or structure of the cysts.

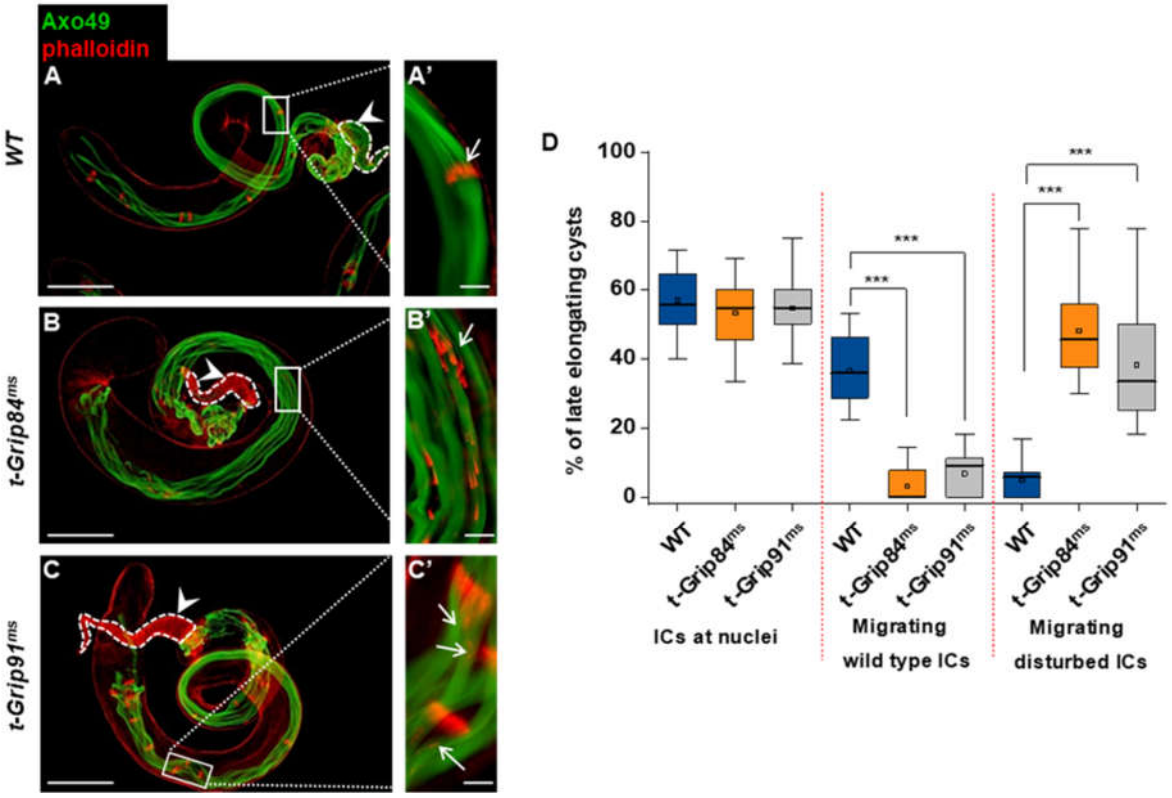

Figure 14. Phenotypic characterization of mutants of t-γ-TuRC members. A-C. Polyglycylated elongated axonemes are visualized by polyglycylated tubulin (AXO49) (green) staining and ICs stained with Phalloidin (red). (A-C) Axoneme elongation of *t-Grip84*^{ms} and *t-Grip91*^{ms} mutants is similar to WT. (A') The movement of the investment cones is synchronized (arrow) and the seminal vesicle is filled with mature sperm (arrowhead) in WT testis. (B'-C') Scattered investment cones (arrows) and (B-C) empty seminal vesicles (arrowhead) are present in *t-Grip84*^{ms} and *t-Grip91*^{ms} mutants. Scale bars: A-C 100 µm, A'-C' 20 µm. **D.** We used DAPI and Phalloidin staining to count nuclear bundles, and ICs in WT, *t-Grip84*^{ms} and *t-Grip91*^{ms} mutant testes (n=30 testes in each genotype) The number of ICs at the nuclei and normal or disturbed migration of ICs were counted in each genotype. Statistical significance was determined by one-way ANOVA ($p<0.001$).

We tested the individualization in *t-Grip84*^{ms} and *t-Grip91*^{ms} mutants by visualizing the IC using phalloidin staining. We found that the actin cones are formed, and their structure and size are similar to wild type at the onset of individualization; however, their movement lost synchrony and they became scattered in the individualizing cysts of both *t-Grip84*^{ms} and *t-Grip91*^{ms} mutants (**Figure 14 B, C**). We analyzed the data statistically and found that 40% and 35% of the migrating

IC were abnormal in *t-Grip84*^{ms} and *t-Grip91*^{ms} mutants respectively (**Figure 14D**). Parallel with the abnormal actin cone movement, we also noticed a scattering of the nuclei in the late stages of elongation in *t-Grip84*^{ms} and *t-Grip91*^{ms} mutants (**Figure 18 B, C**).

Considering the disturbed actin cones, we were interested in the proper activation of the non-apoptotic Caspase-cascade in late elongating spermatids. We tested caspase activity, with cleaved Caspase3 antibody and found that it was activated, however, its distribution is more dispersed in the *t-Grip84*^{ms} and *t-Grip91*^{ms} mutants (**Figure 15**). Based on these results we believe that the abnormal caspase activity is a secondary phenotype due to the disturbance in actin cone migration.

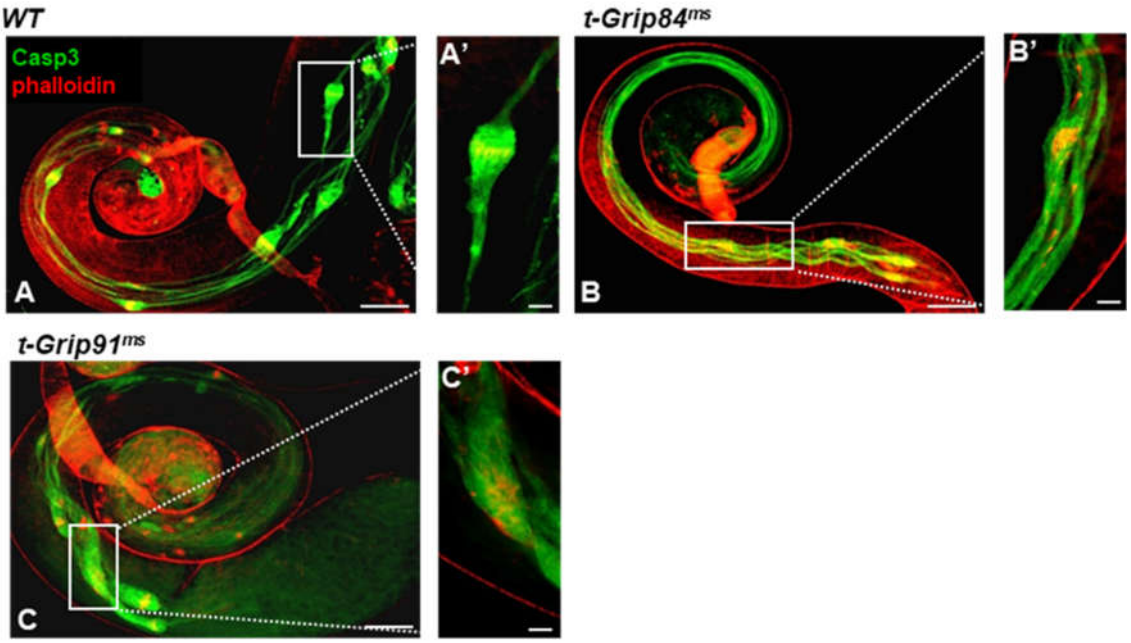

Figure 15. Caspase activation in t-γ-TuRC mutants. Cleaved-Caspase3 (green) is present in t-γ-TuRC mutants *t-Grip84*^{ms} and *t-Grip91*^{ms}. investment cones stained with Phalloidin (red). Scale bars 100 μm, insets 20 μm.

Transmission electron microscopy (TEM) is the most suitable method to test the integrity and components of the elongated cyst with the developing spermatids. We prepared samples from WT and the strongest mutant of t-γ-TuRC members, *t-Grip84*^{ms} and analyze the fine structure of the axoneme and the mitochondrial derivatives by TEM. We found normal morphology and wild type accumulation of the paracrystalline material in the developing mitochondrial derivatives in the cross-section of spermatids of *t-Grip84*^{ms} mutant. The number and distribution of the axoneme

independent cytoplasmic MTs and that of the axoneme itself develop like the wild type in spermatids of *t-Grip84*^{ms} mutant (**Figure 16**).

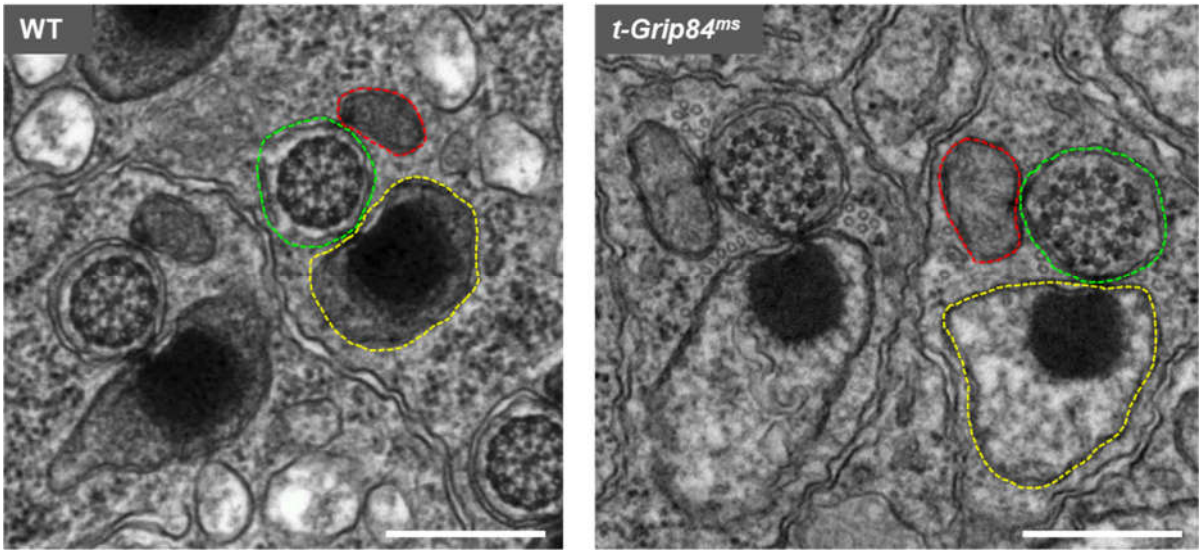

Figure 16. Transmission electron microscopy of testis of *t-Grip84*^{ms}. Testis of the mutant *t-Grip84*^{ms} shows no difference in the structure of the axoneme, and mitochondrial derivatives compare to the WT testis. Green dashed line: axial membrane, yellow dashed line: large mitochondrial derivative, red dashed line: small mitochondrial derivative. Scale bars. 0.5 µm.

The asynchronous movement of the ICs may be the result of a situation where the basal body fails to dock at the spermatid nucleus or to maintain the connection if it is established. Similar phenotypes were described in the case of dynein and Pericentrin-like protein mutants (Galletta et al., 2020). To test this more carefully, we expressed the basal body localized protein GFP-PACT in the *t-Grip84*^{ms} and *t-Grip91*^{ms} mutant background. GFP-PACT localize to the basal body when it was embedded into the nuclear envelope in the round stage spermatids both in WT and *t-Grip84*^{ms} and *t-Grip91*^{ms} mutants (**Figure 17**). GFP-PACT stays close to the elongating nuclei in WT, however, it is separated from the nuclei in the *t-Grip84*^{ms} and *t-Grip91*^{ms} mutant spermatids (**Figure 18**).

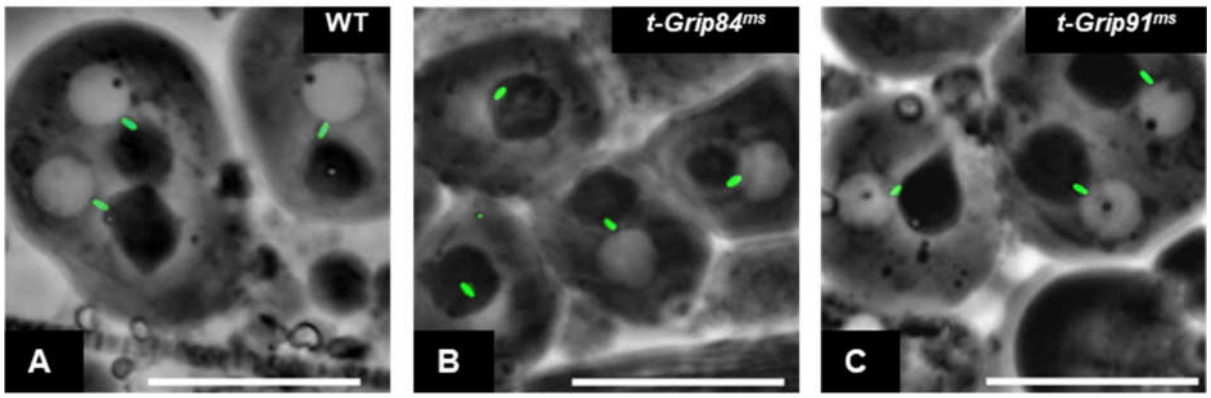

Figure 17. GFP-PACT localization in round spermatids. GFP-PACT signal is on the basal body, which is embedded in the nuclear envelope in round spermatids of WT (**A**), *t-Grip84*^{ms} (**B**) and *t-Grip91*^{ms} (**C**) mutants. Scale bars: 20 µm.

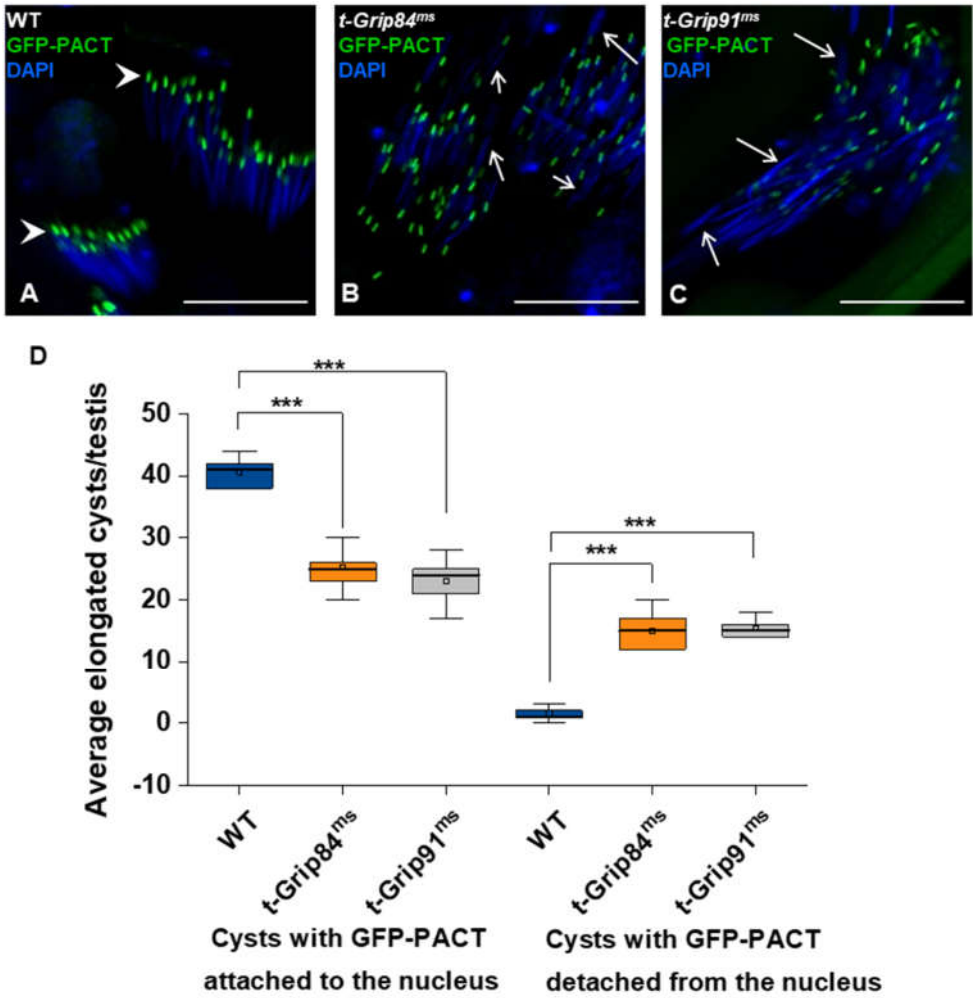

Figure 18. Basal body-nucleus connection is disturbed in t-γ-TuRC mutants. (**A-C**) GFP-PACT (green) is localizing to the basal body in WT (A, arrowhead), *t-Grip84*^{ms} and *t-Grip91*^{ms} (B, C respectively) spermatids, but nuclei are scattered in the elongated cysts of *t-Grip84*^{ms} and *t-Grip91*^{ms} mutants (B, C arrows). (**D**) GFP-PACT localization to the nucleus was counted in the elongated cysts of WT and *t-Grip84*^{ms} and *t-Grip91*^{ms} mutants (n=12 pairs of testes in each genotype). GFP-PACT signal represents the basal body, which is detached from the nuclei in the t-γ-TuRC mutants. Statistical significance was determined by one-way ANOVA ($p<0.001$). Scale bars: 20 μm**.**

In light of these findings, we wanted to test if the centriole adjunct and the basal body are disintegrated in *t-Grip84* or *t-Grip91* mutants. We tested the localization of the centriole component Ana1, Asterless and the PCM/ centriole PACT, in *t-Grip84*^{ms} and *t-Grip91*^{ms} mutants (Martinez-Campos et al., 2004; Fu et al., 2016; Galletta et al., 2020). GFP-PACT, Ana1 and Asterless were found on the basal body of *t-Grip84*^{ms} and *t-Grip91*^{ms} mutant spermatids. However, we observed their nuclear scattering during the later stages of individualization, as well as the partial detachment of the GFP-PACT, Ana1 and Asterless labelled basal body from the nucleus in both mutants (**Figure 19**).

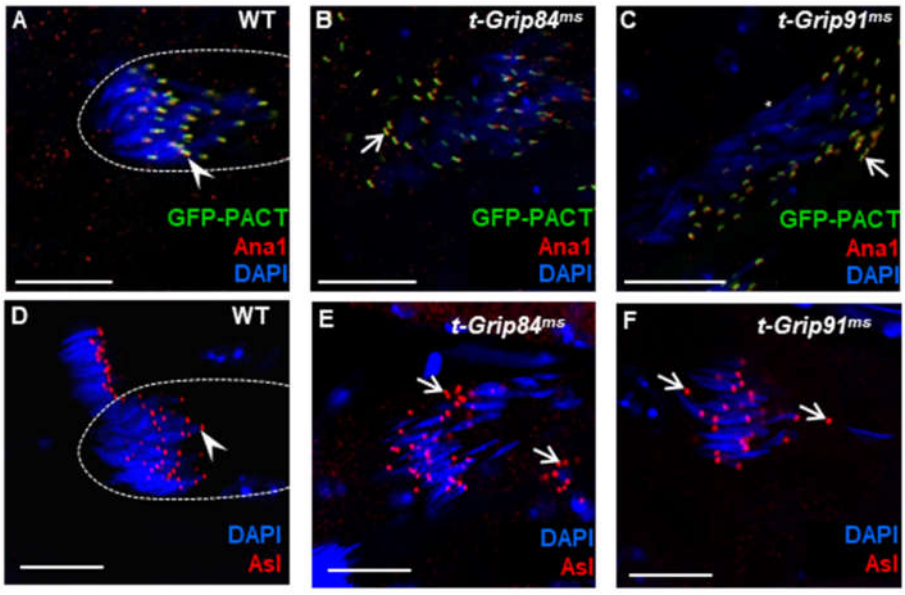

Figure 19. Localization of basal body proteins in t-γ-TuRC mutants. Ana1, GFP-PACT and Asl are localizing to the basal body of the WT (**A**, **D** arrowhead). In *t-Grip84*^{ms} (**B**, **E**) and *t-Grip91*^{ms} (**C**, **F**) their signal can be detected at the basal body; however, the basal bodies were scattered in the cyst (detached from the nuclei) (arrows). Scale bars: 20 μm.

Despite the lack of sterile phenotype in *t-Grip128*$^{\Delta 65}$ mutant, we tested the localization of Asl and γ-tubulin in *t-Grip128*$^{\Delta 65}$ mutant. Both proteins localize normally to the centriole adjuncts and show normal centriole adjunct-nucleus attachment in *t-Grip128*$^{\Delta 65}$ mutant (**Figure 20**).

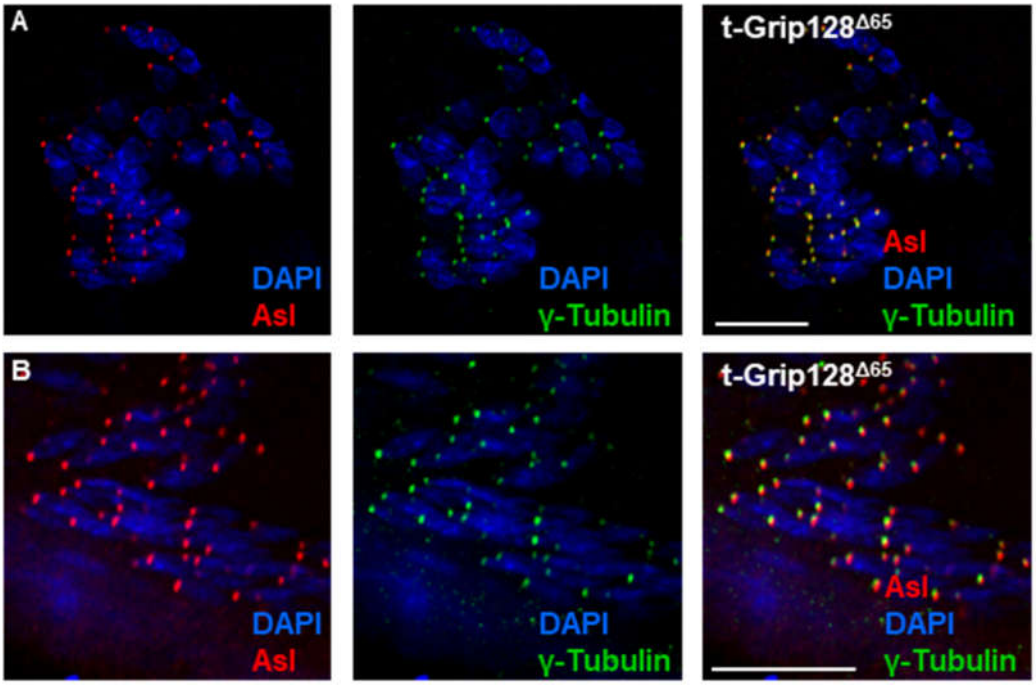

Figure 20. Asl and γ-tubulin localization in *t-Grip128*$^{\Delta 65}$ mutant. Asl and γ-tubulin localize normally to the centriole adjuncts in the *t-Grip128*$^{\Delta 65}$ mutant. Scale bars: 20 µm.

4.4 *t-Grip84* expression in Drosophila tissue culture cells

It is well known that γ-TuRC is localized to the centrosome in somatic cells (Gunawardane et al., 2000). Therefore, we were curious to test whether t-γ-TuRC members can be built into the ubiquitous complex and localize to the centrosome in tissue culture cells. To test this idea, we fused *t-Grip84* with GFP and cloned it into a vector, where the expression of the fusion transcript was driven by an *actin5C* promoter. We did a transient transfection in Dmel2 Drosophila tissue culture cells, and we visualized the centrosomes by immunolabelling centrosomal proteins. t-Grip84-GFP was able to localize to the centrosome and strongly colocalized with the centrosomal markers, γ-tubulin and Spd2 (**Figure 21**).

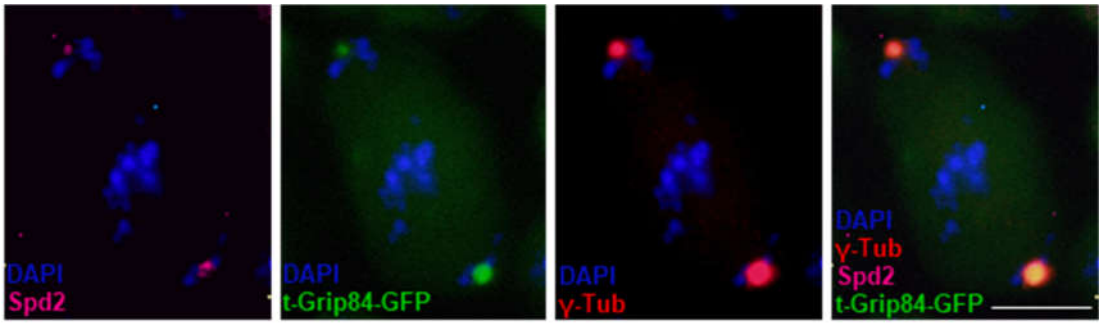

Figure 21. t-Grip84-GFP localization in Dmel2 cells. t-Grip84-GFP (green) localizes to the centrosome and colocalizes with γ-tubulin (red) and Spd2 (magenta) in Dmel2 cells. Nuclei stained with DAPI (blue). Scale bar: 10 μm.

4.5 The localization pattern of t-γ-TuRC proteins during spermatogenesis

Due to the centrosomal accumulation of t-Grip84-GFP in tissue culture cells, we generated the tagged version of the t-γ-TuRC proteins. We tagged t-Grip84 with mCherry (t-Grip84-mCh) and GFP (t-Grip84-GFP), t-Grip91 and t-Grip128 with 3 copies of hemagglutinin tag (HA) (HA-t-Grip91 and HA-t-Grip128) and γ-Tub23C with GFP (γ-Tub23C-GFP). To provide the endogenous expression of the transgenes in the testis, we cloned their own 5' genomic regions and the coding region into fly transformation vectors. This allows us to study the expression pattern and subcellular distribution of the t-γ-TuRC components during spermatogenesis (**Figure 22**). We established independent transgenic lines and tested their rescuing capacity in the mutant background. t-Grip84-mCh and HA-t-Grip91 were able to rescue the male sterility and the nuclear detachment abnormality in *t-Grip84*^{ms} and *t-Grip91*^{ms} mutants respectively, proving that the tags are not interfering with t-Grip84 or t-Grip91 function (**Figure 11B and 23**).

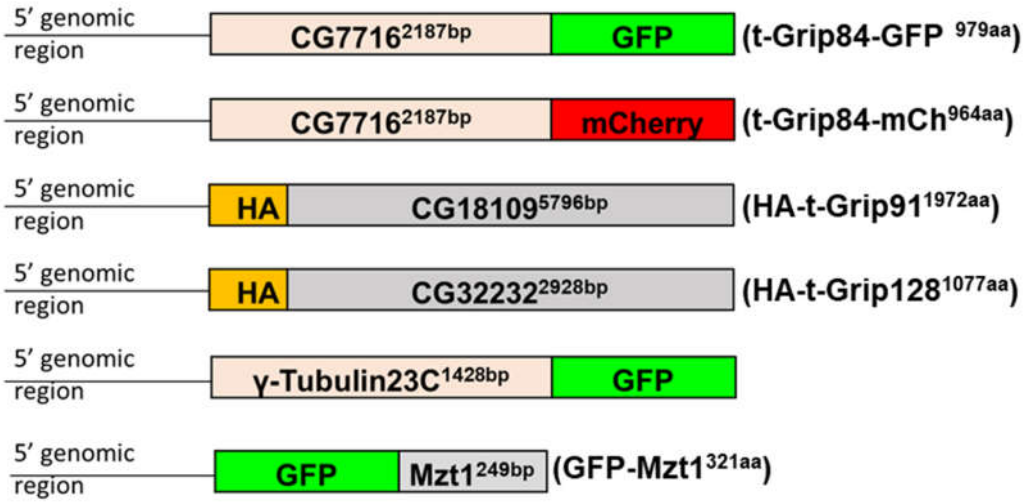

Figure 22. Graphical representation of the t-γ-TuRC transgenes. To study the localization of different t-γ-TuRC proteins we made transgenic lines with different tags, where we cloned the endogenous 5' genomic region and the coding sequence of the gene in frame with the indicated tag either N- or C-terminal.

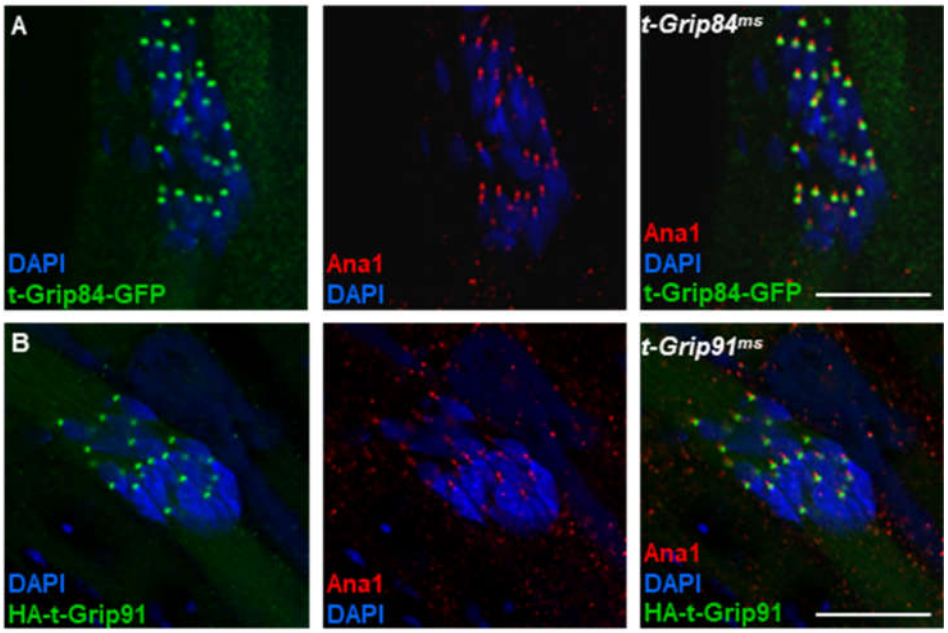

Figure 23. Transgenes of t-γ-TuSC mutant proteins rescued the basal body nucleus detachment abnormality in the mutants. Ana1 signal is localizing to the basal body and colocalizing with t-Grip84-GFP (**A**), and HA-t-Grip91(**B**). The basal bodies are attached to the nuclei in the presence of wild type transgenes in the stocks of *t-Grip84*^{ms} and *t-Grip91*^{ms} (A, B). Nuclei stained with DAPI (blue). Scale bars: 20 µm.

In the next step, we systematically tested the localization pattern of the transgenes in various tissues. We could not detect the expression of the transgenes in somatic tissues or in the ovary (**Figure 24**). All tested t-γ-TuRC proteins are expressed only in the germline cells during spermatogenesis, and neither is expressed in the somatic cyst or epithelial cells of the testis **(Figure 24 and 25)**. Signals of t-Grip84-mCherry, HA-t-Grip91, and HA-t-Grip128 first appear at the centriole adjunct during nuclear elongation of the round spermatids **(Figure 25)**. Centriole adjunct localization of t-Grip84-mCh/t-Grip84-GFP, HA-t-Grip91, and HA-t-Grip128 during different stages of spermatogenesis was further confirmed by simultaneous labelling with γ-tubulin **(Figure 25 and 26).**

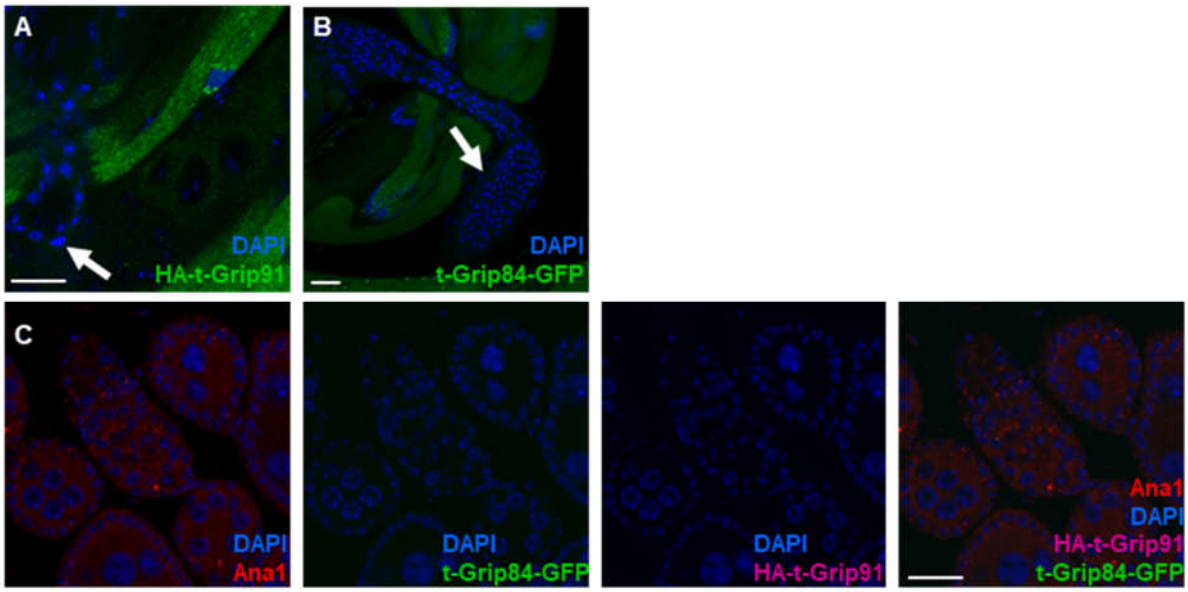

Figure 24. t-γ-TuRC proteins are not localizing to the epithelial tissue of the testis (A, B arrows) nor the ovaries (C). Nuclei stained with DAPI (blue). Scale bars: 20 μm

The transgenic lines made it possible to express them simultaneously and test their colocalization during stages of spermatogenesis. We found a complete overlap between t-Grip84-mCh, HA-t-Grip91, HA-t-Grip128 and γ-tubulin (γ-Tub23C-GFP) at the centriole adjunct during spermatid elongation **(Figure 26 and Supplementary Figure 3)**.

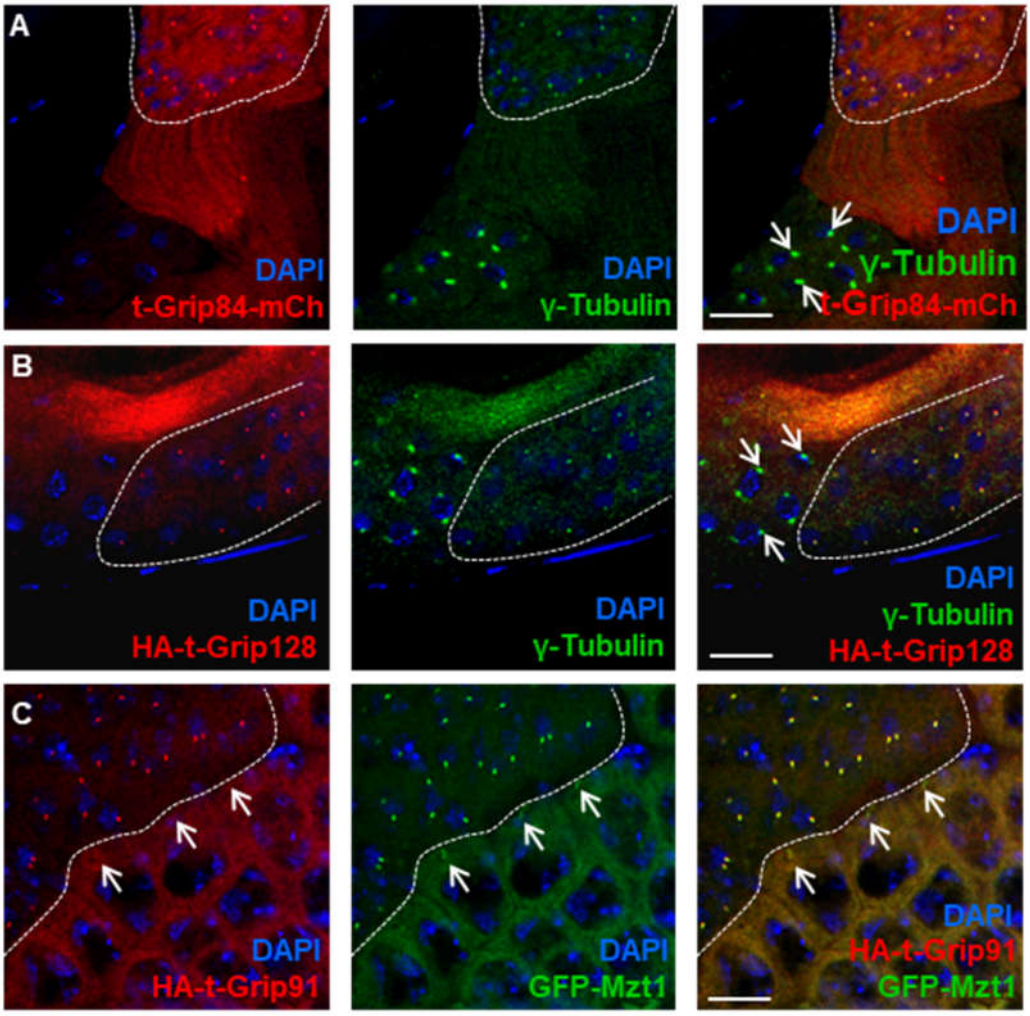

Figure 25. Localization of t-γ-TuRC proteins in early stages of spermatogenesis. (**A**) t-Grip84-mCh (red), (**B**) HA-t-Grip128 (red) and (**C**) HA-t-Grip91 (red) localize to the centriole adjunct but are not present on the centrosome of the primary or secondary spermatocytes. The centrosome and the basal body (arrows) are visualized by γ-tubulin (green). In round spermatids signals of t-Grip84-mCh, HA-t-Grip128 and HA-t-Grip91 (red) are visible on the centriole adjunct and colocalize with γ-tubulin (green) (dashed lines highlighting cysts). Nuclei stained with DAPI (blue). Scale bars: 20 μm.

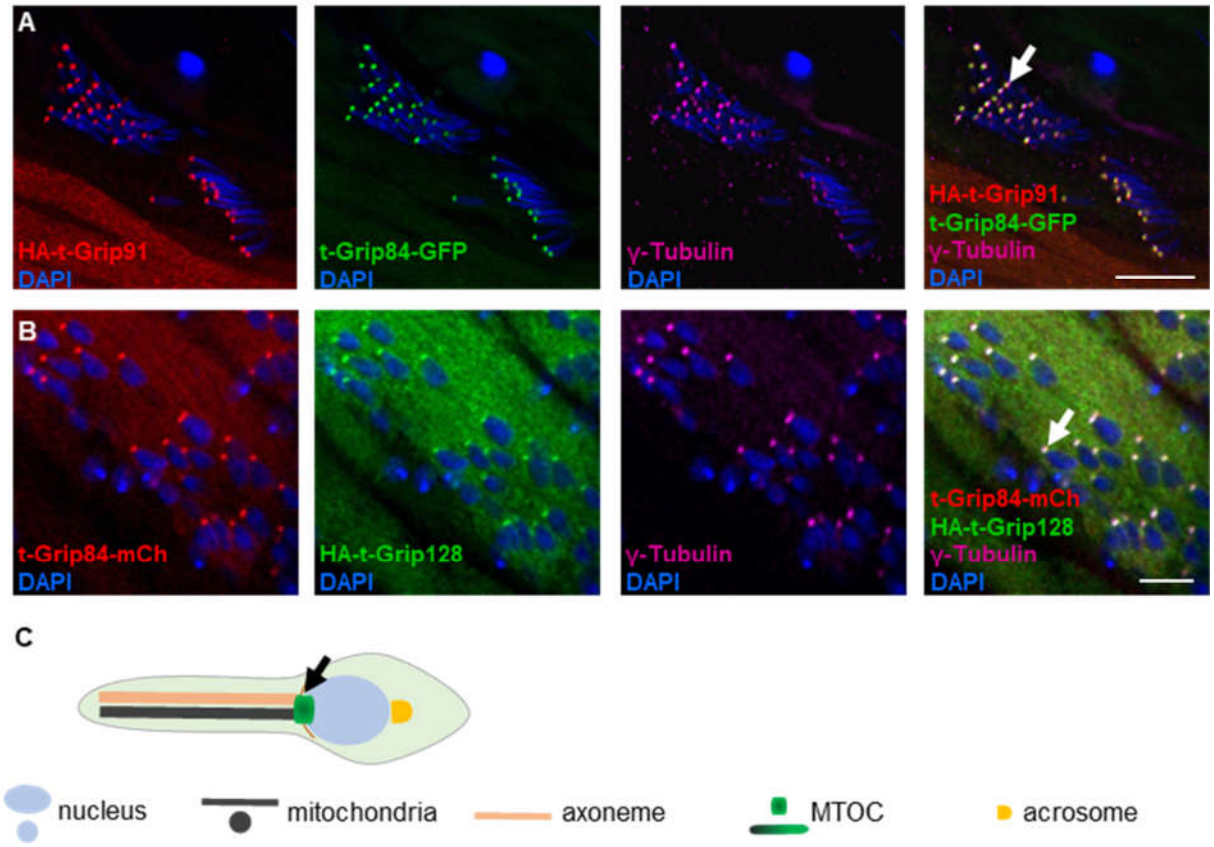

Figure 26. Localization of t-γ-TuRC proteins during spermatogenesis. A. HA-t-Grip91 (red) is colocalizing with t-Grip84-GFP (green) and γ-tubulin (magenta) at the centriole adjunct in elongating spermatids. **B.** t-Grip84-mCh (red) is colocalizing with HA-t-Grip128 (green) and with γ-tubulin (magenta) at the centriole adjunct in early elongating spermatids. Nuclei stained with DAPI (blue) **C.** Graphical illustration of the early elongating spermatid with the localization focus of the centriole adjunct (arrow). Nuclei stained with DAPI (blue). Scale bars: 10 μm.

We concluded that t-γ-TuRC members colocalize with γ-tubulin and with each other at the centriole adjunct in the post-meiotic spermatids but diminish in the fully elongated cysts **(Figure 27A)**.

Detailed observation of the different stages of spermatogenesis revealed an additional localization focus of the t-γ-TuRC proteins in the elongating cysts. Parallel with the centriole adjunct localization, t-Grip84-GFP, HA-t-Grip91, and HA-t-Grip128 were localized at the apical tip of the elongating nucleus **(Figure 27 B, C)**.

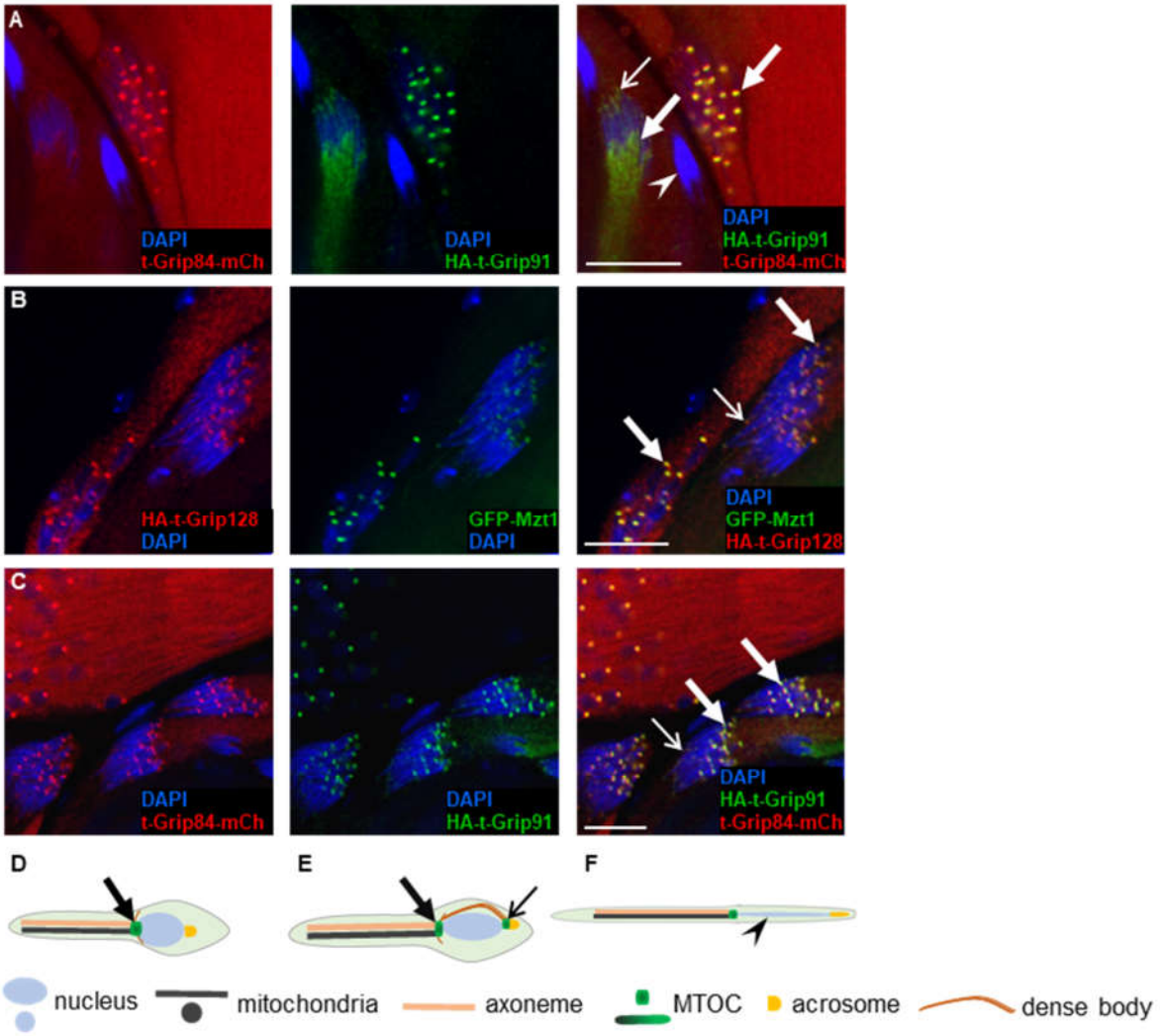

Figure 27. The localization pattern of t-γ-TuRC proteins. A. t-γ-TuRC proteins localization persists through elongation (arrows) but is not present in the fully elongated spermatids (arrowhead) **B, C.** HA-t-Grip128 (red) and Mzt1 (green) (B) t-Grip84-mCh (red), HA-t-Grip91 (green) (C), localize to the anterior tip of the nucleus (B, C arrows) and the centriole adjunct. (B, C bold arrows). **D, E.** Graphical representation of an early and late elongating spermatid with the localization sites of t-γ-TuRC proteins (arrows) **F.** Graphical representation of an elongated spermatid (for key see figure 30). Nuclei stained with DAPI, scale bars 20 μm.

Centriole adjunct localization of t-γ-TuRC proteins was further confirmed by immunostaining with already characterized protein components of the structure. We checked the localization of GFP-PACT, Ana1, the ubiquitous γ-TuRC protein Grip163 and Asterless and found overlapping localization between GFP-PACT, Ana1, Grip163, Asterless and t-γ-TuRC proteins (**Figure 28**).

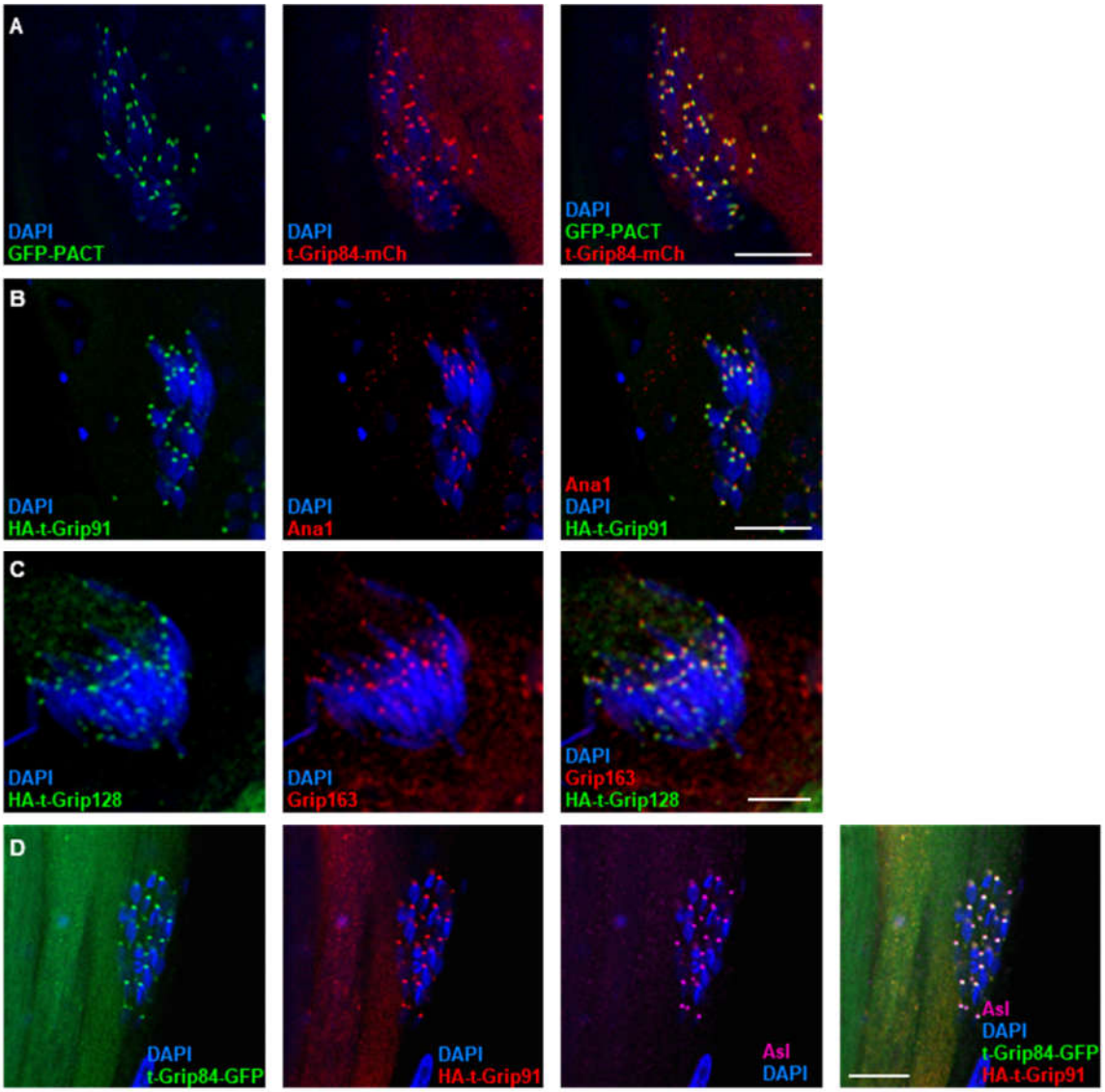

Figure 28. The colocalization between the t-γ-TuRC proteins with centriole, PCM and ubiquitous γ-TuRC proteins. A. t-Grip84-mCh colocalizes with the PCM marker GFP-PACT. **B**. HA-t-Grip91 colocalizes with the centriole adjunct and centrosome protein Ana1. **C**. HA-t-Grip128 (green) colocalizes with the ubiquitous γ-TuRC protein Grip163 (red) **D.** t-Grip84-GFP (green) and HA-t-Grip91(red) colocalize with the centriole adjunct marker Asterless (magenta) in elongating spermatids. Nuclei stained with DAPI (blue). Scale bars 20 µm.

We observed a third localization focus for the t-γ-TuRC proteins in the tail region near the mitochondria of the late elongating spermatids (**Figure 27 C**). We confirmed HA-t-Grip91, HA-t-Grip128 and t-Grip84-GFP mitochondrial localization by staining with Mitotracker red-fluorescent dye that decorates the mitochondria in living cells and its accumulation is membrane

potential-dependent (**Supplementary Figure 4**). We also coexpressed t-Grip84-GFP with the mitochondrial outer membrane protein Tom20-mCh and found an overlap between the signals on the mitochondria (**Figure 29**) (Zhang et al., 2016).

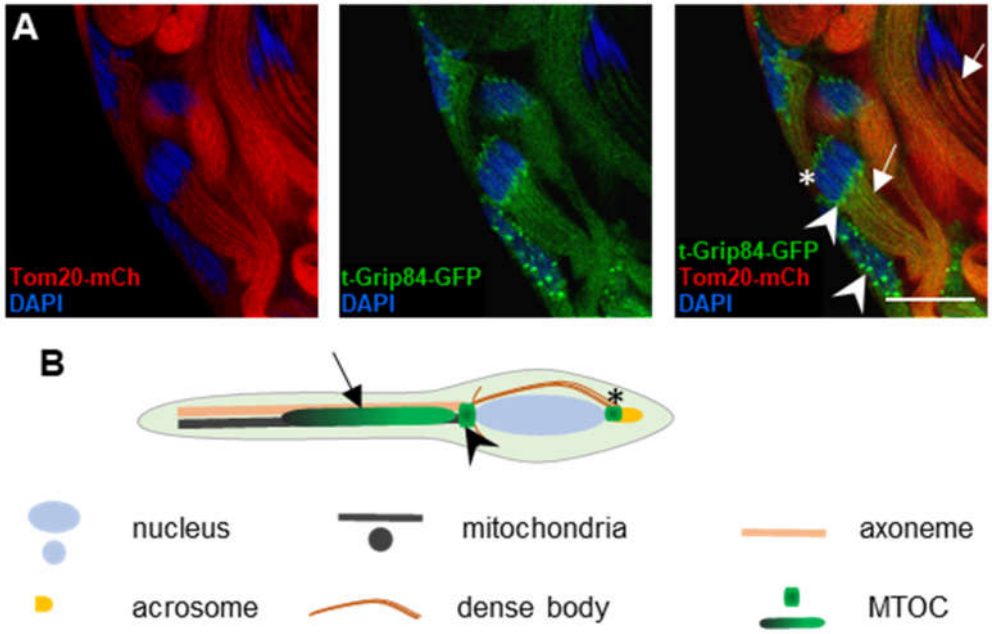

Figure 29. t-γ-TuRC component localize to the apical tip of the nucleus, centriole adjunct and on the surface of the mitochondria in the late elongating spermatids. **A.** t-Grip84-GFP (green) colocalizes with the mitochondrial marker Tom20-mCh (red)(arrow), simultaneously with the centriole adjunct (arrowhead) and the nuclear tip (asterisk) localization in the elongating spermatids. **B.** Graphical representation of Drosophila spermatid showing t-γ-TuRC proteins different localization points during spermatogenesis. Nuclei stained with DAPI (blue). Scale bar: 20 µm.

We conclude that the t-γ-TuRC proteins are only present in the post-meiotic stages and localize first to the centriole adjunct, later to the apical tip of the nuclei and finally to the surface of the elongating mitochondria (**Figure 30**).

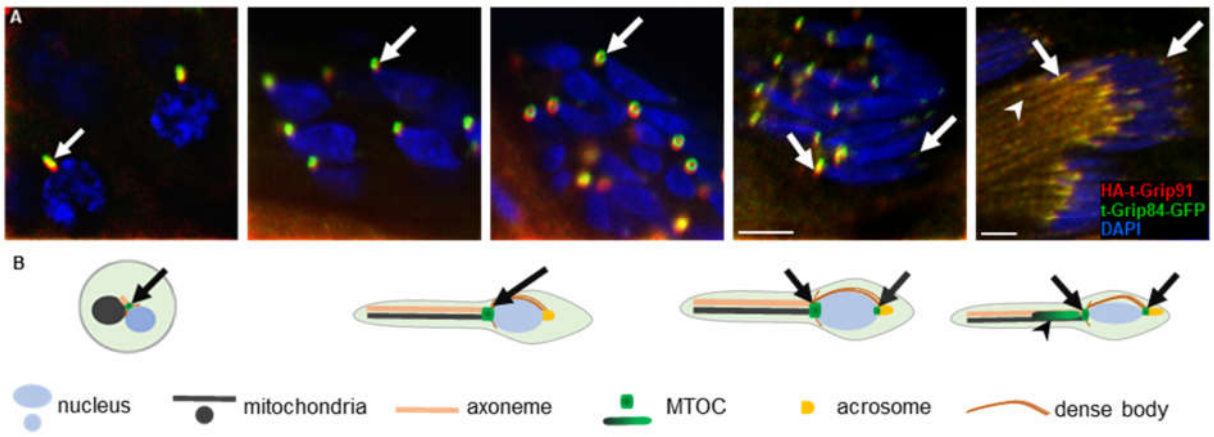

Figure 30. Summary of t-γ-TuRC localization during spermatogenesis. A. t-γ-TuRC proteins start to localize at the centriole adjuncts of round spermatids this localization persists through elongation and disappears from elongated spermatids. Later during elongation t-γ-TuRC localizes at the apical tip of the elongating nucleus and finally t-γ-TuRC in late elongating spermatids localizes near the mitochondria. **B**. Graphical summary of t-γ-TuRC localization throughout spermatogenesis. Nuclei stained with DAPI (blue). Scale bars 5 µm.

Mzt1, the newly identified γ-TuRC protein exhibits a very similar localization pattern to the t-γ-TuRC in the late stages of spermatogenesis. (Tovey et al., 2018). Mzt1 was shown to interact with the ubiquitous Grip91 and Grip128 protein using yeast two-hybrid analysis (Tovey et al., 2018), therefore it was logical to test the relation between Mzt1 and the t-γ-TuRC. To test the colocalization of Mzt1 and the t-γ-TuRC proteins, first, we engineered an endogenous promoter-driven GFP-Mzt1 transgene. To our surprise, GFP-Mzt1 signal is present already from the early stages of spermatogenesis on the centrosomes of the mitotic spermatocytes and shows centrosomal and mitochondrial association during the meiotic division (**Figure 31A**). After meiosis GFP-Mzt1 localize to the centriole adjunct and show a strong colocalization with all three t-γ-TuRC proteins, as it was published previously (Tovey et al., 2018) (**Figure 31 B, C**). With the examination of the additional t-γ-TuRC localization sites, we detected GFP-Mzt1 at the tip of the nuclei, similarly to the t-γ-TuRC proteins (**Figure 31 B**). Moreover, we detected a strong signal along the tail region of the elongating spermatids, closely to the late elongating mitochondria. We confirmed this mitochondrial localization by coexpressing GFP-Mzt1 and the mitochondrial protein, Tom20-mCh (**Figure 31 C**). Taken together, our results strongly support, that Mzt1 is part of both the ubiquitous and the testis-specific γ-TuRC.

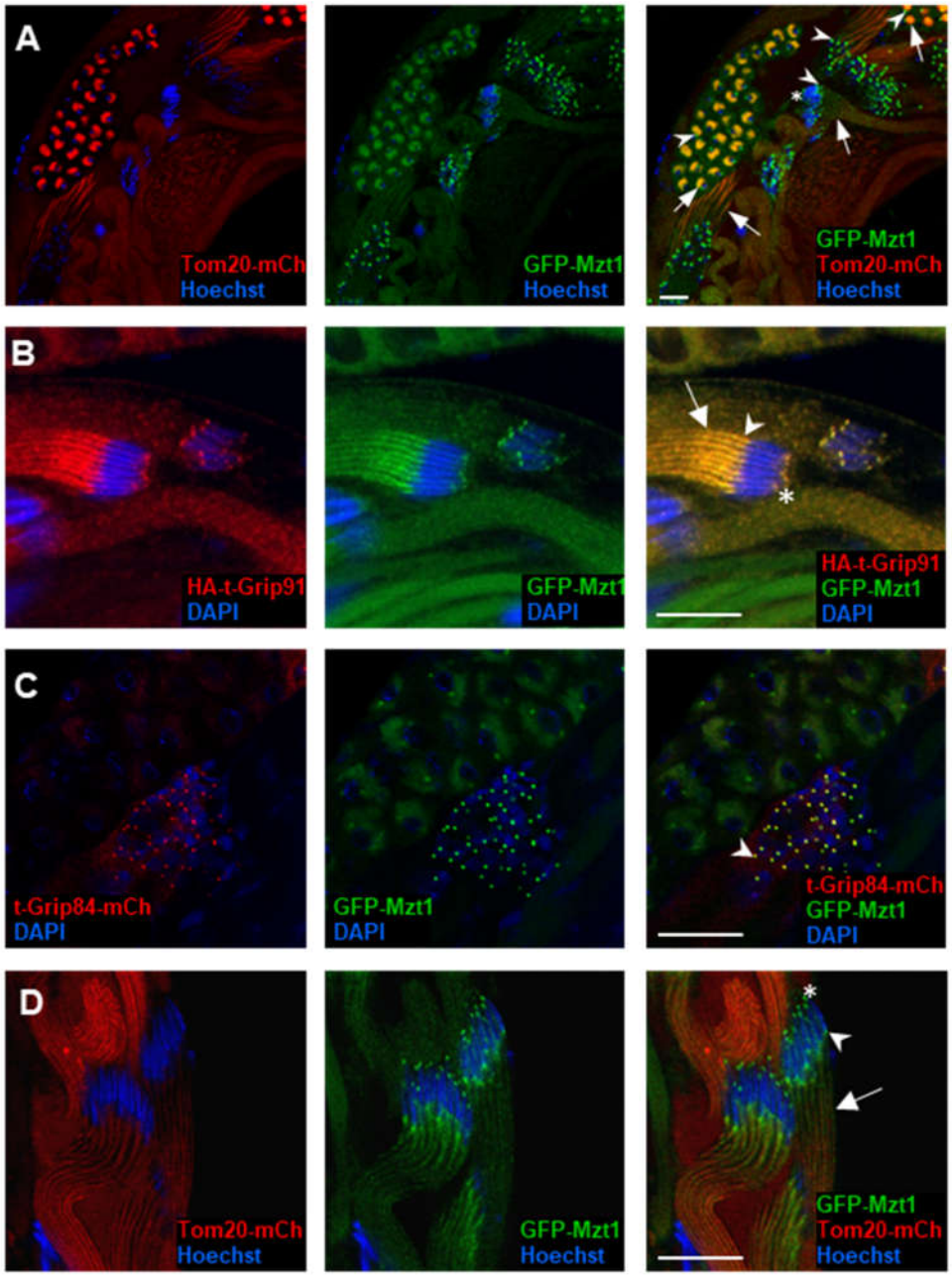

Figure 31. GFP-Mzt1 localization during Drosophila spermatogenesis. A. GFP-Mzt1 localizes to the centrosome (arrowhead) and overlaps with the mitochondrial marker Tom20-mCh of the meiotic spermatocytes (arrow). Mzt1 is also present at the centriole adjuncts and on the surface of the mitochondria in the elongating spermatid (arrowhead, arrow). **B.** HA-t-Grip91 colocalizes with GFP-Mzt1 at the centriole adjuncts (arrowhead), the nucleus tip (asterisk) and the elongating cyst (arrow). **C.** t-Grip84-mCh is colocalizing with GFP-Mzt1 at the centriole adjuncts of the elongating spermatids (arrowhead). **D.** GFP-Mzt1 overlaps with the mitochondrial marker Tom20-mCh at the mitochondria of the late elongating cyst. Nuclei stained with DAPI (blue). Scale bars: 20 µm.

Moreover, it was shown that a testis-specific isoform of the centrosomal protein centrosomin, (CnnT) is also expressed and localized to the surface of the elongated mitochondria during spermatogenesis (Chen et al., 2017). Based on this, and the above presented localization patterns, we can speculate that t-γ-TuRC with testis-specific proteins (t-Grip84, t-Grip-91, t-Grip128, CnnT, Mzt1) is assembled after meiosis.

Next, we tested the mutual dependence of the diverse localization of the t-γ-TuRC proteins. We found that neither HA-t-Grip91 nor t-Grip84-GFP localizes to the centriole adjunct or nuclear tip in the round or early elongating spermatids of *t-Grip84*^{ms} or *t-Grip91*^{ms} mutants, respectively (**Figure 32 A-C**). Afterwards, we analyzed the distribution of γ-tubulin and Mzt1, the two potential interactor proteins of the complex in the mutant background. We found that both γ-tubulin and GFP-Mzt1 are present on the centrosome of spermatocytes in *t-Grip84*^{ms} and *t-Grip91*^{ms} mutants (**Figure 33**), however, from the round spermatid stage onward, their localizations disappear and, they become cytoplasmic (**Figure 32 D-I**). These results provide additional evidence that t-γ-TuRC function is restricted to the post-meiotic stages and is not essential for centrosomal recruitment of the γ-TuRC interacting proteins (Alzyoud et al., 2021).

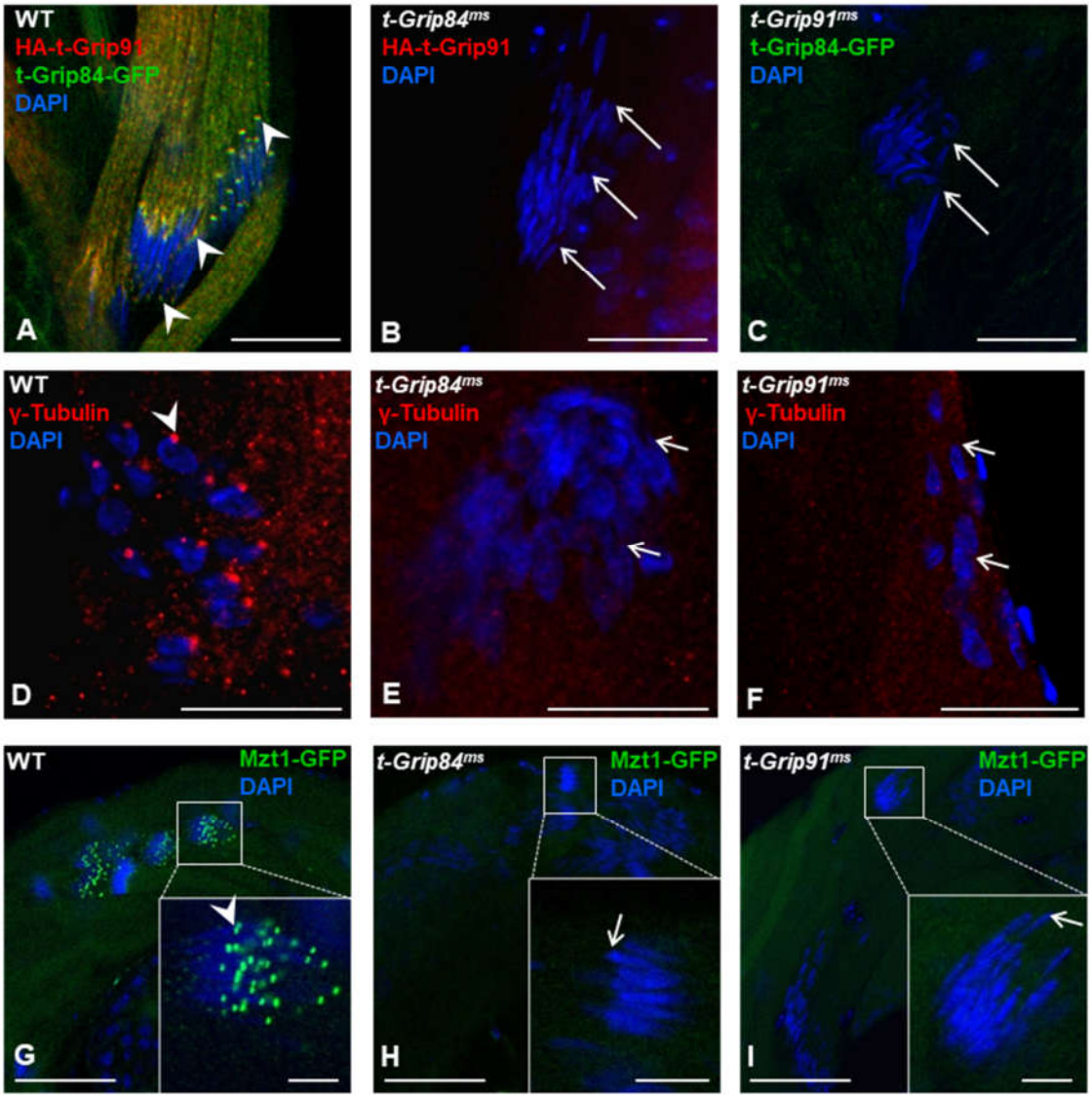

Figure 32. Distribution of t-γ-TuRC proteins in t-γ-TuRC mutants. A. HA-t-Grip91 and t-Grip84-GFP colocalizing at the centriole adjunct and the nuclear tip. **B, C.** HA-t-Grip91 and t-Grip84-GFP became cytosolic in *t-Grip84*^{ms} and *t-Grip91*^{ms} mutants respectively. **D-I.** γ-tubulin (D, E, F) and Mzt1 (G, H, I) both became cytosolic, and they lost their WT localization profile in *t-Grip84*^{ms} and *t-Grip91*^{ms} mutants. Scale bars: Scale bars: (A–F) 20 µm, G-I 50 µm, insets 10 µm.

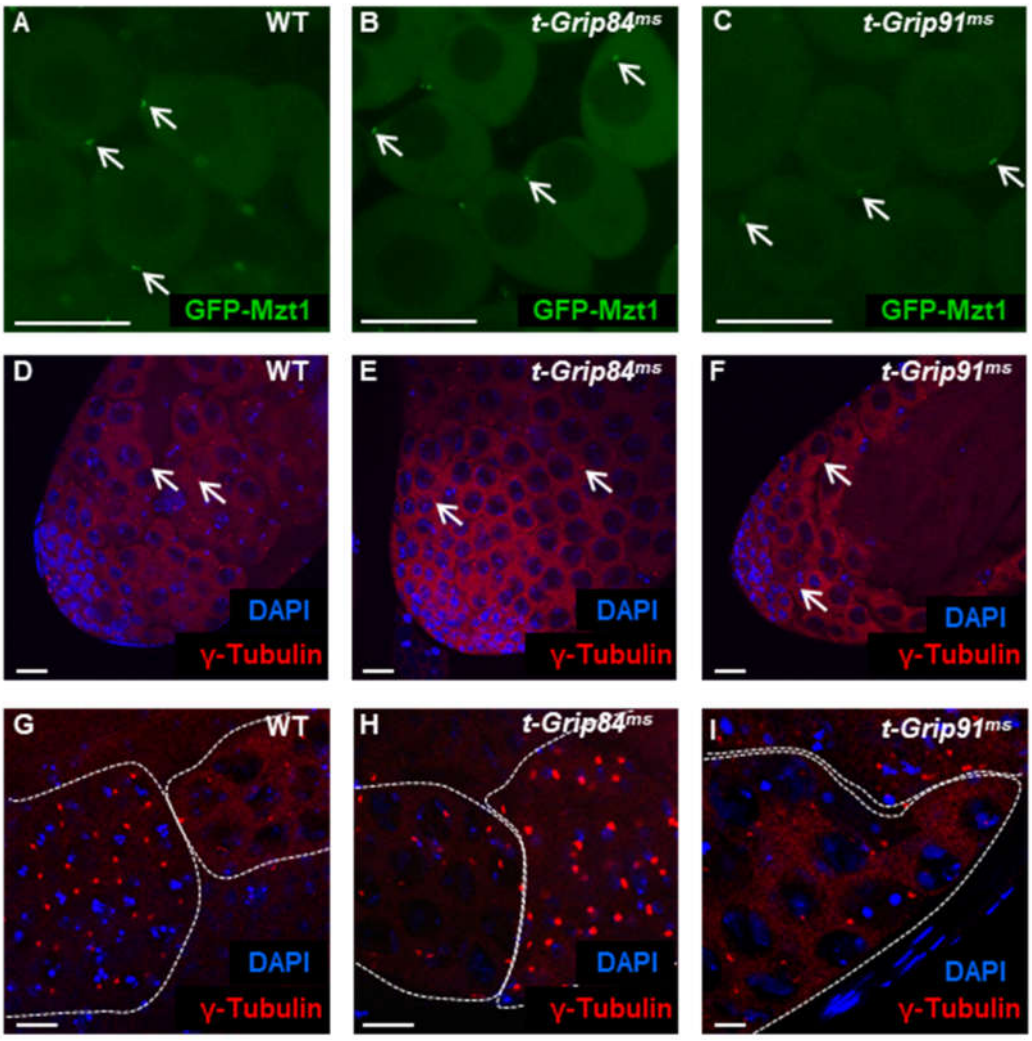

Figure 33. Localization of GFP-Mzt1 and γ-tubulin in t-γ-TuRC mutants. GFP-Mzt1 and γ-tubulin localize to the centrosome (arrows) in WT (**A**, **D**, **G**), *t-Grip84*^{ms} (**B**, **E**, **H**) and *t-Grip91*^{ms} (**C**, **F**, **I**) `spermatocytes`. Nuclei stained with DAPI (blue). Scale bars: 20 μm.

We concluded that the t-γ-TuRC members influence each other's localization and despite normal axoneme assembly, basal body attachment to the nucleus and integrity of the cysts are disturbed in the *t-Grip84*^{ms} and *t-Grip91*^{ms} mutants. Taken together, these results suggest that the observed abnormalities in the mutants are not due to the disappearance of centriole adjunct or general failure of sperm development (Alzyoud et al., 2021).

4.6 Interactions of t-γ-TuRC and partner proteins

γ-Tubulin exists in two related complexes, the γ-TuSC and the γ-TuRC in Drosophila (Oegema et al., 1999). The ubiquitous Grip84 and Grip91 containing γ-TuSC is a structural subunit of the γ-TuRC, a larger complex with additional proteins, such as Grip128, Grip163, Grip75, Grip71 and Mzt1 (Gunawardane et al., 2000). The genetic results and the localization pattern of the t-γ-TuRC suggested that an alternative γ-TuRC could assemble in the post-meiotic stages of spermatogenesis, but its molecular composition is unknown. To get an insight into the t-γ-TuRC structure, first, we performed a yeast two-hybrid analysis (Y2H) to test the interactions between t-γ-TuRC proteins in every combination. We also included γ-tubulin in this analysis, due to the known interaction with the ubiquitous γ-TuRC.

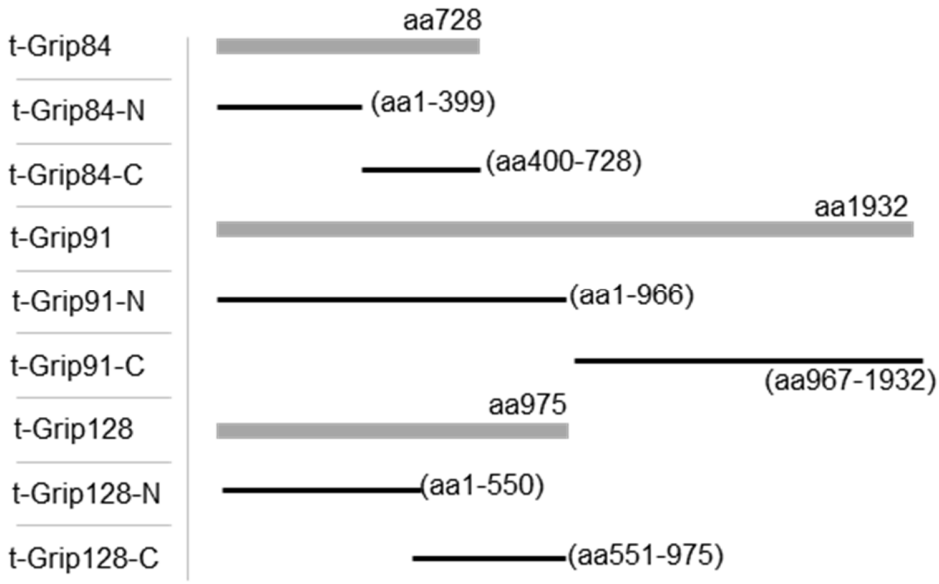

Figure 34. t-γ-TuRC protein fragments used in the yeast two-hybrid analysis. N- and C-terminal fragments of t-γ-TuRC proteins were used in yeast two-hybrid experiments. Full protein length is indicated, while breakpoints are labelled in the case of fragments.

Due to the large size of the proteins, we divided all three t-γ-TuRC proteins into an N-terminal and a C-terminal part (**Figure 34)** and cloned them into pGAD424 and pGBT9 prey and bait vectors. First, we tested the interaction between the t-γ-TuRC proteins and γ-Tubulin. Drosophila encodes two γ-Tubulin, γ-Tub23C and γ-Tub37C. γ-Tub37C expresses only in the female

germline, and it was proven to be a maternal gamma-tubulin, therefore we used γ-Tub23C in the Y2H. We found that t-Grip84-N, t-Grip91-N, and t-Grip128-C bind to the ubiquitously expressed γ-Tub23C (**Figure 35 A, B**).

Next, we tested the interaction between fragments of t-γ-TuRC proteins and found that t-Grip84-N interacts with both t-Grip91-N and t-Grip91-C. Moreover, t-Grip91-C shows binding with t-Grip84-C and t-Grip128-C. t-Grip91-N also shows binding with both t-Grip128-N and t-Grip128-C in yeast two-hybrid assays (**Figure 35 A, B**).

Interaction of the N-terminal of ubiquitous Grip91 and Mzt1 was previously reported, however, the precise subcellular location of this interaction was not investigated before (Tovey et al., 2018). Based on the strong colocalization between GFP-Mzt1 and the tagged t-γ-TuRC proteins in the post-meiotic spermatids, we predicted direct interaction between them. We found that only t-Grip91-N shows interaction with Mzt1 in Y2H (**Figure 35 A, B** and **Supplementary Figure 5**) (Alzyoud et al., 2021).

A

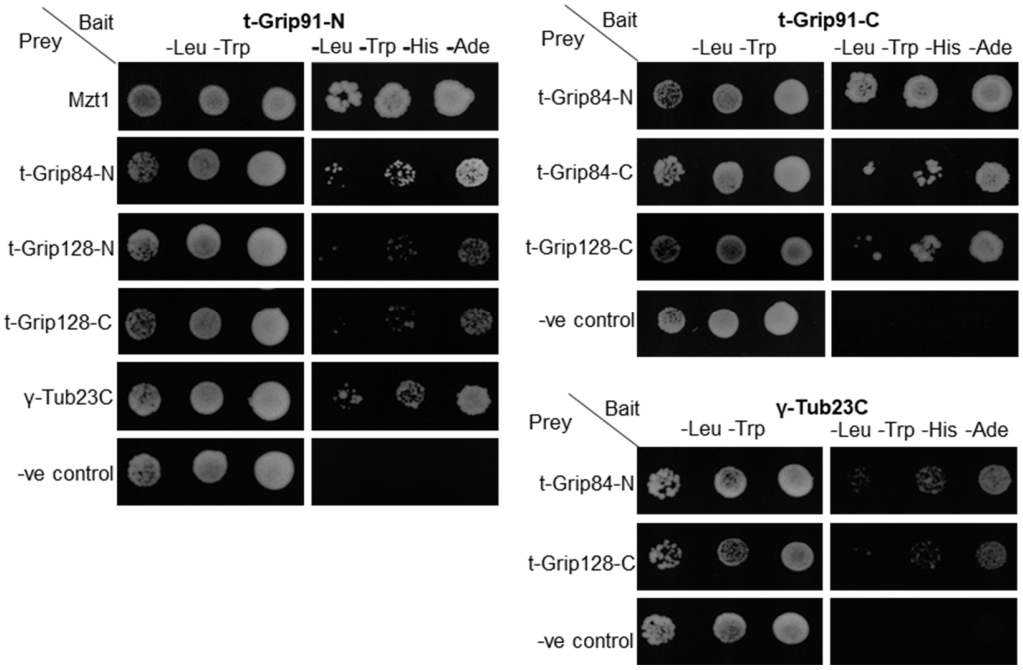

B

	t-Grip84-N	t-Grip84-C	t-Grip91-N	t-Grip91-C	t-Grip128-N	t-Grip128-C
γ-Tub23-C	+	-	+	-	-	+
Mzt1	-	-	+	-	-	-
t-Grip84-N			+	+	-	-
t-Grip84-C			-	+	-	-
t-Grip91-N					+	+
t-Grip91-C					-	+

Figure 35. Summary of the Y2H interactions of t-γ-TuRC proteins. A. Yeast containing the bait and the prey vectors was grown on -Leu, -Trp plates (control), -Leu, -Trp, -His, -Ade plates (test). **B**. Summary of the positive and the negative Y2H results.

To confirm the Y2H results, we performed direct binding experiments. To do so, we expressed, the GST tagged version of the t-γ-TuRC proteins (N- or C-terminal parts as bait). We also cloned the coding region of the protein fragments downstream of a T7 promoter, which enabled us of producing preys with a coupled *in vitro* transcription-translation (IVTT) system. Bait proteins were mixed with ^{35}S-methionine-labelled preys, and physical interactions were detected by autoradiography of the protein samples from the interaction experiments. Results of the *in vitro* binding experiments supported the yeast two-hybrid findings (**Figure 36** and **Supplementary Figure 6**).

Consequently, we proved with two independent experimental systems that all three t-γ-TuRC proteins could bind to each other and to γ-tubulin, but only the N-terminal t-Grip91 shows interaction with Mzt1 (**Figure 36** and **Supplementary Figure 6**, **7**). Furthermore, our results suggest complex and diverse t-γ-TuRC composition, which implies the possibility of multiple t-γ-TuRCs with diverse localization abilities during the post-meiotic stages of spermatogenesis.

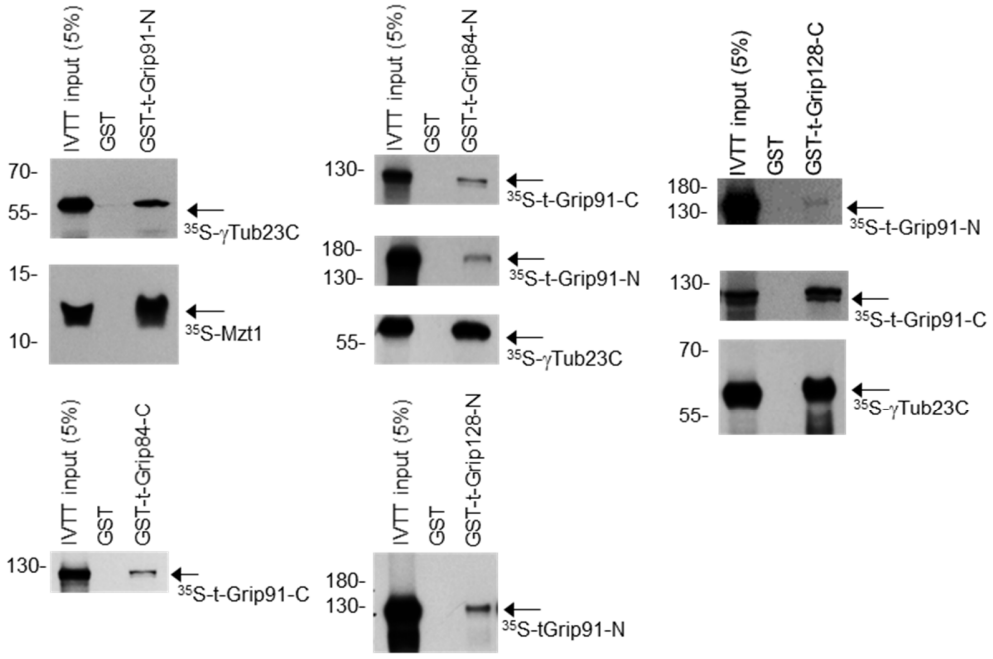

Figure 36. t-γ-TuRC interacting partners by IVTT system. Autoradiography for the interactions between GST tagged fragments of t-γ-TuRC proteins and ^{35}S-methionine labelled t-γ-TuRC component proteins.

5 Discussion

MTs are an essential part of the eukaryotic cytoskeleton, playing crucial roles in cell division, and intracellular transport between organelles and cellular compartments. MTs are mainly formed *de novo* at specific positions in the cell, termed MT organization centers (MTOCs). Depending on their location in the cell, centrosomal and non-centrosomal MTOCs can be distinguished. The nucleation of MTs from α and β-tubulin dimers is an essential cellular process; however, they are operating with a distinct set of participating proteins in the different MTOCs. There is one common factor likely required for MT nucleation in all different locations, γ-tubulin. This protein is conserved throughout eukaryotes and shares high homology with α-tubulin and β-tubulin. γ-tubulin is a member of γ-TuRC, a complex with conserved composition and function.

Recruitment of γ-TuRCs to different MTOCs at different time points influences MT array establishment, but how this is regulated is not completely understood. It is also not clear whether all γ-TuRCs have the same composition within the same organism and the heterogeneity in localization and function might be the result of the different compositions of the γ-TuRCs. Upon assembly γ-TuRC has basal microtubule nucleation activity only, activators incorporation stimulates microtubule nucleation (Wiese and Zheng, 2006). γ-TuRC consists of γ-tubulin, five related γ-tubulin complex proteins, (GCP2, GCP3, GCP4, GCP5, GCP6) and (variable) additional γ-TuRC proteins (Oakley et al., 2015). γ-tubulin is part of a complex, namely the 300 kDa γ-TuSC, which contains γ-tubulin complex proteins GCP2 and GCP3 and forms the MT nucleator in *Saccharomyces cerevisiae* (Oegema et al., 1999). In higher eukaryotes, the 2.2 MDa γ-TuRC contains the γ-TuSC in multiple copies, as well as GCP4, GCP5 and GCP6 (Zheng et al., 1995; Martin et al., 1998; Moritz et al., 1998; Murphy et al., 1998; Fava et al., 1999; Oegema et al., 1999). We believe that the variety of these MTOCs has a different protein composition based on their subcellular position and function, γ-TuRCs might play a role in the diversification of these MTOCs.

D. melanogaster is an ideal model to study the assembly and regulation of conserved protein complexes, related to the cytoskeletal organization in somatic and germ cells. Sequence analysis of γ-TuRC subunits revealed that the γ-TuRC is conserved, composing of γ-TuSC with the Grip84 and Grip91 and with the addition of Grip75, Grip128 and Grip163, γ-TuRC is formed in Drosophila (Gunawardane et al., 2000). More and more evidence suggests that testis-specific gene products contribute to the MTOCs during Drosophila spermatogenesis (Chen et al., 2017; Tovey

et al., 2018). Based on sequence homology analysis we found that *Drosophila melanogaster* genome encodes three testis-specific γ-TuRC paralogues of the evolutionary conserved genes (*Grip84*, *Grip91* and *Grip128),* namely *t-Grip84*, *t-Grip91*, and *t-Grip128*. Gene duplication is an important process in molecular evolution, providing the possibility of neofunctionalization and subfunctionalization of the duplicated gene (White-Cooper and Bausek, 2010). Gene duplications provide a possibility for the testis-specific duplicates to adapt and evolve for the specialized sperm-specific organelles, without compromising the function and regulation of the ubiquitous counterpart. It was shown that many genes related to metabolism, protein degradation and cytoskeletal organization have duplicated retrogenes with testis-specific transcript enrichment patterns in the late stages of spermatogenesis (Vlasschaert et al., 2017; Vedelek et al., 2018). ubiquitous γ-TuRC components have a typical gene structure with multiple exons and introns. The newly identified testis-specific γ-TuRC proteins have one exon and no introns, which is a typical gene structure of retrogenes. The duplication of γ-TuRC genes in Drosophila could be beneficial is to meet the high demand for MT nucleation during spermatogenesis, where a 12um spermatocyte elongates to a 1.8 mm long spermatid. Additionally, the testis-specific genes might contribute to the regulation of MTs dynamics during spermatogenesis, when the spermatids are going through intensive morphological changes.

The protein structure of the ubiquitous Grip84, Grip91 and Grip128 is typical γ-TuRC protein structures. All ubiquitous Grip proteins share two short (100–200 amino acids) homologous regions, termed the GCP-N and GCP-C motifs (Gunawardane et al., 2000; Murphy et al., 2001), as well as non-homologous coiled-coil domains. While the GCP-N motif is involved in lateral contact surfaces between Grips within γ-TuRCs, GCP-C forms a part of the conserved γ-tubulin-binding interface (Kollman et al., 2010; Guillet et al., 2011). In the testis-specific γ-TuRC proteins only t-Grip84 has GCP-N and GCP-C domains, in the case of t-Grip91 and t-Grip128 they only have GCP-N domain; however, we found direct binding between these proteins and γ-tubulin. These results suggest that γ-tubulin-binding of t-Grip91 and t-Grip128 is independent of the GCP-C domain. We found that *t-Grip84*, *t-Grip91*, and *t-Grip128* all have high transcript enrichment in the middle-basal part of the testis with a high testis specificity index. However, transcript enrichment of the ubiquitous γ-TuRC components was restricted to the apical part of the testis with lower testis specificity index. We believe that the newly identified γ-TuRC proteins form a testis-specific γ-TuRC (t-γ-TuRC) in the post-meiotic stages of spermatogenesis. This was supported by

the analysis of the localization of t-γ-TuRC proteins. We found that they start to localize first after meiosis in the round spermatids, but not in the stem cells or the mitotic or meiotic spermatocytes. This may indicate that Drosophila spermatogenesis operates with two different γ-TuRCs, starting with the general centrosomally localizing γ-TuRC in the mitotic and meiotic spermatocytes and after meiosis, t-γ-TuRC assembles and incorporates into different MTOCs of the developing spermatids. The first appearance of the tagged t-Grip84, t-Grip91 and t-Grip128 is at the centriole adjunct of the round spermatid. Centriole adjunct localization of the t-γ-TuRC proteins persisted through spermatid elongation and disappeared in the fully elongated spermatids. Several components of the spermatids basal body and centriole adjunct are not present in the mature sperm, suggesting their reduction in late spermiogenesis (e.g. γ-Tubulin, Sas4, Sas6) (Raynaud-Messina et al., 2001; Blachon et al., 2014; Alzyoud et al., 2021).

Additional localization for the t-γ-TuRC proteins was proven during spermatid elongation. We found t-γ-TuRC specific signals at the apical tip of the elongating nucleus, opposite to the centriole adjunct. It was proved recently that γ-tubulin localizes to ncMTOC at the apical tip of the elongating nucleus (Riparbelli et al., 2020). The centrosome associated proteins Rb188 and Spd-2 were found on the apical tip of the nucleus previously as well (Riparbelli et al., 1997, 2020; Feng et al., 2017) Here we show that t-γ-TuRC proteins could be members of this ncMTOC. Neither CnnT nor Cnn was reported to localize at the apical tip of the nucleus; however, Spd2 is localizing to the nucleus tip. Spd2 is a known Cnn binding protein, therefore, it is possible that Spd2 alone is involved in t-γ-TuRC recruitment to the apical tip of the nucleolar associated ncMTOC (Chen et al., 2017; Riparbelli et al., 2020) It is also an open question what proteins are responsible for recruiting t-γ-TuRC to the elongating nucleus. Apical nucleolar tip localized ncMTOC might contribute to proper nuclear elongation, through the perinuclear MTs. It could be involved in the organization of the apically localized acroblast and later the acrosome. Further experiments are necessary to describe the function of this alternative ncMTOC.

During late spermatid elongation, we found a third localization focus for both the t-γ-TuRC proteins and Mzt1 at the surface of elongating mitochondria. Mzt1 is a small, conserved protein involved in γ-TuRC recruitment to MTOCs (Masuda et al., 2013). Our accurate description of Mzt1 complements the previously reported basal body-specific localization of Mzt1 (Tovey et al., 2018). We localized Mzt1 to the centrosome, basal body, centriole adjunct, nuclear apical tip and to the surface of the mitochondria throughout spermatogenesis. We found Mzt1 simultaneously at

the basal body and the mitochondria of meiotic spermatocytes. It was even colocalized with the t-γ-TuRC in all 3 different localization foci, which suggests that Mzt1 is involved in the ubiquitous γ-TuRC formation before meiosis and got incorporated into the t-γ-TuRC after meiosis in every MTOC focus. It was shown that γ-tubulin has an overlapping localization with mitochondrial marker ATP5. The testis-specific isoform of Centrosomin (CnnT), the binding partner of γ-tubulin, can recruit the human ubiquitous γ-TuRC proteins, GCP2 and GCP5, to the mitochondria in Hek293 cells and CnnT itself localizes on the surface of spermatid mitochondria, converting mitochondria into MTOCs during spermatid development (Chen et al., 2017). Mutation in CnnT did not affect the mitochondrial elongation which suggests the existence of compensation for the disruption of the mitochondrial surface ncMTOC (Chen et al., 2017). It is tempting to speculate that, despite both Mzt1 and γ-tubulin bind to the ubiquitous γ-TuRC prior to the meiotic stages, following meiosis, Mzt1, and probably γ-tubulin, can also be recruited to different ncMTOCs by the t-γ-TuRC. Additional experiments are necessary to test whether CnnT is a direct binding partner of t-γ-TuRC, and to test the significance of the mitochondrial association of t-γ-TuRC and its interactor proteins (Alzyoud et al., 2021).

MTOCs containing t-γ-TuRC could participate in MT nucleation, playing a role in the dynamics of the intensive morphological changes during spermatogenesis. An alternative possible role t-γ-TuRC could be to have a function in the stabilization of the already existing MTs, which was reported previously in Drosophila S2 cells (Bouissou et al., 2009). MTs surrounding the elongating nuclei could be held or anchored by t-γ-TuRC, which localized at the nuclear tip MTOC. While in the case of the mitochondria surface MTOC starts to form after meiosis, where t-γ-TuRC proteins are not localizing to the mitochondria. Mitochondrial surface MTOC could be the first source of MTs, guiding and controlling mitochondrial elongation. t-γ-TuRC localize to the surface of the late elongating mitochondria only, which further supports that their main role could be to stabilize the existing MTs maintaining the length of the mitochondria.

Mutants for the t-γ-TuSC components *t-Grip84* and *t-Grip91* were found to be male sterile and male semi-sterile respectively, in homozygous, trans-heterozygous and hemizygous combinations; however, *t-Grip128* mutant is fertile. Early stages of spermatogenesis before meiosis were normal similar to WT in $t\text{-}Grip84^{ms}$ and $t\text{-}Grip91^{ms}$ mutants, which is expected since the t-γ-TuRC start to localize during spermiogenesis exclusively after meiosis. We checked the axoneme formation and development in t-γ-TuSC mutants $t\text{-}Grip84^{ms}$ and $t\text{-}Grip91^{ms}$ and found that axonemes were

normally developed and elongated in t-γ-TuSC mutants. Post-meiotic localization of γ-tubulin and Mzt1 was found to be disrupted in *t-Grip84*^{ms} and *t-Grip91*^{ms}mutants. While the basal bodies were detached from the nuclei, which suggests that the t-γ-TuSC proteins are important for maintaining the basal body nucleus attachment. Mutants for the ubiquitous γ-TuRC proteins *Grip75* and *Grip128* are male sterile, with a phenotype manifest in the post-meiotic stages of spermatogenesis, resembling *t-Grip84* and *t-Grip91* mutants. (Vogt, 2006). *Grip75* and *Grip128* mutants phenotype is similar to *t-Grip84* and *t-Grip91* mutants, as they result in a scattered nuclei during elongation as well as the production of elongated non motile sperms (Vogt, 2006). This means that neither the ubiquitous nor the testis-specific γ-TuRC is essential for axoneme development during Drosophila spermatogenesis (Fabian and Brill, 2012).

Taking these results together with earlier findings, we suggest that t-Grip128, Mzt1 and CnnT could have a moderator or redundant roles, in contrast to t-Grip84, t-Grip91, Grip75 and Grip128, which likely have more fundamental roles in spermatid development (Vogt, 2006; Chen et al., 2017; Tovey et al., 2018).

Targeting γ-tubulin to the elongating spermatids is not dependent on Grip75 or Grip128, despite the γ-tubulin binding capacity of both proteins (Vogt, 2006). While all tested γ-TuRC and t-γ-TuRC proteins could bind to γ-tubulin *in vitro*, the localization of γ-tubulin is disturbed only in the post-meiotic cysts of the *t-Grip84*^{ms} and *t*-Grip91^{ms} mutants. This strongly suggests that t-Grip84 and t-Grip91 are fundamental in the centriole adjunct, nuclear tip and mitochondrial recruitment of γ-tubulin in the post-meiotic stages. Based on the late spermatogenesis phenotype of *Grip75* and *Grip128* mutants, and the fact that Grip163 (GCP6) was shown to be part of the Drosophila sperm proteome, we can imagine that some of the ubiquitous γ-TuRC proteins could be present in the t-γ-TuRC and inherited through the sperm following fertilization (Vogt, 2006; Wasbrough et al., 2010).

We believe that our results open a new avenue to understand the composition of alternative γ-TuRCs in different specialized cell types, such as the spermatids, and the function of MTOCs' heterogeneity (Alzyoud et al., 2021).

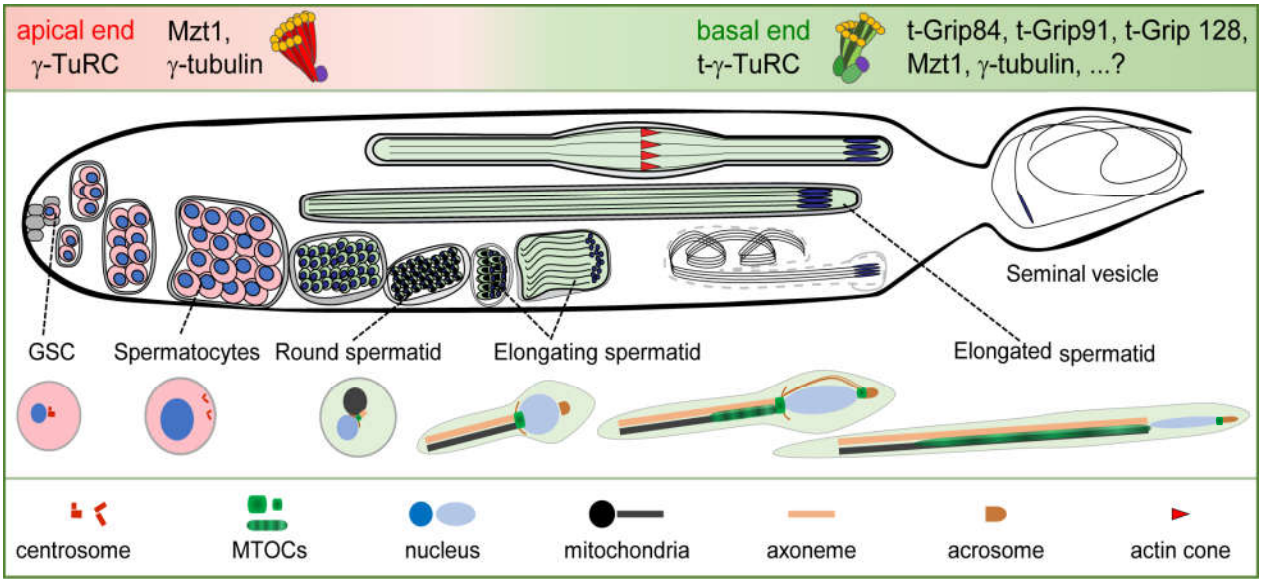

Summary of the various stages of spermatogenesis with highlighting the stage specific MTOCs. Core γ-TuRC and its binding proteins localize to the centrosome in spermatocytes. From the round spermatid stage t-γ-TuRC, γ-Tubulin and Mzt1 accumulate first on the centriole adjunct and besides the centriole adjunct also on at the apical tip of the nuclei and on the surface of the elongating mitochondria of spermatids.

6 Summary

Drosophila melanogaster spermatogenesis harbor various MTOCs, which makes it a good model to study MTOCs and their components, like γ-TuRC. In addition, spermatogenesis and sperm structure show a high degree of conservation among different organisms. In this study, we identified 3 testis-specific γ-TuRC component proteins, t-Grip84, t-Grip91 and t-Grip128. Transcripts of t-γ-TuRC genes accumulate in the middle-basal part of the testis with a high testis specificity index. Transcripts of the ubiquitous *Grip84*, *Grip91* and *Grip128* accumulate at the apical region of the testis with a low testis-specificity index. The mutant lines of *t-Grip84, t-Grip91* and *t-Grip128* were analyzed in detail in this study. Mutants of *t-Grip84* were male sterile in homozygous, hemizygotes and transheterozygous, while *t-Grip91* mutants were male semi-sterile in homozygous and hemizygotes. *t-Grip128* mutant *t-Grip128$^{\Delta 65}$* was male-fertile, with fertility comparable to the wild type. We found that transcripts of *t-Grip84*, *t-Grip91* and *t-Grip128* were highly reduced in testis extracts of *t-Grip84^{ms}*, *t-Grip91^{ms}* and *t-Grip128$^{\Delta 65}$* mutants respectively, which indicates that those mutants are null alleles. Since t-Grip84 has a typical Grip protein structure we checked t-Grip84 localization to the centrosome of the Drosophila Dmel2 cells. We found that t-Grip84-GFP was able to localize to the centrosome of Drosophila Dmel2 cells. We established transgenic lines for the t-γ-TuRC proteins with different tags to test their subcellular distribution. We did not find t-Grip84-GFP, t-Grip84-mCh, HA-t-Grip91 or HA-t-Grip128 proteins in epithelial tissue or ovaries. t-γ-TuRC proteins appeared only in the testis during spermatogenesis. t-Grip84-mCh (GFP), HA-t-Grip91 and HA-t-Grip128 have a dynamic localization pattern during spermatogenesis, the proteins were not present during the early stages of spermatogenesis in GSCs, mitotic or meiotic cells. t-γ-TuRC proteins start to localize after meiosis at the centriole adjuncts of the round spermatid and their localization persists during elongation at the centriole adjuncts but disappears in the elongated spermatids. Later during elongation, the t-γ-TuRC proteins appear at the anterior tip of the elongated nucleus. Moreover, a third localization focus of the proteins starts to emerge on the surface of the mitochondria. We tested the colocalization between the t-γ-TuRC proteins, γ-tubulin and the t-γ-TuRC interacting protein Mzt1. t-Grip84, t-Grip91 and t-Grip128 all colocalize with each, other with γ-tubulin and Mzt1 at the centriole adjuncts during elongation. The anterior tip localization was shared between all t-γ-TuRC proteins, t-Grip84-mCh (GFP) HA-t-Grip91 and HA-t-Grip128. In the case of GFP-

Mzt1, the signal starts to localize at the beginning of spermatogenesis to the centrosome of spermatocytes. Later at meiotic spermatids, GFP-Mzt1 signal was visible at the centrosome and the mitochondria. During later stages of elongation GFP-Mzt1 and γ-Tub23C-GFP colocalized with the t-γ-TuRC proteins at the centriole adjunct, the apical tip of the nuclei and the surface of the elongating mitochondria. t-γ-TuRC proteins colocalized with the PCM proteins PACT and Ana1 in addition to the centrosomal protein Asl and the ubiquitous γ-TuRC protein Grip163. In *t-Grip84*^{ms} and *t-Grip91*^{ms} mutants, early stages of spermatogenesis were normal. The axonemes of *t-Grip84*^{ms} and *t-Grip91*^{ms} mutants were normally developed and elongated. During elongation, the basal bodies detached from the nuclei where the nuclei were scattered in the cytoplasm. The ICs were normally formed but their movement was disturbed as they start their migration. ICs became scattered in *t-Grip84*^{ms} and *t-Grip91*^{ms} mutants. Neither t-Grip84-GFP nor HA-t-Grip91 were able to localize in *t-Grip91*^{ms} and *t-Grip84*^{ms} respectively. The same γ-tubulin and GFP-Mzt1 were not localized to the elongating spermatids in the mutants of *t-Grip91*^{ms} and *t-Grip84*^{ms}. We divided the t-γ-TuRC proteins into two parts N- and C- terminal parts to test their interactions biochemically using yeast two-hybrid and IVTT. All t-Grip84, t-Grip91 and t-Grip128 bind to each other and γ-tubulin, while only the N-terminal part of t-Grip91 binds to Mzt1.

In conclusion, we identified three testis-specific γ-TuRC proteins, which have dynamic localization throughout spermatogenesis. They start to localize to the centriole adjunct after meiosis, then simultaneously localize to the apical tip of the nucleus and the basal body and finally during the late elongation stages they localize near the surface of the mitochondria. t-γ-TuRC proteins bind to each other and γ-tubulin while only t-Grip91-N binds to Mzt1. This all suggests that Drosophila spermatogenesis functions with two different γ-TuRC, the ubiquitous γ-TuRC and the newly identified t-γ-TuRC. The ubiquitous γ-TuRC is involved in MTOCs organization till the end of the meiosis, whereas t-γ-TuRC is involved in MTOCs after meiosis. Since the majority of Drosophila and human genes share high homology, studying and modelling the organization and composition of different MTOCs in flies could have great potential to understand better several human diseases such as microcephalies, ciliopathies and even cancer.

7 Összefoglaló

A spermatogenesis folyamata és az érett spermiumok szerkezete magas fokú evolúciós konzerváltságot mutat. A fejlődő Drosophila spermatidákban számos mikrotubulus szervező központ kialakulása figyelhető meg. Célunk volt 3 tesztisz-specifikus γ-TuRC genetikai és molekuláris jellemzése. A részletes genetikai jellemzés megmutatta, hogy a t-Grip84 és t-Grip91 mutánsok hímsterilek, míg a t-Grip128 null mutánsa fertilis. A t-Grip84 és t-Grip91 mutánsokban a korai spermatogenezis normális, a spermatidák farki részében kilakul az axonéma. Az elongáció során a mutánsokban a magmembránba ágyazott bazális testek leválnak és a sejtmagok szinkronizált mozgása sérült, és érett egyedi spermiumok nem figyelhetők meg a szeminális vezikulumokban.

A GFP jelölt t-Grip84 képes volt a szomatikus sejtek centroszómájába belépülni Dmel-2 sejtekben. Transzgenikus vonalakat hoztunk létre, ahol a saját genomi szabályozásása által vezérelt t-γ-TuRC fehérjékhez különböző jelzőfehérjéket építve vizsgáltuk a tesztiszen belüli szubcelluláris lokalizációjukat. A t-γ-TuRC fehérjék csak a herében fejeződnek ki. A t-γ-TuRC fehérjék a meiózist követően kezdenek lokalizálódni a kerek spermatidák bazális testeinek környékén. Később az elongáció során a t-γ-TuRC fehérjék megjelennek a megnyúlt mag elülső csúcsán, a mag megnyúlásával párhuzamosan. Ezenkívül a mitokondriumok felszínén is megfigyelhető a t-γ-TuRC lokalizáció, ahol a t-γ-TuRC fehérjék a γ-tubulinnal és Mzt1-gyel is együtt lokalizálódnak. A mutánsokban a paralog t-γ-TuRC fehérjék lokalizációja hibás. Sem a γ-tubulin, sem a Mzt1 nem lokalizálódott a megnyúló spermatidákban a t-Grip91ms és t Grip84ms mutánsaiban, jelezve ezzel, hogy a komplex kialakításához a t-γ-TuRC fehérjék elengedhetetlenek. A t-γ-TuRC fehérjék biokémiai tesztelése élesztő kettős hybrid és IVTT technológiával megmutatta, hogy a t-Grip84, t-Grip91 és t-Grip128 fehérjék kötődnek egymáshoz és a γ-tubulinhoz. Bizonyítottuk, hogy a t-Grip91 N-terminális része specifikusan kötődik a Mzt1-hez.

Összefoglalva, három here-specifikus γ-TuRC fehérjét azonosítottunk, amelyek dinamikus lokalizációval rendelkeznek a spermatogenezis során. A t-γ-TuRC fehérjék a sejtmag megnyúlásában, illetve a mitokondrium felszínén létrejövő nem-centroszómális mikrotubulus szervező központok kialakításában kulcsfontosságúak és nélkülözhetetlenek a normális fertilitáshoz.

8 Acknowledgment

I would like to thank my supervisor Dr. Rita Sinka for accepting me in her group, for all the guidance and the advice throughout my PhD time and for the opportunity she provided me to learn and practice a whole set of genetic and molecular techniques. I am grateful to Dr. Viktor Vedelek for the advice, suggestions and help through my work time. I am grateful for all members of Drosophila spermatogenesis group for all the support and the help they gave me. I am grateful also for the Department of Genetics.

I would like to thank Dr. Zoltan Lipinszki for the tissue culture and the IVTT experiment. I would like to spread my thanks for Prof. Gábor Juhász and Dr. Attila L. Kovács for the electron microscopy, and the injection facility of ELKH-BRC, Szeged. I would deeply thank Dr. Zsolt Datki and Dr. Ferenc Jankovics for reading my thesis and for the constructive thoughts and comments they made.

Also, I express my appreciation for my friends especially Alexandra, Nizar, Bence and Afnan who made my time here pleasant and smooth.

Last but not least, many thanks to my parents and siblings for all the support and the encouragement! Reham, Mohammed and Hamidi, you enlightened my times alone, thanks for you.

Funding:

This work was supported by the NKFIH_OTKA 132155 and GINOP 2.3.2-15-2016-00032

9 References

Alzyoud, E., Vedelek, V., Réthi-Nagy, Z., Lipinszki, Z., and Sinka, R. (2021). Microtubule Organizing Centers Contain Testis-Specific γ-TuRC Proteins in Spermatids of Drosophila. *Front. Cell Dev. Biol.* 9, 727264. doi:10.3389/fcell.2021.727264.

Anders, A., Lourenço, P. C. C., and Sawin, K. E. (2006). Noncore components of the fission yeast gamma-tubulin complex. *Mol. Biol. Cell* 17, 5075–5093. doi:10.1091/mbc.e05-11-1009.

Atwood, S. X., Li, M., Lee, A., Tang, J. Y., and Oro, A. E. (2013). GLI activation by atypical protein kinase C ι/λ regulates the growth of basal cell carcinomas. *Nature* 494, 484–488. doi:10.1038/nature11889.

Bai, Y., Casola, C., Feschotte, C., and Betrán, E. (2007). Comparative genomics reveals a constant rate of origination and convergent acquisition of functional retrogenes in Drosophila. *Genome Biol.* 8, 1–9. doi:10.1186/gb-2007-8-1-r11.

Baker, J. D., Adhikarakunnathu, S., and Kernan, M. J. (2004). Mechanosensory-defective, male-sterile unc mutants identify anovel basal body protein required for ciliogenesis inDrosophila. *Development* 131, 3411–3422. doi:10.1242/dev.01229.

Barbosa, V., Yamamoto, R. R., Henderson, D. S., and Glover, D. M. (2000). Mutation of a Drosophila gamma tubulin ring complex subunit encoded by discs degenerate-4 differentially disrupts centrosomal protein localization. *Genes Dev.* 14, 3126–3139. doi:10.1101/gad.182800.

Basto, R., Gergely, F., Draviam, V. M., Ohkura, H., Liley, K., and Raff, J. W. (2007). Hsp90 is required to localise cyclin B and Msps/ch-TOG to the mitotic spindle in Drosophila and humans. *J. Cell Sci.* 120, 1278–1287. doi:10.1242/jcs.000604.

Basto, R., Lau, J., Vinogradova, T., Gardiol, A., Woods, C. G., Khodjakov, A., et al. (2006). Flies without Centrioles. 1375–1386. doi:10.1016/j.cell.2006.05.025.

Bergkessel, M., and Guthrie, C. (2013). "Chapter Twenty Five - Colony PCR," in *Laboratory Methods in Enzymology: DNA*, ed. J. B. T.-M. in E. Lorsch (Academic Press), 299–309. doi:https://doi.org/10.1016/B978-0-12-418687-3.00025-2.

Bilitou, A., Watson, J., Gartner, A., and Ohnuma, S.-I. (2009). The NM23 family in development. *Mol. Cell. Biochem.* 329, 17–33. doi:10.1007/s11010-009-0121-6.

Blachon, S., Khire, A., and Avidor-Reiss, T. (2014). The Origin of the Second Centriole in the Zygote of Drosophila melanogaster. *Genetics* 197, 199–205. doi:10.1534/genetics.113.160523.

Bouissou, A., Vérollet, C., Sousa, A., Sampaio, P., Wright, M., Sunkel, C. E., et al. (2009). {gamma}-Tubulin ring complexes regulate microtubule plus end dynamics. *J. Cell Biol.* 187, 327–334. doi:10.1083/jcb.200905060.

Carvalho-Santos, Z., Machado, P., Alvarez-Martins, I., Gouveia, S. M., Jana, S. C., Duarte, P., et al. (2012). BLD10/CEP135 Is a Microtubule-Associated Protein that Controls the Formation of the Flagellum Central Microtubule Pair. *Dev. Cell* 23, 412–424.

doi:10.1016/j.devcel.2012.06.001.

Carvalho, A. B., Lazzaro, B. P., and Clark, A. G. (2000). Y chromosomal fertility factors kl-2 and kl-3 of Drosophila melanogaster encode dynein heavy chain polypeptides. 97, 13239–13244. doi:10.1073/pnas.230438397.

Chen, J. V, Buchwalter, R. A., Kao, L.-R., and Megraw, T. L. (2017). A Splice Variant of Centrosomin Converts Mitochondria to Microtubule-Organizing Centers. *Curr. Biol.* 27, 1928-1940.e6. doi:10.1016/j.cub.2017.05.090.

Colombié, N., Vérollet, C., Sampaio, P., Moisand, A., Sunkel, C., Bourbon, H.-M., et al. (2006). The Drosophila gamma-tubulin small complex subunit Dgrip84 is required for structural and functional integrity of the spindle apparatus. *Mol. Biol. Cell* 17, 272–282. doi:10.1091/mbc.e05-08-0722.

Cota, R. R., Teixidó-Travesa, N., Ezquerra, A., Eibes, S., Lacasa, C., Roig, J., et al. (2017). MZT1 regulates microtubule nucleation by linking γTuRC assembly to adapter-mediated targeting and activation. *J. Cell Sci.* 130, 406–419. doi:10.1242/jcs.195321.

D'Angiolella, V., Donato, V., Vijayakumar, S., Saraf, A., Florens, L., Washburn, M. P., et al. (2010). SCF(Cyclin F) controls centrosome homeostasis and mitotic fidelity through CP110 degradation. *Nature* 466, 138–142. doi:10.1038/nature09140.

Dallai, R., Gottardo, M., Mercati, D., Machida, R., Mashimo, Y., Matsumura, Y., et al. (2014). Giant spermatozoa and a huge spermatheca: a case of coevolution of male and female reproductive organs in the ground louse Zorotypus impolitus (Insecta, Zoraptera). *Arthropod Struct. Dev.* 43, 135–51. doi:10.1016/j.asd.2013.10.002.

de Cuevas, M., and Matunis, E. L. (2011). The stem cell niche: Lessons from the Drosophila testis. *Development* 138, 2861–2869. doi:10.1242/dev.056242.

Demarco, R. S., Eikenes, Å. H., Haglund, K., and Jones, D. L. (2014). Investigating spermatogenesis in Drosophila melanogaster. *Methods* 68, 218–227. doi:10.1016/j.ymeth.2014.04.020.

Díaz-Castillo, C., and Ranz, J. M. (2012). Nuclear chromosome dynamics in the drosophila male germ line contribute to the nonrandom genomic distribution of retrogenes. *Mol. Biol. Evol.* 29, 2105–2108. doi:10.1093/molbev/mss096.

Dominado, N., La Marca, J. E., Siddall, N. A., Heaney, J., Tran, M., Cai, Y., et al. (2016). Rbf Regulates Drosophila Spermatogenesis via Control of Somatic Stem and Progenitor Cell Fate in the Larval Testis. *Stem cell reports* 7, 1152–1163. doi:10.1016/j.stemcr.2016.11.007.

Doxsey, S., Zimmerman, W., and Mikule, K. (2005). Centrosome control of the cell cycle. *Trends Cell Biol.* 15, 303–311. doi:10.1016/j.tcb.2005.04.008.

Dumont, J., and Desai, A. (2012). Acentrosomal spindle assembly and chromosome segregation during oocyte meiosis. *Trends Cell Biol.* 22, 241–249. doi:10.1016/j.tcb.2012.02.007.

Enjolras, C., Thomas, J., Chhin, B., Cortier, E., Duteyrat, J.-L., Soulavie, F., et al. (2012). Drosophila chibby is required for basal body formation and ciliogenesis but not for Wg

signaling. *J. Cell Biol.* 197, 313–325. doi:10.1083/jcb.201109148.

Fabian, L., and Brill, J. A. (2012). Drosophila spermiogenesis: Big things come from little packages. *Spermatogenesis* 2, 197–212. doi:10.4161/spmg.21798.

Fabrizio, J. J., Hime, G., Lemmon, S. K., and Bazinet, C. (1998). Genetic dissection of sperm individualization in Drosophila melanogaster. *Development* 125, 1833–1843. doi:10.1242/dev.125.10.1833.

Farache, D., Jauneau, A., Chemin, C., Chartrain, M., Rémy, M.-H., Merdes, A., et al. (2016). Functional Analysis of γ-Tubulin Complex Proteins Indicates Specific Lateral Association via Their N-terminal Domains. *J. Biol. Chem.* 291, 23112–23125. doi:10.1074/jbc.M116.744862.

Fári, K., Takács, S., Ungár, D., and Sinka, R. (2016). The role of acroblast formation during Drosophila spermatogenesis. *Biol. Open* 5, 1102–1110. doi:10.1242/bio.018275.

Fava, F., Raynaud-Messina, B., Leung-Tack, J., Mazzolini, L., Li, M., Guillemot, J. C., et al. (1999). Human 76p: A new member of the gamma-tubulin-associated protein family. *J. Cell Biol.* 147, 857–868. doi:10.1083/jcb.147.4.857.

Feng, Z., Caballe, A., Wainman, A., Johnson, S., Haensele, A. F. M., Cottee, M. A., et al. (2017). Structural Basis for Mitotic Centrosome Assembly in Flies. *Cell* 169, 1078-1089.e13. doi:10.1016/j.cell.2017.05.030.

Filigheddu, N., Gnocchi, V. F., Coscia, M., Cappelli, M., Porporato, P. E., and Taulli, R. (2007). Santiago M. Di Pietro,* Juan M. Falco ´n-Pe ´rez,* Danie `le Tenza,† Subba R.G. Setty,‡ Michael S. Marks,‡ Grac ¸a Raposo,† and Esteban C. Dell'Angelica*. *Mol. Biol. Cell* 18, 986–994. doi:10.1091/mbc.E06.

Fry, A. M., Sampson, J., Shak, C., and Shackleton, S. (2017). Recent advances in pericentriolar material organization: ordered layers and scaffolding gels. *F1000Research* 6, 1622. doi:10.12688/f1000research.11652.1.

Fu, J., Lipinszki, Z., Rangone, H., Min, M., Mykura, C., Chao-Chu, J., et al. (2016). Conserved molecular interactions in centriole-to-centrosome conversion. *Nat. Cell Biol.* 18, 87–99. doi:10.1038/ncb3274.

Galletta, B. J., Ortega, J. M., Smith, S. L., Fagerstrom, C. J., Fear, J. M., Mahadevaraju, S., et al. (2020). Sperm Head-Tail Linkage Requires Restriction of Pericentriolar Material to the Proximal Centriole End. *Dev. Cell* 53, 86-101.e7. doi:10.1016/j.devcel.2020.02.006.

Giet, R., McLean, D., Descamps, S., Lee, M. J., Raff, J. W., Prigent, C., et al. (2002). Drosophila Aurora A kinase is required to localize D-TACC to centrosomes and to regulate astral microtubules. *J. Cell Biol.* 156, 437–451. doi:10.1083/jcb.200108135.

Glover, D. M., Leibowitz, M. H., McLean, D. A., and Parry, H. (1995). Mutations in aurora prevent centrosome separation leading to the formation of monopolar spindles. *Cell* 81, 95–105. doi:10.1016/0092-8674(95)90374-7.

Gönczy, P., and DiNardo, S. (1996). The germ line regulates somatic cyst cell proliferation and fate during Drosophila spermatogenesis. *Development* 122, 2437–2447.

doi:10.1242/dev.122.8.2437.

Gottardo, M., Callaini, G., and Riparbelli, M. G. (2015). The Drosophila centriole - conversion of doublets into triplets within the stem cell niche. *J. Cell Sci.* 128, 2437–2442. doi:10.1242/jcs.172627.

Griffith, E., Walker, S., Martin, C.-A., Vagnarelli, P., Stiff, T., Vernay, B., et al. (2008). Mutations in pericentrin cause Seckel syndrome with defective ATR-dependent DNA damage signaling. *Nat. Genet.* 40, 232–236. doi:10.1038/ng.2007.80.

Guillet, V., Knibiehler, M., Gregory-Pauron, L., Remy, M.-H., Chemin, C., Raynaud-Messina, B., et al. (2011). Crystal structure of γ-tubulin complex protein GCP4 provides insight into microtubule nucleation. *Nat. Struct. Mol. Biol.* 18, 915–919. doi:10.1038/nsmb.2083.

Gunawardane, R. N., Martin, O. C., Cao, K., Zhang, L., Dej, K., Iwamatsu, A., et al. (2000). Characterization and Reconstitution of Drosophila γ-Tubulin Ring Complex Subunits. *J. Cell Biol.* 151, 1513–1524. doi:10.1083/jcb.151.7.1513.

Gunawardane, R. N., Martin, O. C., and Zheng, Y. (2003). Characterization of a New γTuRC Subunit with WD Repeats. *Mol. Biol. Cell* 14, 1017–1026. doi:10.1091/mbc.e02-01-0034.

Hales, K. G., Korey, C. A., Larracuente, A. M., and Roberts, D. M. (2015). Genetics on the fly: A primer on the drosophila model system. *Genetics* 201, 815–842. doi:10.1534/genetics.115.183392.

Helps, N. R., Brewis, N. D., Lineruth, K., Davis, T., Kaiser, K., and Cohen, P. T. (1998). Protein phosphatase 4 is an essential enzyme required for organisation of microtubules at centrosomes in Drosophila embryos. *J. Cell Sci.* 111 (Pt 1, 1331–1340. doi:10.1242/jcs.111.10.1331.

Hughes, S. E., Beeler, J. S., Seat, A., Slaughter, B. D., Unruh, J. R., Bauerly, E., et al. (2011). Gamma-tubulin is required for bipolar spindle assembly and for proper kinetochore microtubule attachments during prometaphase I in Drosophila oocytes. *PLoS Genet.* 7, e1002209. doi:10.1371/journal.pgen.1002209.

Hutchins, J. R. A., Toyoda, Y., Hegemann, B., Poser, I., Hériché, J.-K., Sykora, M. M., et al. (2010). Systematic analysis of human protein complexes identifies chromosome segregation proteins. *Science* 328, 593–599. doi:10.1126/science.1181348.

Jana, S. C., Bettencourt-Dias, M., Durand, B., and Megraw, T. L. (2016). Drosophila melanogaster as a model for basal body research. *Cilia* 5, 22. doi:10.1186/s13630-016-0041-5.

Karman, Z., Rethi-Nagy, Z., Abraham, E., Fabri-Ordogh, L., Csonka, A., Vilmos, P., et al. (2020). Novel perspectives of target-binding by the evolutionarily conserved PP4 phosphatase. *Open Biol.* 10, 200343. doi:10.1098/rsob.200343.

Kobayashi, T., and Dynlacht, B. D. (2011). Regulating the transition from centriole to basal body. *J. Cell Biol.* 193, 435–444. doi:10.1083/jcb.201101005.

Kollman, J. M., Merdes, A., Mourey, L., and Agard, D. A. (2011). Microtubule nucleation by γ-tubulin complexes. *Nat. Rev. Mol. Cell Biol.* 12, 709–721. doi:10.1038/nrm3209.

Kollman, J. M., Polka, J. K., Zelter, A., Davis, T. N., and Agard, D. A. (2010). Microtubule nucleating gamma-TuSC assembles structures with 13-fold microtubule-like symmetry. *Nature* 466, 879–882. doi:10.1038/nature09207.

Kumar, P., and Wittmann, T. (2012). +TIPs: SxIPping along microtubule ends. *Trends Cell Biol.* 22, 418–428. doi:10.1016/j.tcb.2012.05.005.

Lattao, R., Kovács, L., and Glover, D. M. (2017). The Centrioles,Centrosomes, Basal Bodies, and Cilia of Drosophila melanogaster. *Genetics* 206, 33–53. doi:10.1534/genetics.116.198168.

Laurinyecz, B., Péter, M., Vedelek, V., Kovács, A. L., Juhász, G., Maróy, P., et al. (2016). Reduced expression of CDP-DAG synthase changes lipid composition and leads to male sterility in Drosophila. *Open Biol.* 6, 50169. doi:10.1098/rsob.150169.

Laurinyecz, B., Vedelek, V., Kovács, A. L., Szilasi, K., Lipinszki, Z., Slezák, C., et al. (2019). Sperm-Leucylaminopeptidases are required for male fertility as structural components of mitochondrial paracrystalline material in Drosophila melanogaster sperm. *PLOS Genet.* 15, e1007987. doi:10.1371/journal.pgen.1007987.

Lengefeld, J., and Barral, Y. (2018). Asymmetric Segregation of Aged Spindle Pole Bodies During Cell Division : Mechanisms and Relevance Beyond Budding Yeast ? 1800038, 1–9. doi:10.1002/bies.201800038.

Liu, P., Würtz, M., Zupa, E., Pfeffer, S., and Schiebel, E. (2021). Microtubule nucleation: The waltz between γ-tubulin ring complex and associated proteins. *Curr. Opin. Cell Biol.* 68, 124–131. doi:10.1016/j.ceb.2020.10.004.

Liu, P., Zupa, E., Neuner, A., Böhler, A., Loerke, J., Flemming, D., et al. (2020). Insights into the assembly and activation of the microtubule nucleator γ-TuRC. *Nature* 578, 467–471. doi:10.1038/s41586-019-1896-6.

Loncarek, J., Hergert, P., Magidson, V., and Khodjakov, A. (2008). Control of daughter centriole formation by the pericentriolar material. *Nat. Cell Biol.* 10, 322–328. doi:10.1038/ncb1694.

Lüders, J., Patel, U. K., and Stearns, T. (2006). GCP-WD is a γ-tubulin targeting factor required for centrosomal and chromatin-mediated microtubule nucleation. *Nat. Cell Biol.* 8, 137–147. doi:10.1038/ncb1349.

Martin, O. C., Gunawardane, R. N., Iwamatsu, A., and Zheng, Y. (1998). Xgrip109: a gamma tubulin-associated protein with an essential role in gamma tubulin ring complex (gammaTuRC) assembly and centrosome function. *J. Cell Biol.* 141, 675–687. doi:10.1083/jcb.141.3.675.

Martinez-Campos, M., Basto, R., Baker, J., Kernan, M., and Raff, J. W. (2004). The Drosophila pericentrin-like protein is essential for cilia/flagella function, but appears to be dispensable for mitosis. *J. Cell Biol.* 165, 673–683. doi:10.1083/jcb.200402130.

Masuda, H., Mori, R., Yukawa, M., and Toda, T. (2013). Fission yeast MOZART1/Mzt1 is an essential γ-tubulin complex component required for complex recruitment to the microtubule organizing center, but not its assembly. *Mol. Biol. Cell* 24, 2894–2906. doi:10.1091/mbc.E13-05-0235.

Megraw, T. L., Kao, L. R., and Kaufman, T. C. (2001). Zygotic development without functional mitotic centrosomes. *Curr. Biol.* 11, 116–120. doi:10.1016/s0960-9822(01)00017-3.

Megraw, T. L., and Kaufman, T. C. (2000). The centrosome in Drosophila oocyte development. *Curr. Top. Dev. Biol.* 49, 385–407. doi:10.1016/s0070-2153(99)49019-2.

Moritz, M., Braunfeld, M. B., Guénebaut, V., Heuser, J., and Agard, D. A. (2000). Structure of the γ-tubulin ring complex: a template for microtubule nucleation. *Nat. Cell Biol.* 2, 365–370. doi:10.1038/35014058.

Moritz, M., Zheng, Y., Alberts, B. M., and Oegema, K. (1998). Recruitment of the gamma-tubulin ring complex to Drosophila salt-stripped centrosome scaffolds. *J. Cell Biol.* 142, 775–786. doi:10.1083/jcb.142.3.775.

Murphy, S. M., Preble, A. M., Patel, U. K., O'Connell, K. L., Dias, D. P., Moritz, M., et al. (2001). GCP5 and GCP6: two new members of the human gamma-tubulin complex. *Mol. Biol. Cell* 12, 3340–3352. doi:10.1091/mbc.12.11.3340.

Murphy, S. M., Urbani, L., and Stearns, T. (1998). The mammalian gamma-tubulin complex contains homologues of the yeast spindle pole body components spc97p and spc98p. *J. Cell Biol.* 141, 663–674. doi:10.1083/jcb.141.3.663.

Nashchekin, D., Fernandes, A. R., and St Johnston, D. (2016). Patronin/Shot Cortical Foci Assemble the Noncentrosomal Microtubule Array that Specifies the Drosophila Anterior-Posterior Axis. *Dev. Cell* 38, 61–72. doi:10.1016/j.devcel.2016.06.010.

Nigg, E. A., and Stearns, T. (2011). The centrosome cycle: Centriole biogenesis, duplication and inherent asymmetries. *Nat. Cell Biol.* 13, 1154–1160. doi:10.1038/ncb2345.

Noguchi, T., Koizumi, M., and Hayashi, S. (2011). Sustained Elongation of Sperm Tail Promoted by Local Remodeling of Giant Mitochondria in Drosophila. *Curr. Biol.* 21, 805–814. doi:10.1016/j.cub.2011.04.016.

Noguchi, T., Koizumi, M., and Hayashi, S. (2012). Mitochondria-driven cell elongation mechanism for competing sperms. *Fly (Austin).* 6, 113–116. doi:10.4161/fly.19862.

Oakley, B. R., Paolillo, V., and Zheng, Y. (2015). γ-Tubulin complexes in microtubule nucleation and beyond. *Mol. Biol. Cell* 26, 2957–2962. doi:10.1091/mbc.E14-11-1514.

Oegema, K., Wiese, C., Martin, O. C., Milligan, R. A., Iwamatsu, A., Mitchison, T. J., et al. (1999). Characterization of two related Drosophila gamma-tubulin complexes that differ in their ability to nucleate microtubules. *J. Cell Biol.* 144, 721–733. doi:10.1083/jcb.144.4.721.

Pitnick, S., Markow, T. A., and Spicer, G. S. (1995). Delayed male maturity is a cost of producing large sperm in Drosophila. *Proc. Natl. Acad. Sci.* 92, 10614–10618. doi:10.1073/pnas.92.23.10614.

Port, F., Chen, H.-M., Lee, T., and Bullock, S. L. (2014). Optimized CRISPR/Cas tools for efficient germline and somatic genome engineering in Drosophila. *Proc. Natl. Acad. Sci.* 111, E2967–E2976. doi:10.1073/pnas.1405500111.

Raynaud-Messina, B., Debec, A., Tollon, Y., Garès, M., and Wright, M. (2001). Differential properties of the two Drosophila γ-tubulin isotypes. *Eur. J. Cell Biol.* 80, 643–649. doi:10.1078/0171-9335-00195.

Riehlman, T. D., Olmsted, Z. T., Branca, C. N., Winnie, A. M., Seo, L., Cruz, L. O., et al. (2013). Functional replacement of fission yeast γ-tubulin small complex proteins Alp4 and Alp6 by human GCP2 and GCP3. *J. Cell Sci.* 126, 4406–4413. doi:10.1242/jcs.128173.

Riparbelli, M. G., Persico, V., and Callaini, G. (2020). The Microtubule Cytoskeleton during the Early Drosophila Spermiogenesis. *Cells* 9, 2684. doi:10.3390/cells9122684.

Riparbelli, M. G., Whitfield, W. G. F., Dallai, R., and Callaini, G. (1997). Assembly of the zygotic centresome in the fertilized Drosophila egg. *Mech. Dev.* 65, 135–144. doi:10.1016/S0925-4773(97)00066-X.

Rogowski, K., Juge, F., van Dijk, J., Wloga, D., Strub, J.-M., Levilliers, N., et al. (2009). Evolutionary Divergence of Enzymatic Mechanisms for Posttranslational Polyglycylation. *Cell* 137, 1076–1087. doi:10.1016/j.cell.2009.05.020.

Roostalu, J., and Surrey, T. (2017). Microtubule nucleation: beyond the template. *Nat. Rev. Mol. Cell Biol.* 18, 702–710. doi:10.1038/nrm.2017.75.

Sanchez, A. D., and Feldman, J. L. (2017). Microtubule-organizing centers: from the centrosome to non-centrosomal sites. *Curr. Opin. Cell Biol.* 44, 93–101. doi:10.1016/j.ceb.2016.09.003.

Santamaria, A., Wang, B., Elowe, S., Malik, R., Zhang, F., Bauer, M., et al. (2011). The Plk1-dependent phosphoproteome of the early mitotic spindle. *Mol. Cell. Proteomics* 10, M110.004457. doi:10.1074/mcp.M110.004457.

Schnorrer, F., Luschnig, S., Koch, I., and Nüsslein-Volhard, C. (2002). γ-Tubulin37C and γ-tubulin ring complex protein 75 Are Essential for bicoid RNA Localization during Drosophila Oogenesis. *Dev. Cell* 3, 685–696. doi:10.1016/S1534-5807(02)00301-5.

Siddall, N. A., and Hime, G. R. (2017). A Drosophila toolkit for defining gene function in spermatogenesis. *Reproduction* 153, R121–R132. doi:10.1530/REP-16-0347.

Spradling, A. C., Nystul, T., Lighthouse, D., Morris, L., Fox, D., Cox, R., et al. (2008). Stem cells and their niches: integrated units that maintain Drosophila tissues. *Cold Spring Harb. Symp. Quant. Biol.* 73, 49–57. doi:10.1101/sqb.2008.73.023.

Sullivan, W., Ashburner, M., and Hawley, R. S. (2000). *Drosophila protocols.* Cold Spring Harbor Laboratory Press.

Takács, Z., Jankovics, F., Vilmos, P., Lénárt, P., Röper, K., and Erdélyi, M. (2017). The spectraplakin Short stop is an essential microtubule regulator involved in epithelial closure in Drosophila. *J. Cell Sci.* 130, 712–724. doi:10.1242/jcs.193003.

Takada, S., Kelkar, A., and Theurkauf, W. E. (2003). Drosophila checkpoint kinase 2 couples centrosome function and spindle assembly to genomic integrity. *Cell* 113, 87–99. doi:10.1016/s0092-8674(03)00202-2.

Tates, A. D. (1971). Cytodifferentiation during spermatogenesis in Drosophila melanogaster: an

electron microscope study. *Ph. D. Thesis. Rijksuniversiteit, Leiden*.

Teixido-Travesa, N., Roig, J., and Luders, J. (2012). The where, when and how of microtubule nucleation - one ring to rule them all. *J. Cell Sci.* 125, 4445–4456. doi:10.1242/jcs.106971.

Tillery, M., Blake-Hedges, C., Zheng, Y., Buchwalter, R., and Megraw, T. (2018). Centrosomal and Non-Centrosomal Microtubule-Organizing Centers (MTOCs) in Drosophila melanogaster. *Cells* 7, 121. doi:10.3390/cells7090121.

Tokuyasu, K. T. (1974a). Dynamics of spermiogenesis in Drosophila melanogaster. 3. Relation between axoneme and mitochondrial derivatives. *Exp. Cell Res.* 84, 239–250. doi:10.1016/0014-4827(74)90402-9.

Tokuyasu, K. T. (1974b). Dynamics of spermiogenesis in Drosophila melanogaster. IV. Nuclear transformation. *J. Ultrastruct. Res.* 48, 284–303. doi:10.1016/s0022-5320(74)80083-3.

Tokuyasu, K. T. (1975). Dynamics of spermiogenesis in Drosophila melanogaster. VI. Significance of "onion" nebenkern formation. *J. Ultrastruct. Res.* 53, 93–112. doi:10.1016/s0022-5320(75)80089-x.

Tokuyasu, K. T., Peacock, W. J., and Hardy, R. W. (1972). Dynamics of spermiogenesis in Drosophila melanogaster. I. Individualization process. *Z. Zellforsch. Mikrosk. Anat.* 124, 479–506. doi:10.1007/BF00335253.

Tovey, C. A., and Conduit, P. T. (2018). Microtubule nucleation by γ-tubulin complexes and beyond. *Essays Biochem.* 62, 765–780. doi:10.1042/EBC20180028.

Tovey, C. A., Tubman, C. E., Hamrud, E., Zhu, Z., Dyas, A. E., Butterfield, A. N., et al. (2018). γ-TuRC Heterogeneity Revealed by Analysis of Mozart1. *Curr. Biol.* 28, 2314-2323.e6. doi:10.1016/j.cub.2018.05.044.

Ugur, B., Chen, K., and Bellen, H. J. (2016). Drosophila tools and assays for the study of human diseases. *DMM Dis. Model. Mech.* 9, 235–244. doi:10.1242/dmm.023762.

van Eeden, F., and St Johnston, D. (1999). The polarisation of the anterior-posterior and dorsal-ventral axes during Drosophila oogenesis. *Curr. Opin. Genet. Dev.* 9, 396–404. doi:10.1016/S0959-437X(99)80060-4.

Vedelek, V., Bodai, L., Grézal, G., Kovács, B., Boros, I. M., Laurinyecz, B., et al. (2018). Analysis of Drosophila melanogaster testis transcriptome. *BMC Genomics* 19, 697. doi:10.1186/s12864-018-5085-z.

Vedelek, V., Laurinyecz, B., Kovács, A. L., Juhász, G., and Sinka, R. (2016). Testis-Specific Bb8 Is Essential in the Development of Spermatid Mitochondria. *PLoS One* 11, e0161289. doi:10.1371/journal.pone.0161289.

Vérollet, C., Colombié, N., Daubon, T., Bourbon, H.-M., Wright, M., and Raynaud-Messina, B. (2006). Drosophila melanogaster γ-TuRC is dispensable for targeting γ-tubulin to the centrosome and microtubule nucleation. *J. Cell Biol.* 172, 517–528. doi:10.1083/jcb.200511071.

Vlasschaert, C., Cook, D., Xia, X., and Gray, D. A. (2017). The Evolution and Functional

Diversification of the Deubiquitinating Enzyme Superfamily. *Genome Biol. Evol.* 9, 558–573. doi:10.1093/gbe/evx020.

Vogt, N. (2006). The TuRC components Grip75 and Grip128 have an essential microtubule-anchoring function in the Drosophila germline. *Development* 133, 3963–3972. doi:10.1242/dev.02570.

Wasbrough, E. R., Dorus, S., Hester, S., Howard-Murkin, J., Lilley, K., Wilkin, E., et al. (2010). The Drosophila melanogaster sperm proteome-II (DmSP-II). *J. Proteomics* 73, 2171–2185. doi:10.1016/j.jprot.2010.09.002.

Wasteneys, G. O. (2002). Microtubule organization in the green kingdom: chaos or self-order? *J. Cell Sci.* 115, 1345–1354. doi:10.1242/jcs.115.7.1345.

White-Cooper, H. (2004). "Spermatogenesis: Analysis of Meiosis and Morphogenesis," in *Drosophila Cytogenetics Protocols* (New Jersey, United States: Humana Press), 45–76. doi:10.1385/1-59259-665-7:45.

White-Cooper, H., and Bausek, N. (2010). Evolution and spermatogenesis. *Philos. Trans. R. Soc. B Biol. Sci.* 365, 1465–1480. doi:10.1098/rstb.2009.0323.

Wiese, C. (2008). Distinct Dgrip84 Isoforms Correlate with Distinct γ-Tubulins in Drosophila. *Mol. Biol. Cell* 19, 368–377. doi:10.1091/mbc.e07-08-0801.

Wiese, C., and Zheng, Y. (2006). Microtubule nucleation: -tubulin and beyond. *J. Cell Sci.* 119, 4143–4153. doi:10.1242/jcs.03226.

Wilson, K. L., Fitch, K. R., Bafus, B. T., and Wakimoto, B. T. (2006). Sperm plasma membrane breakdown during Drosophila fertilization requires Sneaky, an acrosomal membrane protein. *Development* 133, 4871–4879. doi:10.1242/dev.02671.

Woodruff, J. B., Wueseke, O., and Hyman, A. A. (2014). Pericentriolar material structure and dynamics. *Philos. Trans. R. Soc. London. Ser. B, Biol. Sci.* 369. doi:10.1098/rstb.2013.0459.

Yalgin, C., Ebrahimi, S., Delandre, C., Yoong, L. F., Akimoto, S., Tran, H., et al. (2015). Centrosomin represses dendrite branching by orienting microtubule nucleation. *Nat. Neurosci.* 18, 1437–1445. doi:10.1038/nn.4099.

Zhang, L., Keating, T. J., Wilde, A., Borisy, G. G., and Zheng, Y. (2000). The role of Xgrip210 in gamma-tubulin ring complex assembly and centrosome recruitment. *J. Cell Biol.* 151, 1525–1536. doi:10.1083/jcb.151.7.1525.

Zhang, Y., Chen, Y., Gucek, M., and Xu, H. (2016). The mitochondrial outer membrane protein MDI promotes local protein synthesis and mtDNA replication. *EMBO J.* 35, 1045–1057. doi:10.15252/embj.201592994.

Zheng, Y., Wong, M. L., Alberts, B., and Mitchison, T. (1995). Nucleation of microtubule assembly by a gamma-tubulin-containing ring complex. *Nature* 378, 578–583. doi:10.1038/378578a0.

Zimmerman, W., and Doxsey, S. J. (2000). Construction of centrosomes and spindle poles by

molecular motor-driven assembly of protein particles. *Traffic* 1, 927–34. Available at: http://www.ncbi.nlm.nih.gov/pubmed/11208082.

Zupa, E., Liu, P., Würtz, M., Schiebel, E., and Pfeffer, S. (2021). The structure of the γ-TuRC: a 25-years-old molecular puzzle. *Curr. Opin. Struct. Biol.* 66, 15–21. doi:10.1016/j.sbi.2020.08.008.

10 Supplementary material

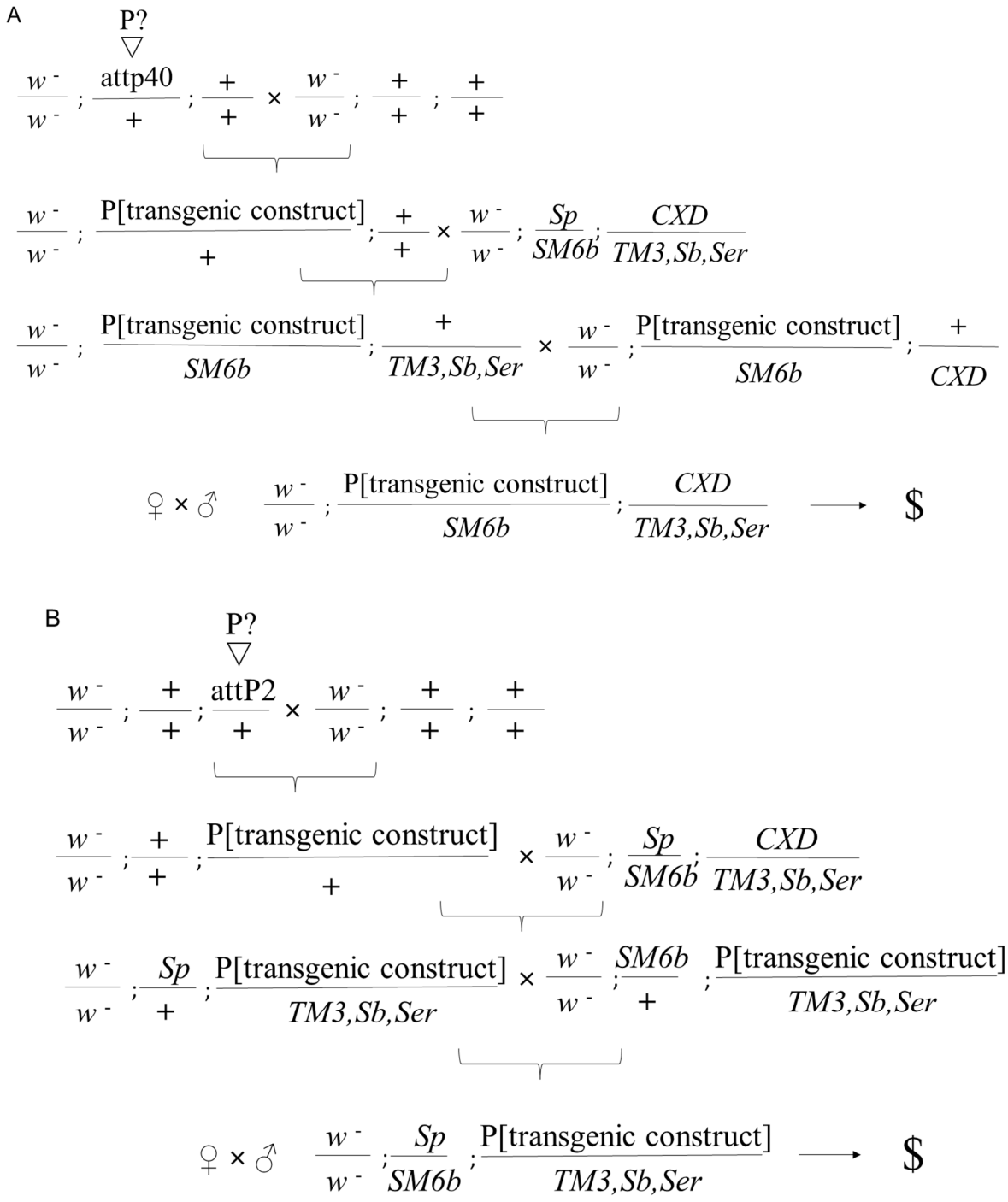

Supplementary Figure 1. Crossing schemes for establishing transgenic lines. **A.** Crossing scheme followed to establish second chromosome transgenic stable fly lines. **B.** Crossing scheme for establishing third chromosome transgenic stable fly lines.

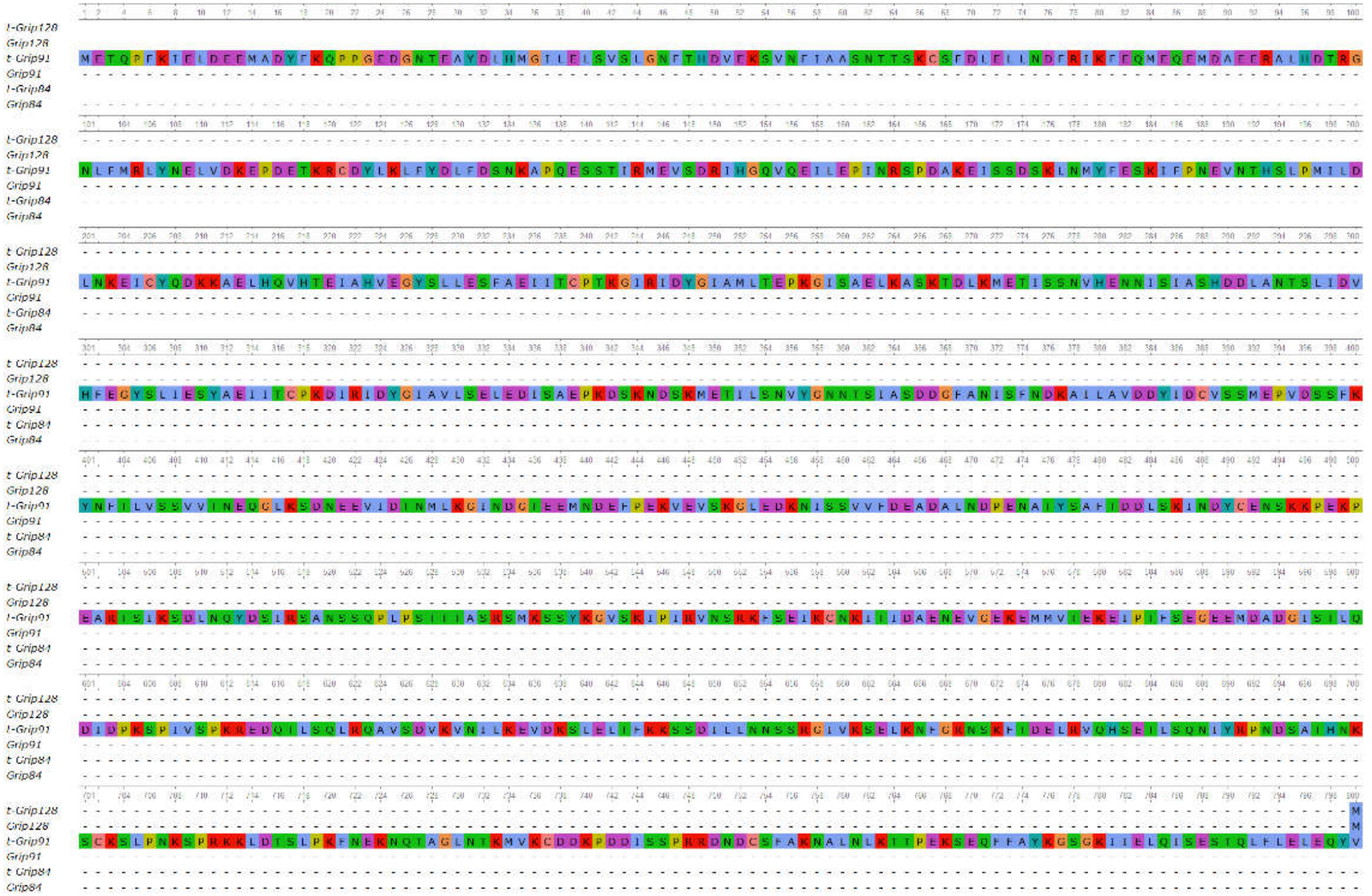
t-Grip128
Grip128
t-Grip91
Grip91
t-Grip84
Grip84

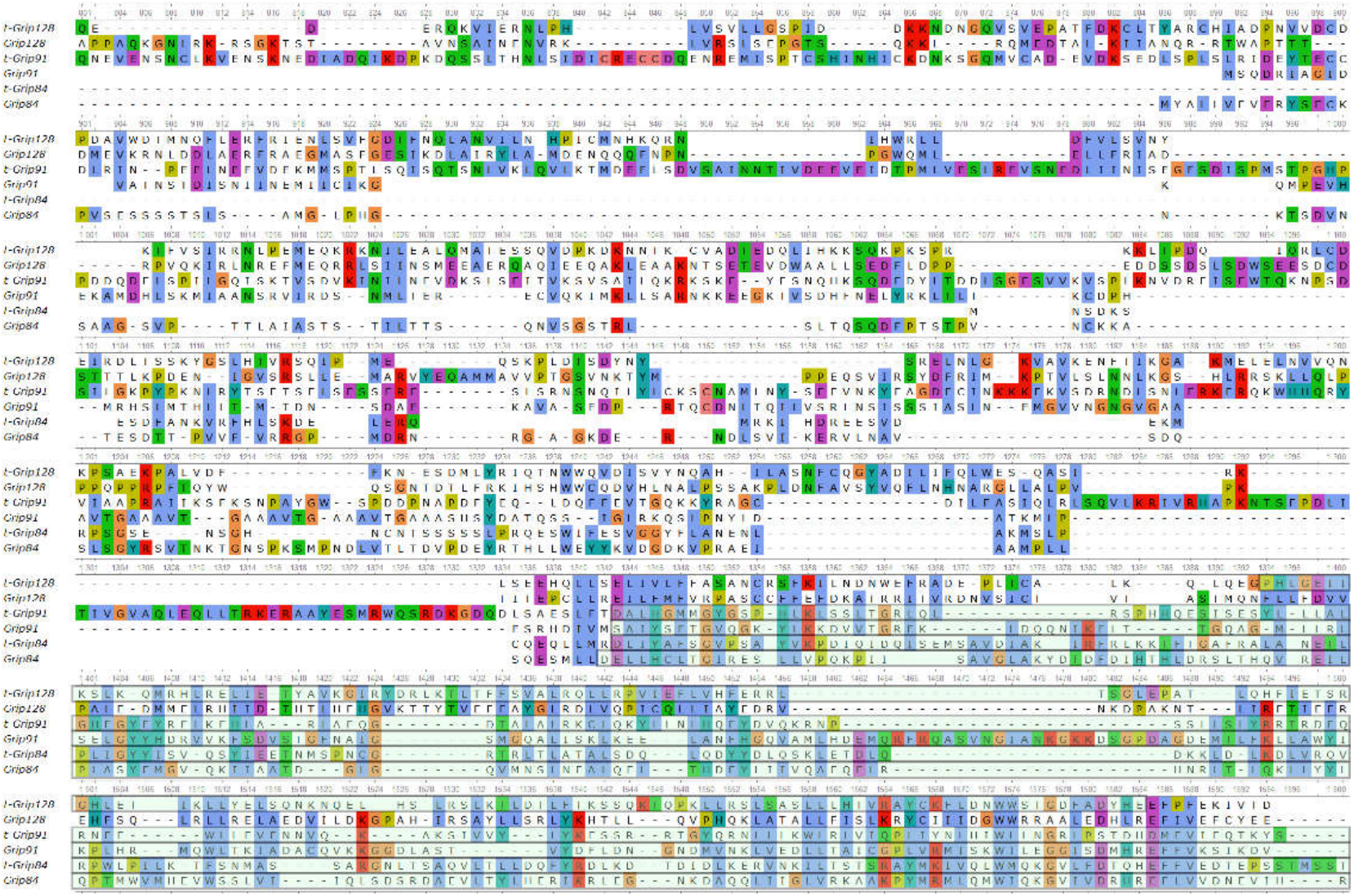
t-Grip178
Grip128
t-Grip91
Grip91
t-Grip84
Grip84

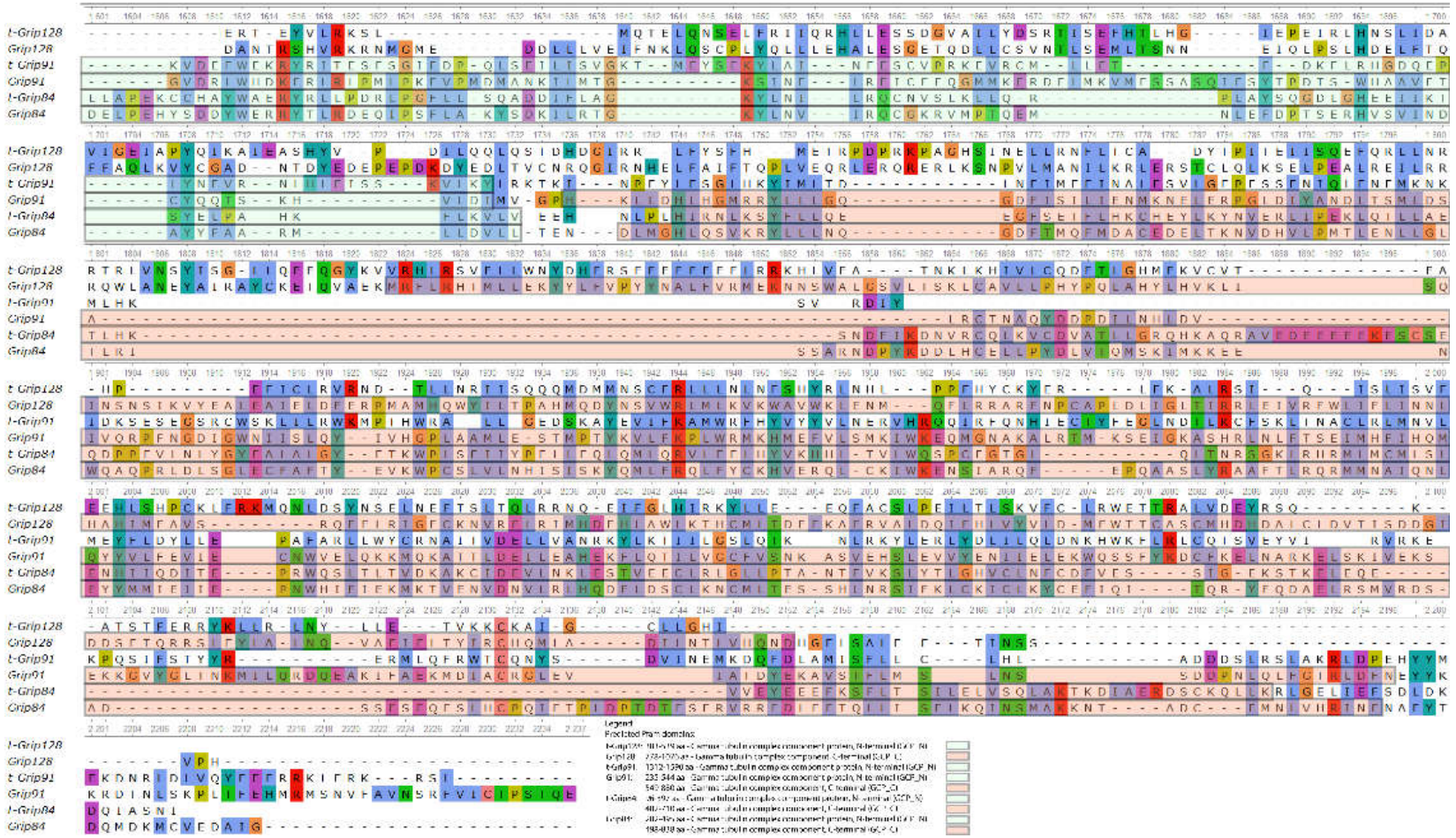
t-Grip128
Grip128
t-Grip91
Grip91
t-Grip84
Grip84
Legend
Predicted Pfam domains

Supplementary Figure 2. Protein sequence alignment for multiple Drosophila γ-TuRC proteins. Pairwise protein alignment for the ubiquitous and testis-specific γ-TuRC proteins. GCP-N (green) and GCP-C (red) domains are highlighted in the figure, key at the bottom of the figure.

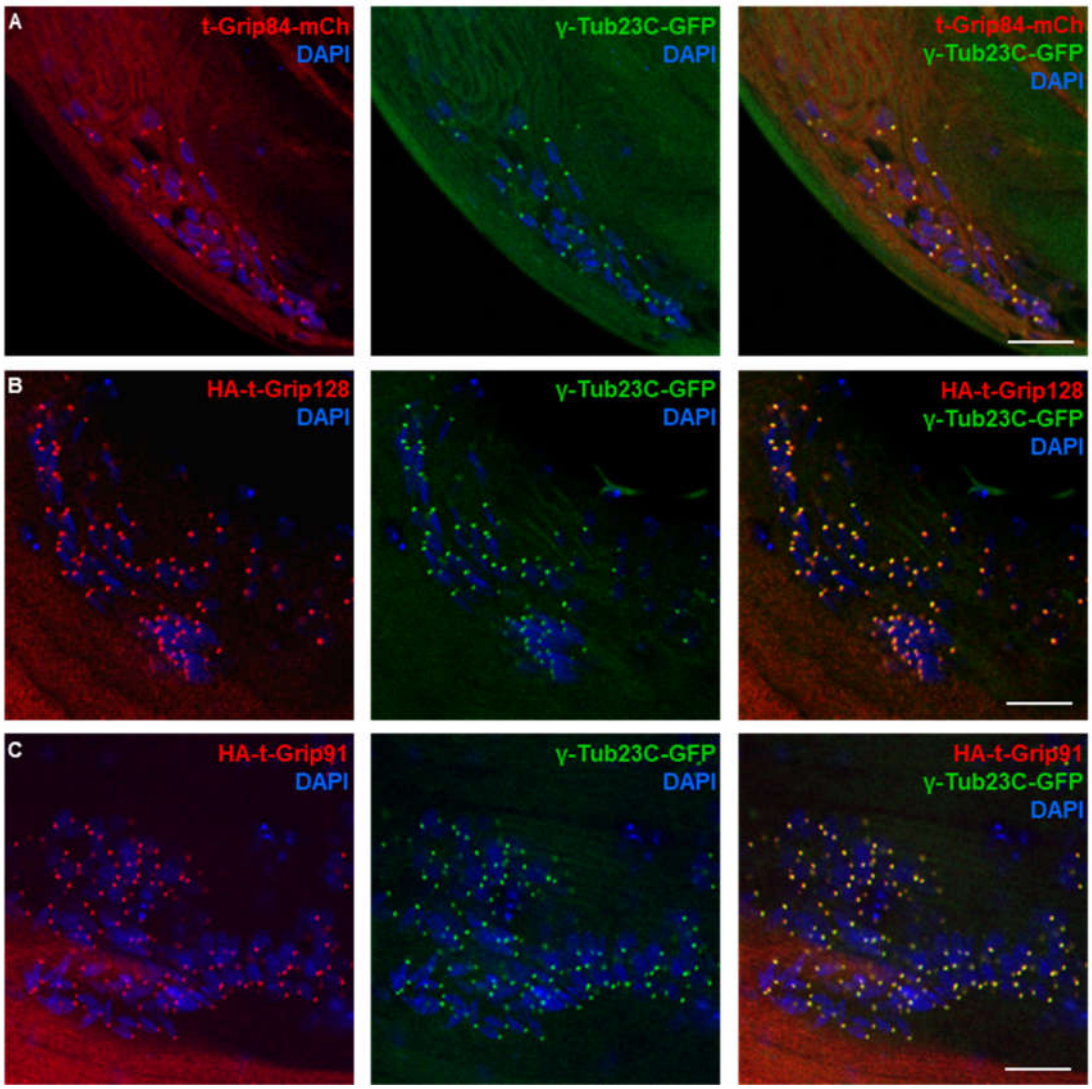

Supplementary Figure 3. Colocalization between t-γ-TuRC proteins and the transgenic line γ-Tub23C-GFP. t-Grip84-mCh (**A**), HA-t-Grip128 (**B**) and HA-t-Grip91 (**C**) all colocalize with γ-Tub23C-GFP at the centriole adjuncts of the elongating spermatids. Scale bars: 20 μm.

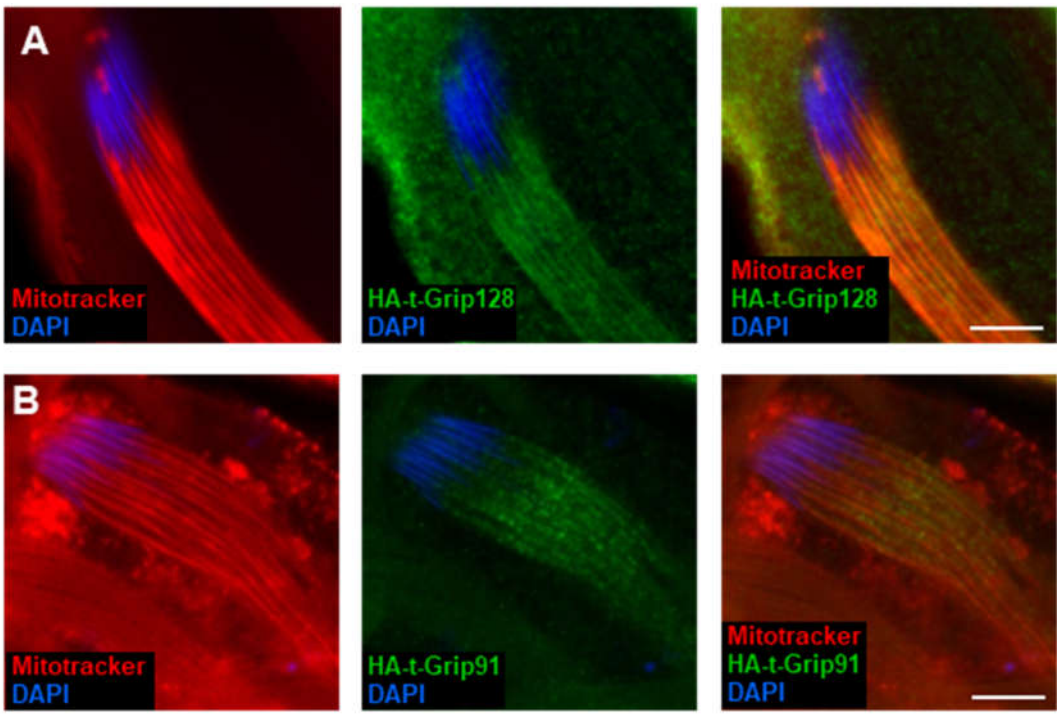

Supplementary Figure 4. Colocalization between t-γ-TuRC proteins and Mitotracker. HA-t-Grip128 (Green) (**A**) and HA-t-Grip91 (Green) (**B)** signal at the mitochondria colocalize with Mitotracker (red) signal. Scale bars: 10 µm.

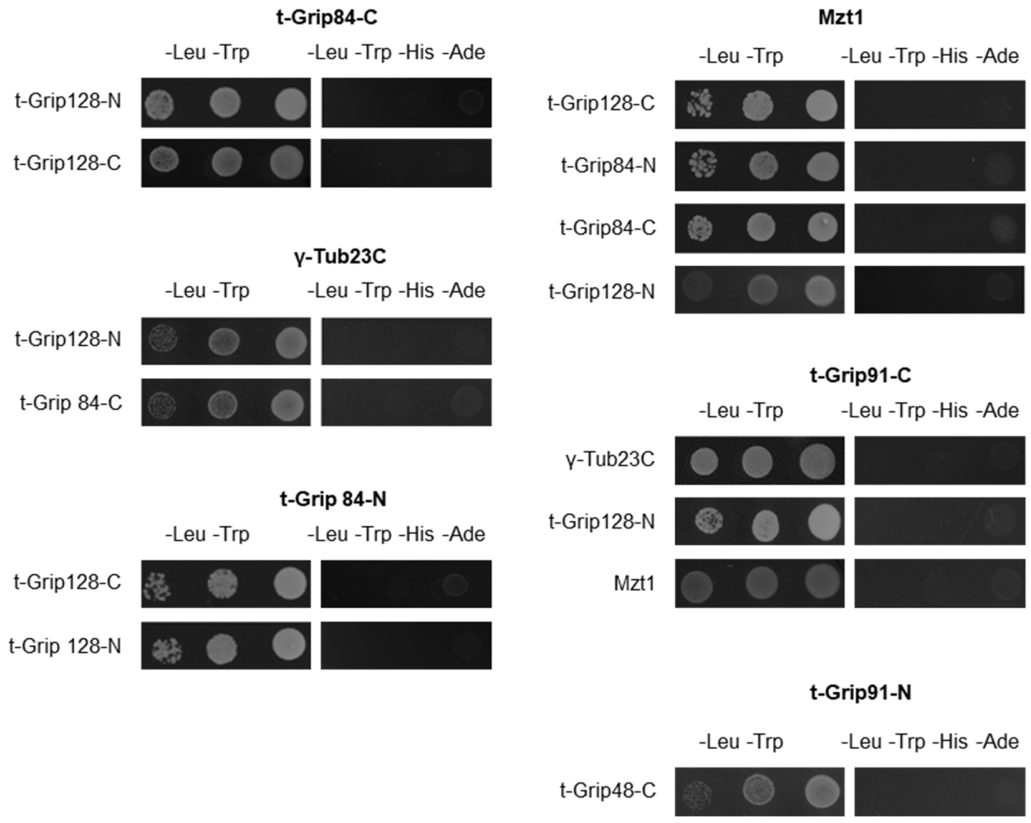

Supplementary Figure 5. The Negative yeast two hybrid results for t-γ-TuRC proteins.

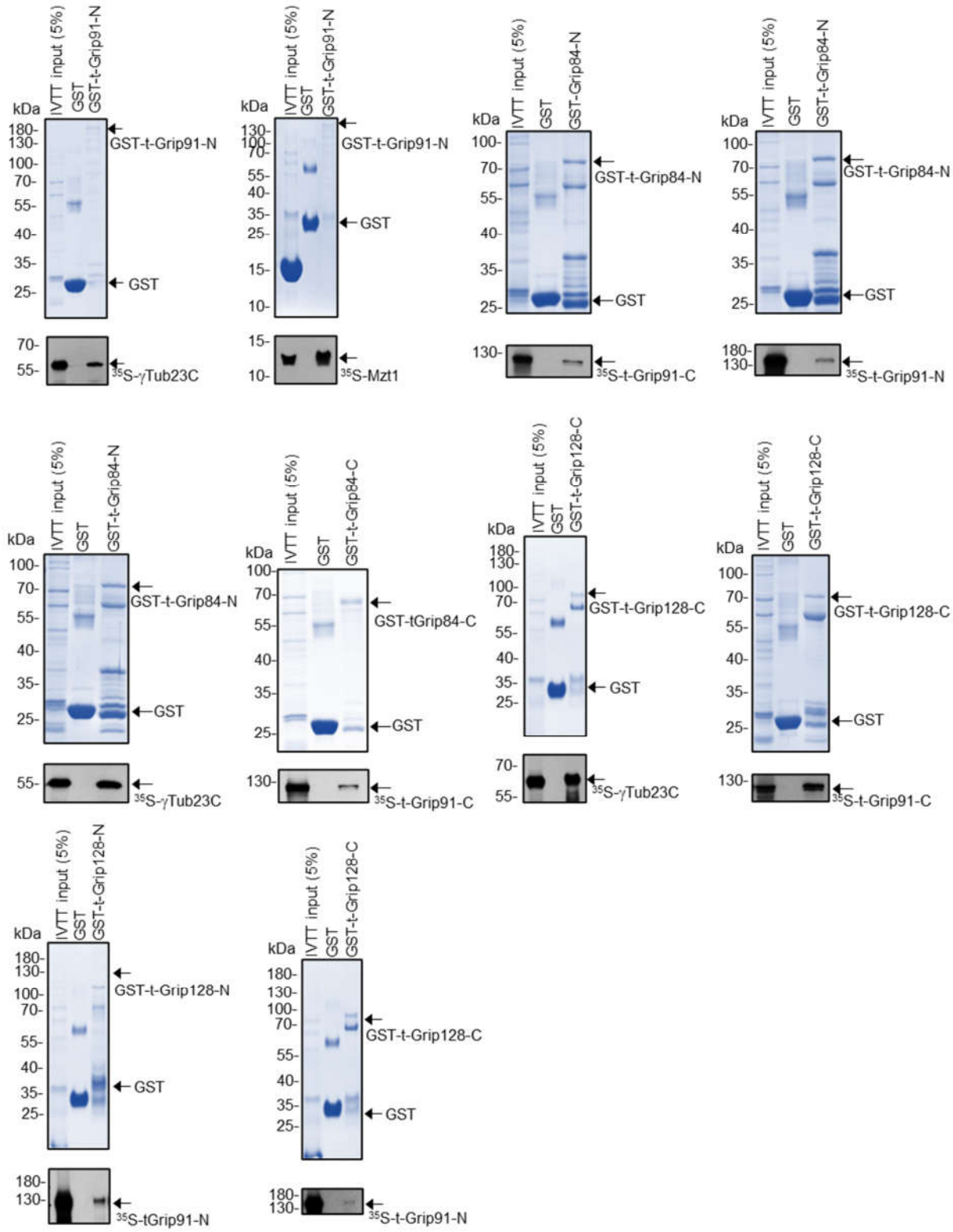

Supplementary Figure 6. IVTT interactions of the t-γ-TuRC proteins. Coomassie-Blue stained PAGE and autoradiograph for the positive interactions between t-γ-TuRC proteins.

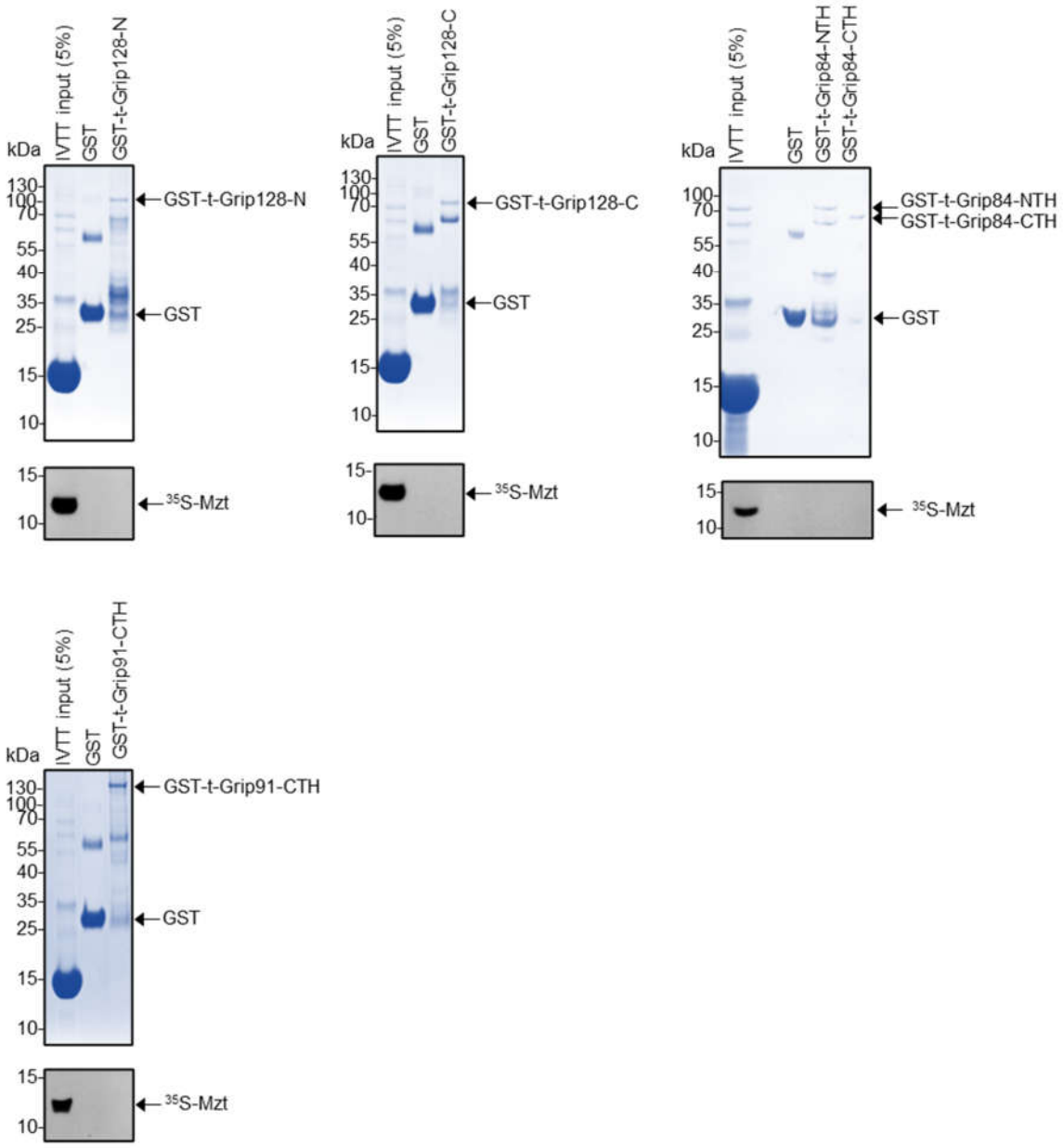

Supplementary Figure 7. Mzt1 IVTT interactions with the t-γ-TuRC proteins. Coomassie-Blue stained PAGE and autoradiograph showing the negative interactions between t-Grip84-N, C terminal, t-Grip128-N, C terminal and t-Grip91-C, and Mzt1.

t-Grip84-mCh_fw	ACTGCGGAATTCTTGAGTGAGTGTGAGCAGTAG
t-Grip84-mCh_rev	ACTGCGGCTAGCATTGGAAGCTATTTGATCCTTATC
HA-t-Grip91_fw	TCCAGATTACGCTATGGAGACGCAGCCATTTAAAATTG
HA-t-Grip91_rev	ATGTCACACCACAGAAGTAAGGTTCATTAAGCTACCAAGGTG ACCACG
HA-t-Grip128_fw	GTTTTCAATAAAAATGGATCTCCACCGCGGTGG
HA-t-Grip128_rev	TGTCCACACCACAGAAGTAAGGTTCTTAAATATGGCCGAGCA AACAGCC
GFP-Mzt1_fw	CTGTACAAGATGTCAGAACAACCGACACAAC
GFP-Mzt1_rev	CACAGAAGTAAGGTTCCTACAAAGTTGAGTCTGTTGATGC
t-Grip84-GFP_fw	GATATATTTTCTTATTCACCATGAACTCCGACAAATCGGAAAG
t-Grip84-GFP_rev	TTGCTCACCATTAGATATCTCGAGTGCGGC
YTH t-Grip91-N_fw	ATCGCCGGAATTCCCAATGGAGACGCAGCCATTTAAAATTG
YTH t-Grip91-N_rev	GGTCGACGGATCCCCTTAAACTAACATAGGGGTATCAATTTC AAC
YTH t-Grip91-C_fw	ATCGCCGGAATTCCCAATGGAAAGTCTTCGTGAAG
YTH t-Grip91-C_rev	GGTCGACGGATCCCCTTACAGTGATCTTTTCCTTTCC
YTH t-Grip84-N_fw	AAAGAGATCGAATTCCCAATGAACTCCGACAAATCG
YTH t-Grip84-N_rev	GGTCGACGGATCCCCTTAATTGTGCTCCTCCACC
YTH t-Grip84-C_fw	AAAGAGATCGAATTCCCAATGTTGCCTTTACACATTCG
YTH t-Grip84-C_rev	GGTCGACGGATCCCCTTAAATATTGGAAGCTATTTGATCC
YTH t-Grip128-N_fw	AAAGAGATCGAATTCCCAATGCAAGAGGACGAGAG
YTH t-Grip128-N_rev	GGTCGACGGATCCCCTTATCGTTCATCGGTCACAATC
YTH t-Grip128-C_fw	AAAGAGATCGAATTCCCAATGACAGAGTACGTCTTAAGAAAAT C
YTH t-Grip128-C_rev	GGTCGACGGATCCCCTTAAATATGGCCGAGCAAAC
YTH γ-Tub23C_fw	AAAGAGATCGAATTCCCAATGCCAAGTGAAATAATTACTTTGC AG
YTH γ-Tub23C_rev	GGTCGACGGATCCCCCTAGGAACCGGCGCTGGTC
YTH Mzt1_fwd	AAAGAGATCGAATTCCCAATGTCAGAACAACCGACAC
YTH Mzt1_rev	GGTCGACGGATCCCCCTACAAAGTTGAGTCTGTTGATG
GST t-Grip91-N_fw	CGACGGTACCATGGAGACGCAGCCATTTAAAAT
GST t-Grip91-N_rev	GCGGCCGCTTAAACTAACATAGGGGTATCAATTTCAAC
GST t-Grip128-N_fw	CGACGGTACCATGCAAGAGGACGAGAGACA
GST t-Grip128-N_rev	GCGGCCGCTTATCGTTCATCGGTCACAATC
GST t-Grip128-C_fw	CGACGGTACCATGACAGAGTACGTCTTAAGAAAATC
GST t-Grip128-C_rev	GCGGCCGCTTAAATATGGCCGAGCAAACA
GST t-Grip84-N_fw	GAATTCAAATGAACTCCGACAAATCGGAAAGTG
GST t-Grip84-N_rev	GCGGCCGCTTAATTGTGCTCCTCCACC
GST t-Grip84-C_fw	GAATTCAAATGTTGCCTTTACACATTCG
GST t-Grip84-C_rev	GCGGCCGCTTAAATATTGGAAGCTATTTGATCC
t-Grip128 $^{\Delta 65}$ CRISPR1	TATATAGGAAAGATATCCGGGTGAACTTC-G AAAACAAGTCTTAAACTCA-GTTTTAGAGCTAGAAATAGCAAG
t-Grip128 $^{\Delta 65}$ CRISPR2	ATTTTAACTTGCTATTTCTAGCTCTAAAAC-GATTCCGTCTAAGTTGAGTC-GACGTTAAATTGAAAATAGGTC
t-Grip84-GFP_fw (D.Mel2)	GAATTCAAATGAACTCCGACAAATCGGAAAGTG
t-Grip84-GFP_rev (D.Mel2)	GCGGCCGCGC AATATTGGAAGCTATTTGATCC

Supplementary Table 1. List of the used primers.